Nasa CR 65363

STUDY OF PROPELLANT VALVE LEAKAGE IN A VACUUM

Phase II Report

14 January 1966 to 7 March 1966

by

Ralph D. Gift
John A. Simmons
Joseph P. Copeland
Jaydee W. Miller
Jack M. Spurlock

for

Manned Spacecraft Center
National Aeronautics and Space Administration

Contract No. NAS9-4494
Control No. PR No. 433-7065

Atlantic Research Corporation
Alexandria, Virginia
6 May, 1966

ATLANTIC RESEARCH CORPORATION

ATLANTIC RESEARCH CORPORATION
HENRY G. SHIRLEY MEMORIAL HIGHWAY AT EDSALL ROAD
ALEXANDRIA, VIRGINIA 703-354-3400 TWX 710-832-9828

May 9, 1966
43-6807

NASA Manned Spacecraft Center
Propulsion and Power Division/EP-2
2101 Webster-Seabrook Road
Houston, Texas 77058

Subject: Phase II Report - Contract NAS 9-4494
Propellant Valve Leakage in a Vacuum

Gentlemen:

Enclosed are twenty-five (25) copies of the Phase II Report, plus one (1) reproducible copy, concerning the subject contract. The Phase II Report covers the studies, using the propellant Aerozine-50, which were accomplished during the period 14 January 1966 to 7 March 1966.

Very truly yours,

ATLANTIC RESEARCH CORPORATION

Jack M. Spurlock
Chief
Engineering Research Group

JMS:am
Enc: Phase II Report

cc: NASA Manned Spacecraft Center
Propulsion & Power Division/BF-33
2101 Webster-Seabrook Road
Houston, Texas 77058 (4 Copies)

NASA Manned Spacecraft Center
Propulsion & Power Division/BG 721
Houston, Texas 77058 (1 Copy)

Mr. Paul J. Martinkovic, RPRPP
Air Force Rocket Propulsion Laboratory
Edwards AFB, California 93523 (1 Copy)

ATLANTIC RESEARCH CORPORATION
ALEXANDRIA, VIRGINIA

STUDY OF PROPELLANT VALVE LEAKAGE IN A VACUUM

Phase II Report

14 January 1966 to 7 March 1966

by

Ralph D. Gift
John A. Simmons
Joseph P. Copeland
Jaydee W. Miller
Jack M. Spurlock

for

Manned Spacecraft Center
National Aeronautics and Space Administration

Contract No.NAS9-4494
Control No. PR No.433-7065

Atlantic Research Corporation
Alexandria, Virginia
6 May, 1966

This report was prepared by the Atlantic Research Corporation under Contract No. NAS9-4494, entitled "Study of Propellant Valve Leakage in a Vacuum", for the NASA Manned Spacecraft Center. The work was administered under the technical direction of the Propulsion Design Section of the Propulsion and Power Division, Manned Spacecraft Center, with Mr. B.B. Sprague serving as project manager.

PHASE II REPORT

TABLE OF CONTENTS

LIST OF FIGURES

1.0 SUMMARY

This report describes the results of an investigation of the adverse effects of Aerozine-50 leakage through propellant valves into injector manifolds exposed to a vacuum environment. The investigation consisted of concurrent theoretical and experimental studies. In the former, a literature survey and analysis was made to elucidate the freezing characteristics of Aerozine-50, and quantitative mathematical relationships between the rate of leakage and the accumulation of frozen propellant within the flow passages of an injector manifold were developed. For the experimental studies, tests with a simulated injector system were performed to characterize the freezing and its dependency on selected parameters, and to determine the extent of any flow stoppages caused by the accumulation of frozen propellant. The test system consisted of a leaky ball valve, a length of glass pipe and a plate with a number of drilled holes, which simulated the propellant valve, manifold and injector, respectively.

The principal results of this investigation are as follows:

(a) The freezing of Aerozine-50 by evaporation involves the vaporization of UDMH from the solution (UDMH is much more volatile than hydrzine) and the simultaneous precipitation of a solid phase of pure hydrazine. As this process continues, the temperature of the freezing mixture steadily decreases. After freezing is complete, the residual material is nearly pure hydrazine.

(b) The tests with the simulated injector manifold (which had a total injector port area of 0.266 in^2) showed that leaking Aerozine-50 can evaporatively freeze and accumulate within the flow passages. With the propellant at an initial temperature of 40°F, the leak-rate range for this occurrence was 0.01 to 2.0 cc/sec.

(c) The freezing did not interfere, in any way, with the operation of the ball valve.

(d) However, the accumulations of frozen propellant did form significant flow stoppages. Flow delays (span of time between valve opening and the start of flow) as long as 75.5 min were experienced for propellant at an

initial temperature of 40°F. For higher initial temperatures the delays were much shorter because of larger thermal convection currents and the attendant increased rate of melting. It is anticipated for a "zero g" situation, initial temperature of the propellant will have little effect on the duration of the stoppage.

(e) Maximum and minimum leak rates for freezing were calculated theoretically for the test system, using estimated data for the vapor pressure of UDMH-hydrazine mixtures. The results agreed reasonably well with the experimental values. For propellant at 40°F in the Apollo SPS engine the calculated leak-rate range is 0.004 to 3.06 cc/sec.

(f) Contrasting with the result for nitrogen tetroxide, the maximum leak rate at first increases with initial propellant temperature, goes through a maximum, which occurs at 80 to 100°F, and then decreases.

2.0 INTRODUCTION

Several cases of evaporative freezing of propellant have occurred during static test-firings of the Apollo Service Module engine (SPS) in a low-pressure environment. Although the freezing caused no apparent difficulties, an investigation seemed advisable to define the situation more fully. The over-all purpose of this program is (1) to define the conditions for which leakage through the propellant valves will result in freezing and impede proper engine operation; (2) to determine the character and extent of such problems; and (3) to suggest remedial action.

The program was begun June 7, 1965, and consists of four phases. The work on two of these phases has been completed and reported previously. Reference 1 presents the results obtained in Phase I, which was a general study of the effects of leakage of nitrogen tetroxide through a propellant valve into an injector manifold exposed to a vacuum. Similarly the results of Phase IV, an investigation of the freezing of propellants in the injector manifolds of the rockets of the Orbit Attitude Maneuvering System and the Re-entry Control System of the Gemini vehicles, have been described in Reference 2. Phase III, an investigation of the effects of the freezing of leaked propellant on hypergolic ignition, is to be completed in the near future.

This report describes the results obtained in Phase II, which was a study similar to Phase I but considering Aerozine-50 instead of nitrogen tetroxide. Aerozine-50, a mixture of hydrazine and unsymmetrical dimethyl hydrazine, has no definite freezing point but instead freezes over a 53°C temperature range. This gives rise to some interesting features of the evaporative freezing of leaking Aerozine-50 in injector manifolds. The characteristics of the freezing of Aerozine-50 and the quantitative relationships defining the range of leak rates permitting the accumulation of frozen material in an injector manifold are presented in Section 3.0. Measurements and observations of the freezing of leaking Aerozine-50 and the resulting formation of flow stoppages in a simulated injector manifold

are described and discussed in Section 4.0. Appendix A presents graphs of the variation of selected measurements with time for most of the tests performed.

The status of the overall program is discussed in Section 5.0.

3.0 THEORETICAL ANALYSIS

The general theory of the accumulation and evaporative freezing of propellant within the flow passages of injector manifolds has been described in the reports for Phase I[1] and Phase IV[2] of this program. The theory applies to propellant either which leaks in through the propellant control valves or which remains after engine shutdown. For the leakage situation, it was shown that flow stoppages caused by accumulations of frozen propellant can occur only if the rate of leakage is within a certain range. The maximum of this range is prescribed by the condition that the rate of heat loss by evaporation,which is determined by the rate of flow of vapor out through the injector ports, be just sufficient to cool and freeze the leaking propellant and remove heat transported in from the surroundings (the valve, the injector itself, radiation from nearby parts of the rocket engine, etc.). The minimum of this range is prescribed by the condition that the propellant be evaporated (or sublimed) as fast as it leaks by the heat transported from the surroundings. The theory has been applied to predict the range of leak rates for the occurrence of freezing and flow stoppages for injector manifolds with nitrogen tetroxide and monomethyl hydrazine. The predictions were verified by experiments.

In this section, application of the theory to injector manifolds with Aerozine-50 is discussed. Nitrogen tetroxide and monomethyl hydrazine are one-component propellants and possess a simple liquid-solid phase transition which occurs at a definite temperature. Aerozine-50 is a two-component propellant, a 1:1 mixture of hydrazine and UDMH (unsymmetrical dimethylhydrazine), and possesses a complex liquid-solid transition involving equilibriums between phases of different compositions over a 63°C temperature range. Although the existence of a range of leak rates for freezing is predicted for a two-component propellant, the detailed dependency of the span of the range on propellant parameters differs significantly from that for one-component propellants.

The freezing characteristics of Aerozine-50 are described in the first subsection below. Derivation of vapor pressure data, which is pertinent to the prediction of the range of leak rates for freezing, also is discussed in this subsection. In the second subsection, the relationships needed to predict the

range of leak rates for Aerozone-50 are derived and discussed. The subsection concludes with the presentation of predicted ranges of leak rates for an actual and a simulated injector. The agreement between the predicted and experimentally determined ranges for the simulated injector (cf. Section 4.0) is also discussed.

The nomenclature for the symbols used in the following discussion and derivations are listed in Table 3-1.

3.1 FREEZING CHARACTERISTICS OF AEROZINE-50

Aerozine-50 does not have a triple point, but freezes over a range of temperatures. As the mixture is cooled the first solid phase, which is pure hydrazine, appears at approximately 18°F (-8°C). Freezing out of hydrazine continues with more cooling, and the liquid phase becomes enriched in UDMH, accompanied by a decrease in the freezing point. Eventually, the liquid reaches the eutectic composition, about 98 per cent (weight) UDMH, which freezes at approximately -78°F (-61°C). If the cooling is caused by evaporation, the entire mixture (solid and solution) is hydrazine enriched, since for solutions with UDMH concentrations greater than 20 per cent (weight) the vapor is nearly pure UDMH. Furthermore, because the heat of vaporization of UDMH is approximately 1.5 times the heat of fusion of hydrazine (based on a unit weight), the solution becomes enriched with UDMH in spite of the loss of UDMH by evaporation. Assuming that the heat of fusion of hydrazine and the heat of vaporization of UDMH from the solutions are the same as for the pure materials, it is estimated that after all the eutectic has been frozen, the over-all composition of the frozen material is approximately 95 per cent (weight) hydrazine. Continued evaporation will cause still more hydrazine enrichment.

Calculation of rates of evaporative cooling, pertinent to the estimation of leak rate ranges for freezing, requires knowledge of the vapor pressures of hydrazine and UDMH above the entire range of the freezing mixtures. These data have never been measured. Only a single total vapor pressure value, 31 torr, has been reported for Aerozine-50 at its initial freezing point of 18°F.[3] However, Reference 3 presents a few data for the vapor pressures of hydrazine and UDMH above various non-freezing solutions at 72°F. Although these data

TABLE 3-1. NOMENCLATURE

ROMAN

A_i	Area of the injector ports, cm^2
A_e	Area of the surface from which evaporation occurs, cm^2
c_v	Vapor phase heat capacity, cal/gm-°K
e	Internal energy (partial molar internal energy divided by molecular weight), cal/gm
K	A parameter defined by equation (3-6)
L	A parameter defined by equation (3-7)
$\dot{M}_o$	Leak rate, gm/sec
MW	Molecular weight, gm/mol
m	Mass, gm
p	Pressure, atm
q_e	Rate of heat transport from the surroundings, cal/sec
R	Universal gas constant, cal/mol-°K
T	Absolute temperature, °K
t	Time, sec
x	Mole fraction of component in solution
y	Mole fraction of component in vapor
Z	A parameter defined by equations (3-8), (3-12), and (3-15)

GREEK

α	Evaporation coefficient
β	Activity coefficient
γ	Specific heat ratio
λ_v	Heat of vaporization, cal/gm
λ_s	Heat of sublimation, cal/gm

TABLE 3-1 (Cont'd.)

GREEK

ρ	Density, gm/cm^3

SUBSCRIPTS AND SUPERSCRIPTS

a	Average
c	Crystalline phase
d	Condensed phase
h	Hydrazine
ℓ	Liquid phase
o	Initial condition
p	Triple point
s	Solution
σ	Saturation condition
u	UDMH
v	Vapor

are not entirely reliable and self-consistent, as determined by application of the Duhem relation, they nevertheless were used to estimate the vapor pressures of freezing solutions. It is believed that the estimates are of sufficient accuracy to provide an insight into the freezing characteristics of leaking Aerozine-50, if not reliable values of the leak rate range.

The estimates of vapor pressure were made by deriving from the data mentioned, the two constants in the van Laar equations for the activity coefficients. Activity coefficients of hydrazine and UDMH in their solutions are defined by the relations

$$\beta_u = \frac{p_{u\sigma}}{x_u p_u^\circ} \quad ,$$

and

$$\beta_h = \frac{p_{h\sigma}}{x_h p_h^\circ} \quad ,$$

where p_u° and p_h° are the vapor pressures of pure UDMH and hydrazine, respectively, at the temperature of interest. The van Laar equations are a well-known, reliable means of extrapolating measured activity coefficients over a large temperature range. The equations are:

$$\ln \beta_u = \frac{B/T}{(1 + A\, x_u/x_h)^2} \quad ,$$

and

$$\ln \beta_h = \frac{AB/T}{(A + x_h/x_u)^2} \quad .$$

The values of the constants derived were A = 0.894 and B = 512. Compositions and temperatures of freezing hydrazine-UDMH solutions are shown in Figure 3-1,

which was taken from Reference 3. The corresponding vapor pressures, calculated from the above equations, are shown in Figure 3-2.

3.2 THE RANGE OF LEAK RATES FOR FREEZING

The derivation of the relationships for the maximum and minimum leak rates of the range for the freezing of a two-component propellant, such as Aerozine-50, proceeds in a manner very similar to that described in Reference 1 for a one-component propellant. Accordingly, attention is focused on the propellant residing at any instant of time in the flow passages of an injector. For freezing mixtures of hydrazine and UDMH this propellant will consist of hydrazine and UDMH vapor, a hydrazine-UDMH solution, and solid hydrazine. The derivation is based on the following assumptions:

(a) Liquid at a temperature, T_o, leaks into the flow passages at a steady rate, $\dot{M}_o$.

(b) Only vapor flows through the injector ports, which have a total area, A_i.

(c) The temperature throughout all phases of the propellant is uniform at the value, T.

(d) Heat, from the surroundings (valve, manifold, rocket engine, etc.) is absorbed by the propellant at the rate q_e, a function of the temperatures of the propellant and the surroundings.

Assumption (b) is necessary to specify the maximum rate since the simultaneous flow of a condensed phase merely reduces the area available for vapor flow and hence reduces the rate of heat removal by evaporation. Assumption (c) is reasonable (but not exact) since the specification of maximum and minimum rates requires that the temperature of the propellant in the manifolds be at a steady-state value. The reason for this is that the maximum utilization of heat removal by evaporation (for the maximum leak rate) or of heat absorbed from the surroundings (for the minimum leak rate) is realized only if the temperature of the propellant is not changing. These conditions also imply that the composition of each phase is uniform throughout.

The derivation is based upon statements of the conservation of mass and energy for the propellant in the flow passages and utilizes the Hertz-

Knudsen evaporation-rate expression and the usual expression for choked-flow of a gas through an orifice. The required conservation statements may be written as follows:

for the conservation of the condensed phases of hydrazine,

$$\frac{d(m_{hs} + m_{hc})}{dt} = 0.5\,\dot{M}_o - K_h \frac{p_{h\sigma} - py_h}{\sqrt{T}} \quad , \tag{3-1}$$

for hydrazine vapor,

$$\frac{dm_{hv}}{dt} = K_h \frac{p_{h\sigma} - py_h}{\sqrt{T}} - \frac{p}{\sqrt{T}} \frac{L\,MW_h y_h}{MW_a} \quad , \tag{3-2}$$

for the condensed phase of UDMH,

$$\frac{dm_{us}}{dt} = 0.5\,\dot{M}_o - K_u \frac{p_{u\sigma} - py_u}{\sqrt{T}} \quad , \tag{3-3}$$

for UDMH vapor,

$$\frac{dm_{uv}}{dt} = K_u \frac{p_{u\sigma} - py_u}{\sqrt{T}} - \frac{p}{\sqrt{T}} \frac{L\,MW_h y_h}{MW_a} \quad , \tag{3-4}$$

for the conservation of energy,

$$\frac{dE}{dt} = \frac{\dot{M}_o}{2}(e^\circ_{hs} + e^\circ_{us}) + q_e - \frac{L\,p}{MW_a\sqrt{T}}\left[y_h MW_h e_{hv} + y_u MW_u e_{uv} + MW_a p/\rho_v\right] \tag{3-5}$$

where $E = m_{hc}e_{hc} + m_{hs}e_{hs} + m_{hv}e_{hv} + m_{us}e_{us} + m_{uv}e_{uv}$, and kinetic energy and pressure-volume work for the condensed phases have been neglected. The quantity K, a parameter of the Hertz-Knudsen evaporation-rate expression, is defined by

the identity

$$K \equiv A_e \alpha \sqrt{\frac{MW}{2\pi R}} \quad , \tag{3-6}$$

and L, a parameter for the expression of choked-flow through the injector ports, is defined by the identity

$$L \equiv A_i \sqrt{\frac{\gamma MW_a}{R}} \left(\frac{2}{\gamma + 1} \right)^{\frac{\gamma + 1}{2(\gamma - 1)}} \quad , \tag{3-7}$$

where $MW_a = y_h MW_h + y_u MW_u$ and $\frac{\gamma - 1}{\gamma} = R/(y_h (c_v)_h + y_u (c_v)_u)$.

As the temperature of the propellant in the flow passages approaches a steady-state value, the quantities dm_{hv}/dt and dm_{uv}/dt become very small compared with the respective vapor fluxes and therefore may be neglected. This permits computation, using equations (3-2) and (3-4), of the quantities py in terms of the respective saturation vapor pressure of each component, which are functions of temperature alone:

$$\frac{L\ MW}{MW_a}\ py = A_i\ Z\ p_\sigma \quad , \tag{3-8}$$

where Z is a function of the parameters L, K, MW, and A_i.

Specification of a steady-state temperature (which is necessary for the determination of maximum and minimum leak rate values), utilizing equations (3-1), (3-3), and (3-8) and realizing that for freezing solutions $m_{hs}/m_{us} = G(T)$, a function of temperature (cf. Figure 3-1), permits equation (3-5) to be written in the form

$$\frac{\dot{M}_o}{2} \left[(e^\circ_{hs} - e_{hc}) + G(T)\ (e_{hc} - e_{hs}) + (e^\circ_{us} - e_{us}) \right] =$$

$$A_i Z_h \frac{p_{h\sigma}}{\sqrt{T}} (\lambda_s)_h + A_i\ Z_u \frac{p_{u\sigma}}{\sqrt{T}} (\lambda_v)_u +$$

$$A_i Z_u \frac{p_{u\sigma}}{\sqrt{T}}\ G(T)\ (e_{hc} - e_{hs}) - q_e \quad . \tag{3-9}$$

The left side of equation (3-9) represents the energy that must be removed to cool the leaking propellant to the steady-state temperature and to freeze whatever amount of hydrazine that is consistent with the composition of the solution at that temperature. The first three terms on the left side represent the energy carried away by the flow of vapor through the injector ports. The last term is the heat transported to the propellant from the surroundings.

Up to this point the derivation has been exactly analogous to that for a one-component propellant. Except for the specification that the steady-state temperature be the triple point temperature, equation (3-9) corresponds exactly to the maximum leak rate expression for a one-component propellant, equation (3) in Reference 1. Since Aerozine-50 and other two-component propellants have no triple point, another criterion for the maximum leak rate is required. Clearly, this must be the condition that there be no net accumulation of solution; only frozen hydrazine can accumulate. This is equivalent to the statement that $\frac{dm_{us}}{dt} = 0$, which when substituted into equation (3-3) yields the relation

$$\frac{M_o}{2} = A_i Z_u \frac{p_{u\sigma}}{\sqrt{T}} \quad . \tag{3-10}$$

Substituting this into equation (3-9) yields the expression

$$\dot{M}_o \frac{(e^\circ_{hs} - e_{hc})}{2} = A_i Z_h \frac{p_h (\lambda_s)_h}{\sqrt{T}} + A_i Z_u \frac{p_{u\sigma} (\lambda^*_v)_u}{\sqrt{T}} - q_e \ , \tag{3-11}$$

where $(\lambda^*_v)_u = (\lambda_v)_u - (e^\circ_{us} - e_{us})$. For the maximum rate it is reasonable to assume that $A_e >> A_i$ (which, in general, only requires the accumulation of enough propellant to fill a cross-section of the flow passage). From this the twin relations

$$Z_{h,u} = \frac{L \, MW_{h,u}}{A_i \, MW_a} \tag{3-12}$$

follow.

For the minimum leak rate the criterion is that the propellant evaporates (sublimes) at the same rate it leaks. Thus from equations (3-1) and (3-3) the relations,

$$\frac{\dot{M}_o}{2} = A_i Z_u \frac{p_{u\sigma}}{\sqrt{T}} = A_i Z_h \frac{p_{h\sigma}}{\sqrt{T}} \quad , \tag{3-13}$$

must follow. Substitution into equation (3-9) yields the additional relation

$$\frac{\dot{M}_o}{2} = \frac{q_e}{[(\lambda_s)_h - (e^\circ_{hs} - e_{hc})] + [(\lambda_v)_u - (e^\circ_{us} - e_{us})]} \tag{3-14}$$

It is assumed that Z_u has whatever value necessary to make equation (3-13) true. Furthermore it is reasonable to assume that $A_e = A_i$ for hydrazine, from which follows the expression

$$Z_h = \frac{L\ MW_h}{A_i\ MW_a\ (\alpha + L\ MW_h / K_h\ MW_a)} \quad . \tag{3-15}$$

Equations (3-10) and (3-11) together with the subsidiary relation (3-12) may be used to compute the maximum leak rate for freezing of Aerozine-50 in any injector configuration and for any initial temperature of the propellant. Similar to the case for a one-component propellant, the equations show, assuming q_e to be small, that the maximum rate is directly proportional to the total injector port area, the vapor pressures of the propellant components in the freezing mixture, and the heats of vaporization. However, the effect of initial temperature (reflected in the terms e°_{us} and e°_{hs}) on the maximum leak rate of Aerozine-50 is more complex: increasing initial temperature, starting from the initial freezing point (18°F), the maximum leak rate at first increases with initial temperature, goes through a maximum and then decreases. The reason for this is that at the maximum leak rate, the temperature of the accumulated propellant in the flow passages increases monotonically with initial temperature. However, as shown in

Figure 3-2, the vapor pressure of UDMH in the freezing mixtures goes through a maximum with increasing temperature. Since nearly all of the cooling results from the evaporation of UDMH, the maximum leak rate must also pass through a maximum value. For a similar reason, increasing the heat transport from the surroundings, for example by using a heater, also increases the maximum leak rate if the initial temperature is less than 80 to 100°F.

The minimum leak rate of Aerozine-50 for any initial temperature in any injector configuration may be computed using equations (3-13) and (3-14) with the subsidiary relation (3-15). Since the right-hand side of equation (3-14) is relatively insensitive to the steady-state temperature of the propellant in the flow passages, equation (3-14) has a much more pronounced influence on the minimum leak rate than does equation (3-13). Accordingly, the minimum leak rate is approximately proportional to q_e, has an inverse dependency on the heats of vaporization of the components, and increases very slowly with the initial temperature of the propellant.

In general the computed values of the minimum leak rate are, at best, only order-of-magnitude estimates. There are two reasons for this. One is the guess of the correct value for A_e which was required to derive equation (3-15). The second, and most important, is the great difficulty associated with determining the correct value for q_e, for which all sources and modes of heat transport must be considered.

The equations just described were used to compute the maximum and minimum leak rates for the simulated injector system used in the tests to be described in Section 4.0. For this system q_e was estimated to be 1.4 cal/sec. The results are shown in Table 3-2 together with experimentally observed values for comparison. Agreement of the minimum leak rate values is excellent and is probably fortuitous. For the maximum leak rate the agreement is only fair. The discrepancy probably arises because of the less than satisfactory data used to estimate the vapor pressures of the propellant components in Section 3.1.

Maximum and minimum leak rates also were computed for leaking Aerozine-50 in the injector manifold of the Apollo Service Propulsion System. The results are listed in Table 3-3. For these calculations, in order to obtain a conservative

TABLE 3-2

COMPUTED MAXIMUM AND MINIMUM LEAK RATES FOR AEROZINE-50 IN AN INJECTOR SYSTEM WITH A TOTAL PORT AREA OF 0.266 in^2

Initial Propellant Temperature (°F)	Calculated Leak Rate Values, cc/sec		Observed Leak Rate Values,[a] cc/sec	
	Maximum	Minimum	Maximum	Minimum
40	0.94	0.007	2.0	0.01
80	3.71	--	--	--
135	1.99	0.009	--	--

a. cf. Section 4.0

TABLE 3-3

COMPUTED MAXIMUM AND MINIMUM LEAK RATES FOR AEROZINE-50 IN THE INJECTOR SYSTEM OF THE APOLLO SPS ENGINE[a]

Initial Propellant Temperature (°F)	Computed Leak Rate (cc/sec)	
	Maximum	Minimum
40	3.06	0.04
80	11.40	--
135	6.98	0.04

a. The injector port area is 0.944 in^2.

value for the minimum rate, an attempt was made to select the lowest reasonable value of q_e consistent with all the various types of thermal environments in which the propulsion system would be used. Accordingly, under most operational circumstances the actual minimum leak rate may be somewhat greater than the values computed.

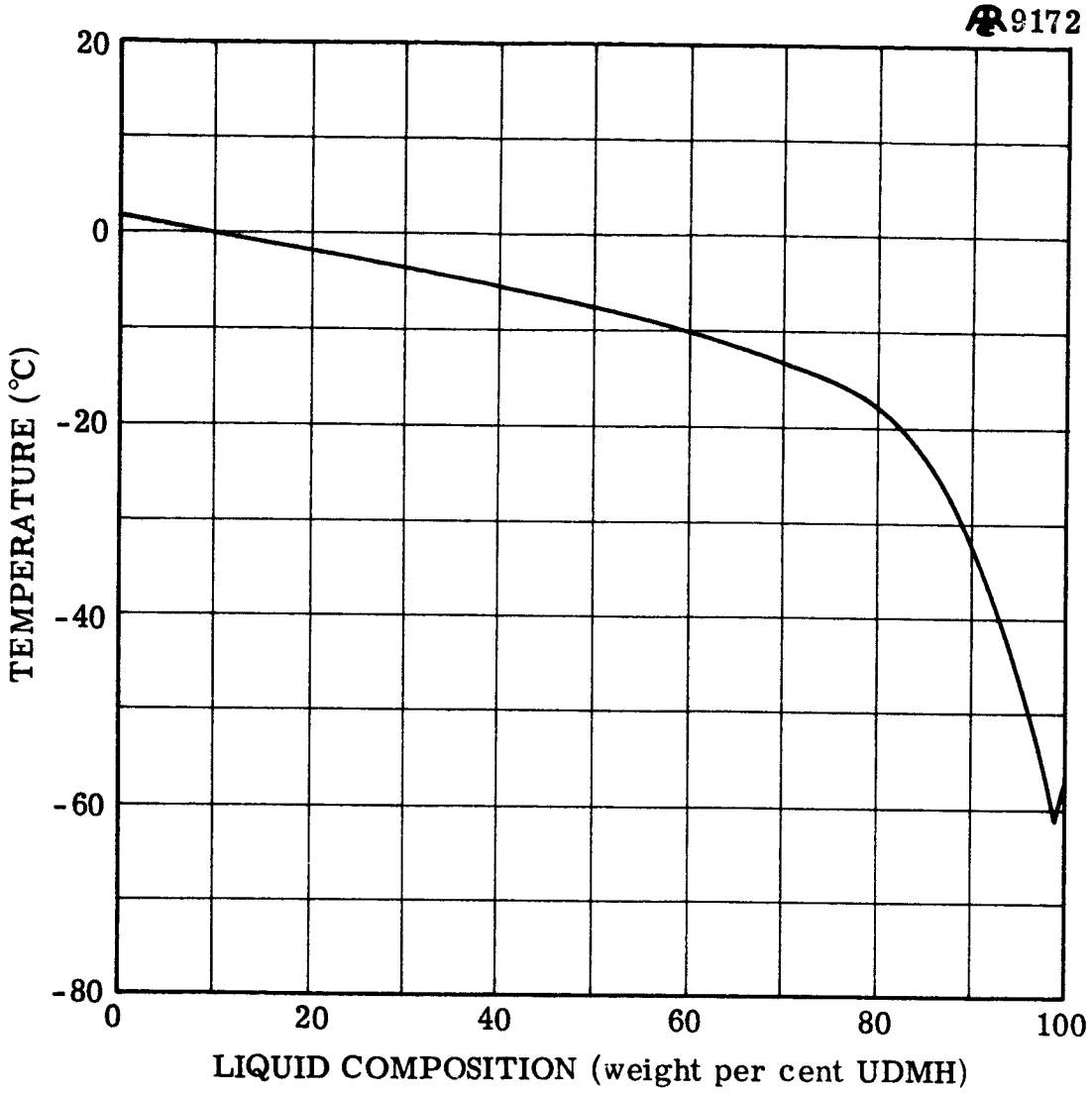

Figure 3-1. Freezing Points of Hydrazine-Unsymmetrical Dimethyl Hydrazine Solutions.

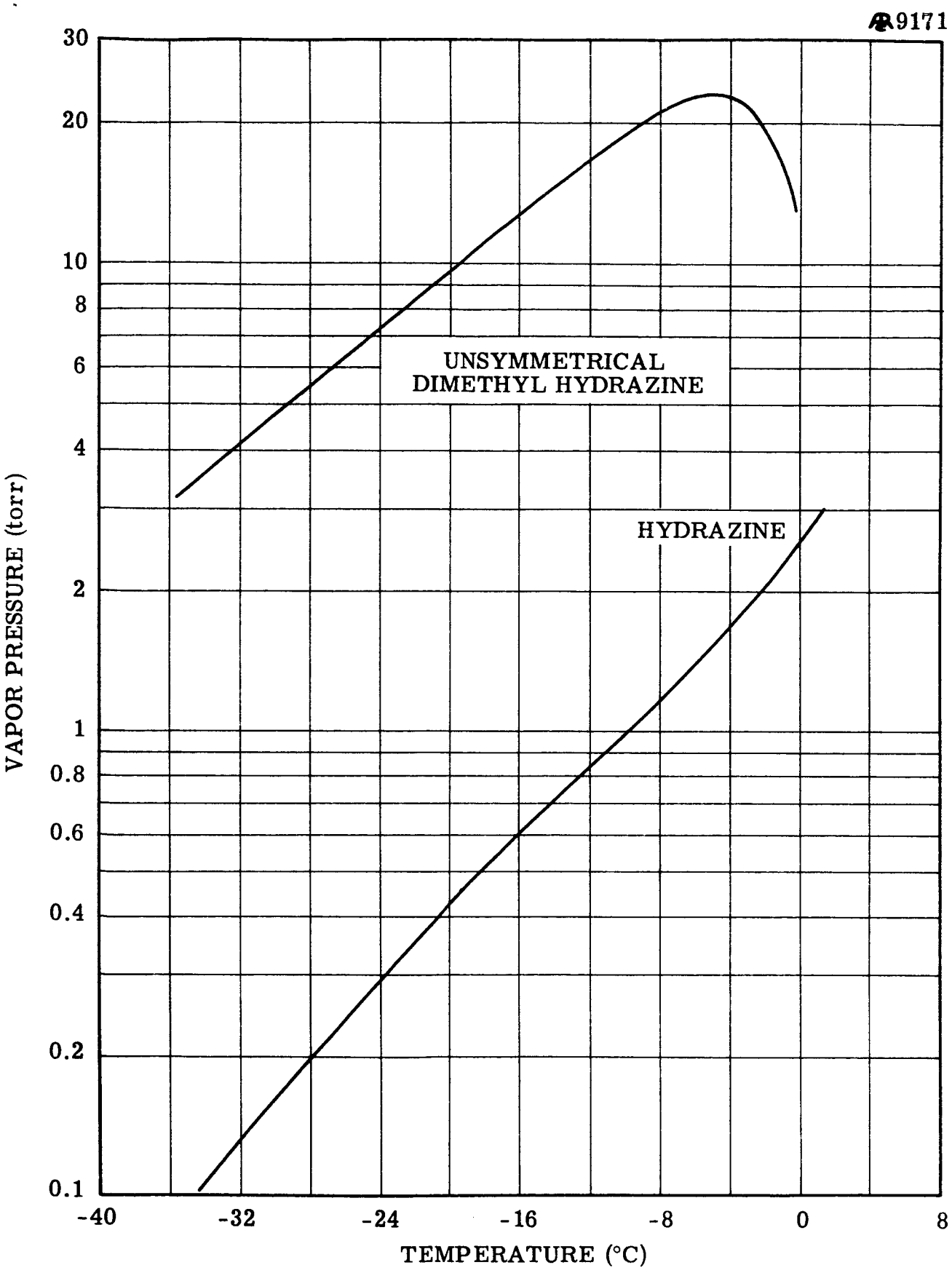

Figure 3-2. Calculated Vapor Pressures of Hydrazine and Unsymmetrical Dimethyl Hydrazine Above Freezing Mixtures.

4.0 EXPERIMENTAL STUDIES

4.1 DISCUSSION

The objective of the Phase II experimental program was to evaluate, in a vacuum environment, the effects of Aerozine-50 leaks through a simulated propellant valve (typical of the main propulsion engines of the Apollo vehicle). One of the likely and important effects is the freezing of Aerozine-50 and blockage of propellant flow systems. This section of the report presents a description of the test apparatus and procedures used in the evaluation, and a discussion of the results obtained.

A set of 81 tests with Aerozine-50 was conducted in this phase of the program. The effects of five variables on leakage-induced freezing phenomena were investigated:

1. Leakage rate
2. Durations of Leaks
3. Propellant temperature
4. Injector orifice area
5. Leak-valve size.

The most important results can be summarized as follows:

1. Evaporative freezing of Aerozine-50 in and around the propellant valve does not affect the torque required to open the valve.
2. Aerozine-50, leaking through the main propellant valve, can evaporatively freeze and block the flow passages between the valve and injector.
3. Leak-rate had a greater effect on the freezing phenomena than did any of the other variables.
4. Aerozine-50, initially cooled to approximately $40^{\circ}F$, produced more persistent blockages and longer flow-delays than did Aerozine-50 initially heated to approximately $135^{\circ}F$. The longest flow-delay experienced with cooled Aerozine-50 was 75.5 minutes, and the longest flow-delay obtained with heated Aerozine-50 was 2.8 minutes.
5. The minimum measured leak-rate for the test system, below which there

was no accumulation of frozen propellant, was about .01 cc/sec.

6. The maximum measured leak rate for the test system, above which Aerozine-50 did not freeze in the flow passages, was about 7.5 cc/sec per in^2 of injection port area.

4.2 TEST APPARATUS

The test equipment used for this phase of the program was, for the most part, the same as or similar to that used for the Phase I tests, described in the Phase I Report[1]. Some of the pertinent facts concerning the apparatus and instrumentation are repeated below.

4.2.1 High Altitude Facility

The major tool used in performing the experiments of this program is the Atlantic Research Corporation high-altitude facility. Figure 4-1 depicts this facility and some of its pertinent characteristics.

The test section consists of a cylindrical stainless steel tunnel, 6 feet in diameter and 25 feet long, which is exhausted by a 5-stage steam ejector system. The tunnel is housed in a building adjacent to the Atlantic Research Corporation Principal Laboratories, located in Alexandria, Virginia.

4.2.2 Flow System

The flow systems for the Phase II test apparatus are shown in Figures 4-2 and 4-3. All metal components in contact with either liquid or gaseous propellant were fabricated of stainless steel. Gaskets and seals were made of teflon.

Liquid Aerozine-50 was contained in the propellant tank attached to one end of a balance beam (the operation of this balance is discussed in Section 4.2.3). Flow was achieved by applying nitrogen pressure to the vapor space at the top of the propellant tank, thereby forcing the propellant into a feed line which ran through the tunnel wall to the leak-valve. A ball-type leak valve was used which is similar to the propellant valves that are em-

ployed on the Apollo SPS engine.

Two other ball valves were installed in the feed line -- a hand-operated valve located outside the tunnel, and a remotely-controlled valve which was installed inside the tunnel just upstream from the leak valve. The reason for the use of these valves is discussed later.

A schematic drawing of the leak valve is given in Figure 4-4. Three alterations were made to this ball valve to induce leakage:

1. The upstream seal was by-passed by drilling a 1/8 inch diameter hole into and perpendicular to the ball cavity. The ball was installed in the valve in a manner such that the relief hold faced upstream when the ball was in the closed position;

2. The downstream seal was scored;

3. The pressure on the downstream seal was varied by adjusting the associated body cap; flow was varied from run to run by changing the adjustment of this cap with the aid of a thickness gauge, as shown in Figure 4-4.

A glass pipe, four inches long, was connected to the outlet of the leak valve to permit observation of any freezing phenomena which might occur. Attached to the end of this pipe was an injector plate that was counterbored in the center such that it was 1/16-inch thick in the area of the hole pattern. As shown in Figure 4-5, a thermocouple was inserted in the side of the plate in a manner such that the junction was located very near the injector holes.

Capability for filling the propellant tank was provided by means of a fill line which ran from a storage tank to the feed line. Approximately 5 psig of nitrogen pressure in the storage tank was sufficient to effect propellant transfer when the propellant tank was vented. A 20 micron filter was installed in the fill line to remove any particulate matter which might be a source of leak-valve clogging.

Figure 4-6 is the flow diagram for the coolant system. The leak-

valve temperature was maintained by a mantle surrounding the valve body. This mantle consisted of several small-diameter copper tubes which were securely clamped onto the valve body. The tube ends were silver-soldered into manifolds located at each end of the valve.

The temperature of the propellant entering the leak valve was controlled by a concentric-tube heat exchanger installed in the feed-line upstream from the cut-off valve. The cut-off valve, identified in Figure 4-3, was the main control valve used to initiate and terminate a run. Test procedure details are presented in Section 4.3. For tests conducted with heated propellant, the concentric-tube heat exchanger was replaced with a section of tubing that was wrapped with an electrical heating tape.

The leak valve was opened and closed by a pneumatic operator which was activated by compressed nitrogen. This device was calibrated before the leak tests were performed so that the torque required to open the valve was known as a function of the gas pressure applied to the operator.

Since motion pictures of the phenomena occurring in the glass pipe and injector plate were desired, these components were mounted in front of a viewing window in the tunnel wall. A flag was affixed to the leak valve operator such that it swung into the viewing field of the camera when the valve was opened. The relative positions of the photographic and test apparatus are shown in Figure 4-7. Primary illumination was obtained by back-lighting, and front-lighting was achieved by taping aluminum-foil reflectors to the tunnel wall.

4.2.3 Instrumentation

All of the pertinent run data were recorded by a multichannel, recording oscillograph. Table 4-1 summarizes the pressure and temperature variables which were measured, indicates the type of sensing elements used, and gives the sensor locations in the test apparatus. In addition to these parameters, the change in weight of the propellant-tank charge was recorded by means of a variable-reluctance-type force transducer that was mounted on the balance. Run-time was obtained from timing marks imposed on the oscillograph trace.

The sensing thermcouples were connected to reference thermocouples

which were maintained at 150°C. Their signals were conditioned by bridge circuits which allowed pre-run balance and electrical calibration. Because of the corrosive nature of the propellant, thermocouples sheathed with stainless-steel were used throughout.

Pressures were measured by means of unbonded strain-gage pressure transducers. These were connected to conditioning circuits which provided the excitation voltage for the strain-gage bridge and allowed pre-run balancing and electrical calibration.

Propellant loss was measured by a specially constructed beam balance shown schematically in Figure 4-3. The beam is suspended from a carriage by a strip of stainless steel shim stock which serves as the beam fulcrum. The propellant tank was securely fastened to one end of the beam and was counterbalanced by a weight clamped to the opposite end.

The force transducer, electrically connected to a carrier-demodulator, was affixed to the balance carriage such that the transducer button touched the beam when the beam was in a horizontal position. When the tank was fully loaded, enough small counterweights were placed on the beam to position the transducer trace at maximum deflection. The size of these weights and their location on the beam were chosen such that when the trace approached zero deflection, due to propellant flow out of the tank, the removal of one of these weights would restore the trace to a nearly full-scale position.

The balance was calibrated by pouring measured quantities of water into the tank and recording the resulting galvanometer deflections. By repeating the process with various amounts of water initially in the tank, it was shown that the calibration did not change significantly with a change in liquid level. The result of this procedure was a constant calibration factor of the dimensional form: grams of weight change per inch of deflection. The magnitude of the factor was determined by the span adjustment in the demodulator circuit and the location of the load cell on the balance beam relative to the balance pivot point. Since the data obtained from the balance were in the form of propellant weight versus time, it was necessary to

differentiate these data to obtain flow rates. By dividing the change in weight by the time interval over which the change occurred, the average mass rate for the interval was obtained. Multiplication of the mass rates by the specific volume of the liquid at the upstream temperature yielded the average volumetric flow rate of the propellant entering the test valve. These rate-data were plotted against time at the mid-point of the intervals over which they were calculated. Since the accuracy of the resulting curve depends on the size of the time intervals, the data were reduced over very small increments in the regions where large changes in slope of the transducer trace were evident.

4.3 TEST PROCEDURE

Before evacuating the tunnel, the test valve (leak valve) was pre-set for a particular flow rate by adjusting the tightness of the body cap. Because of the construction of the valve and the cold-flow property of the teflon seal, this adjustment yielded a flow rate that was only approximately equal to the one desired.

During the tunnel evacuation, the propellant tank was charged by opening the fill line and venting the tank into the tunnel. Also, the remote cut-off and leak valve was opened which permitted the feed line to be evacuated between the injector plate and the hand valve located outside the tunnel. When evacuation of the tunnel was complete, the line was filled by closing the cut-off and opening the hand valve. Then the propellant tank was pressurized with nitrogen, and the force transducer trace was brought to full deflection by placing counterweights on the balance beam. At this point, the flow system was prepared for the leak test.

Two final pre-run operations were performed. The temperature and pressure instruments were balanced and electrically calibrated. The leak valve was opened and closed several times to obtain an opening torque requirement for comparison with a previously established value.

The leak test was initiated by opening the cut-off valve but with

Table 4-1

Pressure and Temperature Measurements

Variable	Sensor	Location of Sensor[a]
Tank pressure	Strain-gage pressure Transducer, 0 - 250 psig	Tank pressurizing line
Tank temperature	Iron-Constantan thermocouple	Bottom of propellant tank
Upstream pressure	Strain-gage pressure transducer, 0-250 psig	Upstream end of leak valve
Upstream temperature	Copper-Constantan thermocouple	Upstream end of leak valve
Downstream pressure	Strain-gage pressure transducer, 0-5 psia	Instrumentation ring located between leak valve and glass tube.
Downstream temperature	Copper-Constantan thermocouple	Instrumentation ring.
Injector temperature	Copper-Constantan thermocouple	Soldered into channel in injector plate
Operator pressure	Strain-gage pressure transducer, 0-75 psig	Opening pressure line to leak-valve operator.
Tunnel pressure	Alphatron Vacuum gage	Tunnel wall near door.

[a] See Figure 4-2 and Figure 4-3

the leak valve closed. The oscillograph chart drive was operated during the entire run, and motion pictures were taken of any freezing or unusual flow phenomena observed in the glass pipe and injector. Whenever the force-transducer trace approached zero, the balance was re-set by removing one of the small counterweights from the beam.

The run was terminated when (1) the leak rate became zero as indicated by the force-transducer trace and visual inspection of the glass pipe, (2) the phenomena observed in the glass pipe and injector were unchanging, or (3) the phenomena were cyclic. When one or more of these occurrences became evident, the leak valve was opened according to the procedure for measuring torque, discussed previously, and was kept open until full flow was achieved. After this the run was terminated by closing the cut-off valve.

The variables studied in these tests were :

1. Valve size: one-inch and two-inch;
2. Downstream line size: one-inch inside diameter;
3. Valve temperature: nominal 40°F, and ambient;
4. Upstream propellant temperature: nominal 40°F, and 135°F;
5. Injector port area: 0.530 sq. in. and 0.265 sq. in.

Data were taken over a wide range of flow rates for each variable or combination of variables. The range extended from a leak rate of about 0.009 cc/sec, which resulted in no accumulation of frozen Aerozine-50 in the valve, up to a rate sufficiently high that no freezing occurred upstream of the injector face.

4.4 RESULTS AND ANALYSIS

The results and conclusions drawn from visual observations, studies of motion pictures taken of each test, and analysis of the recorded data, approximate very closely the theoretical predictions discussed in Section 3.0. Aerozine-50, that leaked past the propellant valve, froze and accumulated between the propellant valve and injector plate during 34

tests. When freezing began in the glass tube, there usually was no sharp interface between solid and liquid, as contrasted with the characteristics observed with N_2O_4 in the Phase I tests, but, rather, a slush was formed which became entrained in the liquid. The differences among the freezing processes of a pure liquid, such as N_2O_4, and a mixture such as Aerozine-50 are explained in Section 3.0.

Different freezing modes were obtained which were somewhat similar to those experienced with N_2O_4 and described in detail in the Phase I Report. As was the case in Phase I, leak-rate was the key variable that defined the various freezing modes, for a fixed injector geometry. The primary differences between the N_2O_4 and Aerozine-50 freezing modes were the manner in which freezing occurred and the rate of boiling just prior to freezing. Boiling of N_2O_4 was more violent than that of Aerozine-50 and resulted in more severe sloshing in the glass tube. This was expected because of the much higher vapor pressure of the N_2O_4. Vapor pressure of N_2O_4 at the freezing temperature is about 2.7 psia compared to less than 0.5 psia for Aerozine-50.

The maximum leak-rate was determined to be approximately 7.5 cc/sec per sq. in. of injector port area. The maximum leak-rate is defined as the value above which accumulation of frozen propellant cannot occur in the flow passages upstream from the injector ports. The minimum leak-rate was determined to be approximately 0.01 cc/sec. The minimum leak-rate is defined as the value below which the rate of sublimation is equal to or greater than the leak-rate, and no frozen propellant accumulates.

Four different types of liquid freezing modes were experienced during the Aerozine-50 tests. For the first mode of freezing which occurs at the higher leak rates, Aerozine-50 accumulated on the downstream face of the injector plate as formations of branched tubes of frozen propellant (hydrazine). The growth of the tubes occurred by the freezing of liquid propellant around the edge of the open end. Occasionally part of the wall of a tube would break away and a new tube would grow at this point, forming a branch. The tubes grew to about six inches in length and 0.5-inch in

diameter at the ends, depending upon the leak rate. Eventually after it became sufficiently heavy, the formation would separate from the injector plate and a new formation began to grow. The formations had sufficient structural integrity to withstand the shock of falling from the injector to the tunnel floor, a distance of about three feet, without breaking apart. Sublimation of the formations of frozen Aerozine-50 (hydrazine), lying on the tunnel floor, was very slow. The formations usually had not completely sublimed or melted by the end of a test, (about 60 minutes) even though the tunnel floor temperature was about 75°F.

Sublimation of the frozen Aerozine-50 (hydrazine), attached to the downstream face of the injector plate, caused the injector plate temperature to decrease to values ranging from approximately 5 to 20°F depending on the test conditions. The injector plate then cooled the Aerozine-50 mixture in the glass tube and caused frozen hydrazine to accumulate on the upstream side of the injector plate. This resulted in a substantial plug formation.

The second freezing mode occurred during tests for which the leak-rates averaged about 5.6 cc/sec per sq.in. of the injector port area. During these tests much of the freezing occurred upstream of the glass tube and chunks of slush, similar to a wet snowball, passed through the glass tube and accumulated on the upstream side of the injector plate. When the leak-valve was opened the pressure of the propellant (165 psia) compressed the slush tightly against the injector and created a stoppage.

The third freezing mode which occurred for just slightly greater than the minimum leak-rate, was the accumulation of frozen propellant (hydrazine) in the vicinity of the leak valve and upstream of the glass tube. At the end of the run, when the leak valve was opened, particles of frozen propellant were observed to be entrained in the liquid deluge which filled the glass tube. This freezing mode produced some significant flow stoppages.

The fourth freezing mode occurred at a leak-rate below which

no significant amount of frozen material accumulated. The apparent absence of solid particles in the liquid deluge obtained when the leak valve was opened was used to distinguish this from the third freezing mode. An analysis of the 16 mm color motion pictures and the oscillograph records showed that the transition from the third to the fourth mode occurs at a leak rate of approximately 0.01 cc/sec. This is the minimum leak-rate value and is strongly dependent on the thermal environment of the flow system but is essentially independent of the injector port area (see Section 3.0 for explanation).

Each test was terminated by opening the leak-valve and measuring the delay, if any, in obtaining propellant flow. The measurement of flow-delay was determined from the elapsed time between the instant the leak valve was opened and the instant at which the downstream thermocouple indicated a temperature increase. Substantially more and longer flow delays were experienced during the tests conducted with propellant at an initial temperature of about 40°F than with propellant at an initial temperature of approximately 135°F. With the cooler propellant 46 per cent of the tests resulted in flow delays ranging from 150 milsec to 75.5 minutes, while with the heated propellant 19 per cent of the tests resulted in flow delays ranging from 1.6 minutes to 2.8 minutes. (These percentages are based on tests having a leak-rate that resulted in the accumulation of frozen propellant in the injector manifold and for which no invalidating experimental difficulties were encountered.) For all the freezing modes, the strength of any plug formed varies cyclically, and therefore the length of the flow-delay experienced depended on the point in the cycle when flow was attempted, relative to the time at which the plug formed. A plug of evaporatively frozen liquid clogging the flow system is dissipated by sublimation at its downstream end and is melted by the warm liquid at its upstream end, after the leak valve is opened. This process weakens the plug and the pressure of trapped propellant breaks it free. This mechanism causes the cyclical variation in plug strength during leakage and the ultimate destruction of the plug after the valve is opened and flow is attempted. This same mechanism also explains the inverse dependency of

length of flow delay on initial propellant temperature.

The effect of initial propellant temperature upon these freezing modes could not be determined from the test results. Although tests were performed with the propellant upstream of the leak valve at two different temperatures, 40°F and 135°F, the leak valve itself was always cooled to 40°F. (This was done in an attempt to simulate a realistic thermal environment of the SPS engine of the Apollo vehicle). It is believed that the rate of cooling also was sufficient to cool significantly the slow trickle of propellant, which occurs during leakage. Thus the effective initial propellant temperature for all tests was approximately 40°F. When the leak valve was opened, however, the cooling was much less significant because of the large thermal convection currents which permitted warming of the entire flow system by the hot propellant upstream, if the flow was blocked by a plug, or because of the large flow rates of liquid if the flow was not blocked.

The data from selected tests for leak-rate, temperature and pressure downstream from the leak valve, and injector and valve temperatures, which were obtained from the oscillograph records, are shown graphically as a function of time in Appendix A.

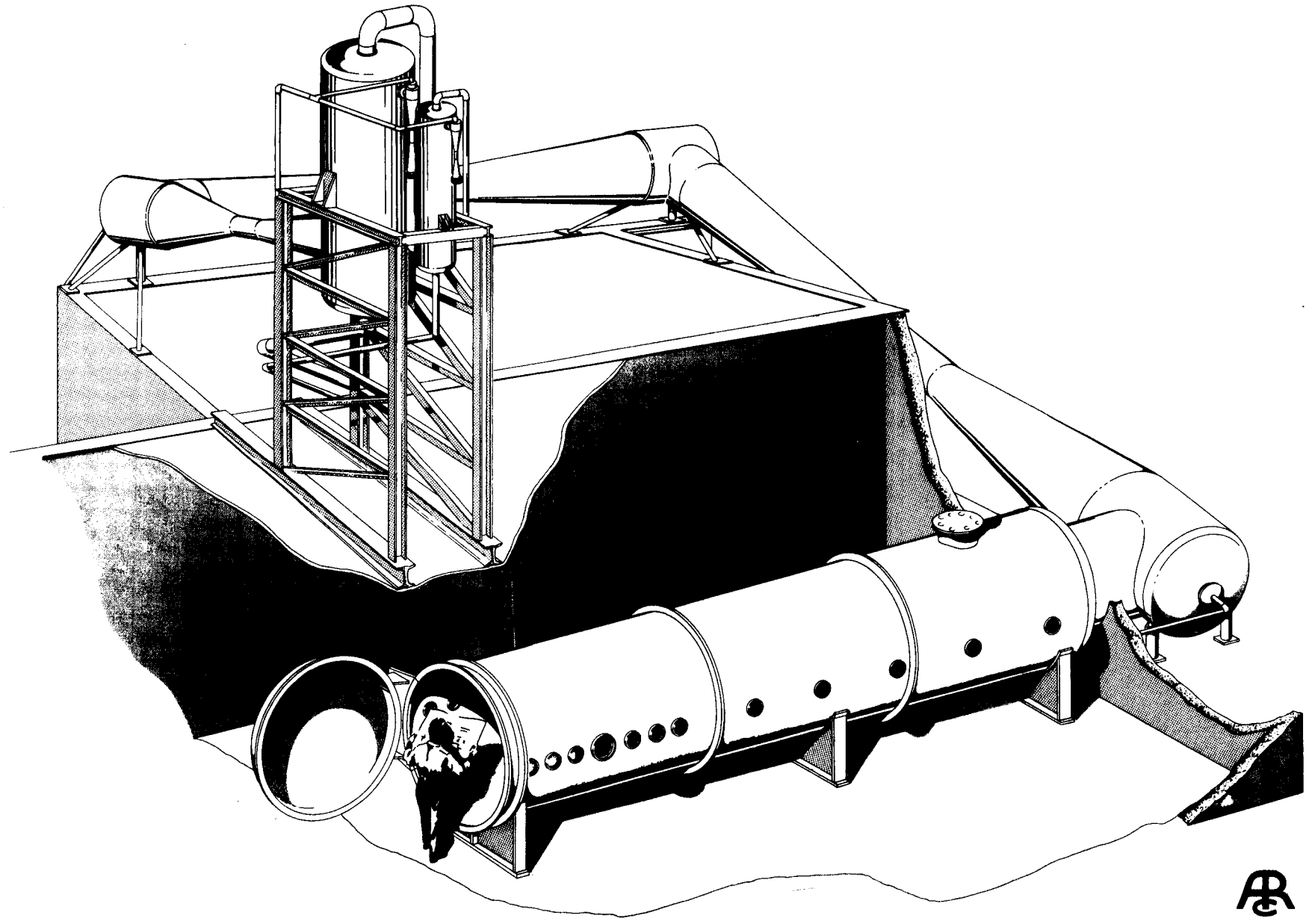

Figure 4.1. High Altitude Research Tunnel.

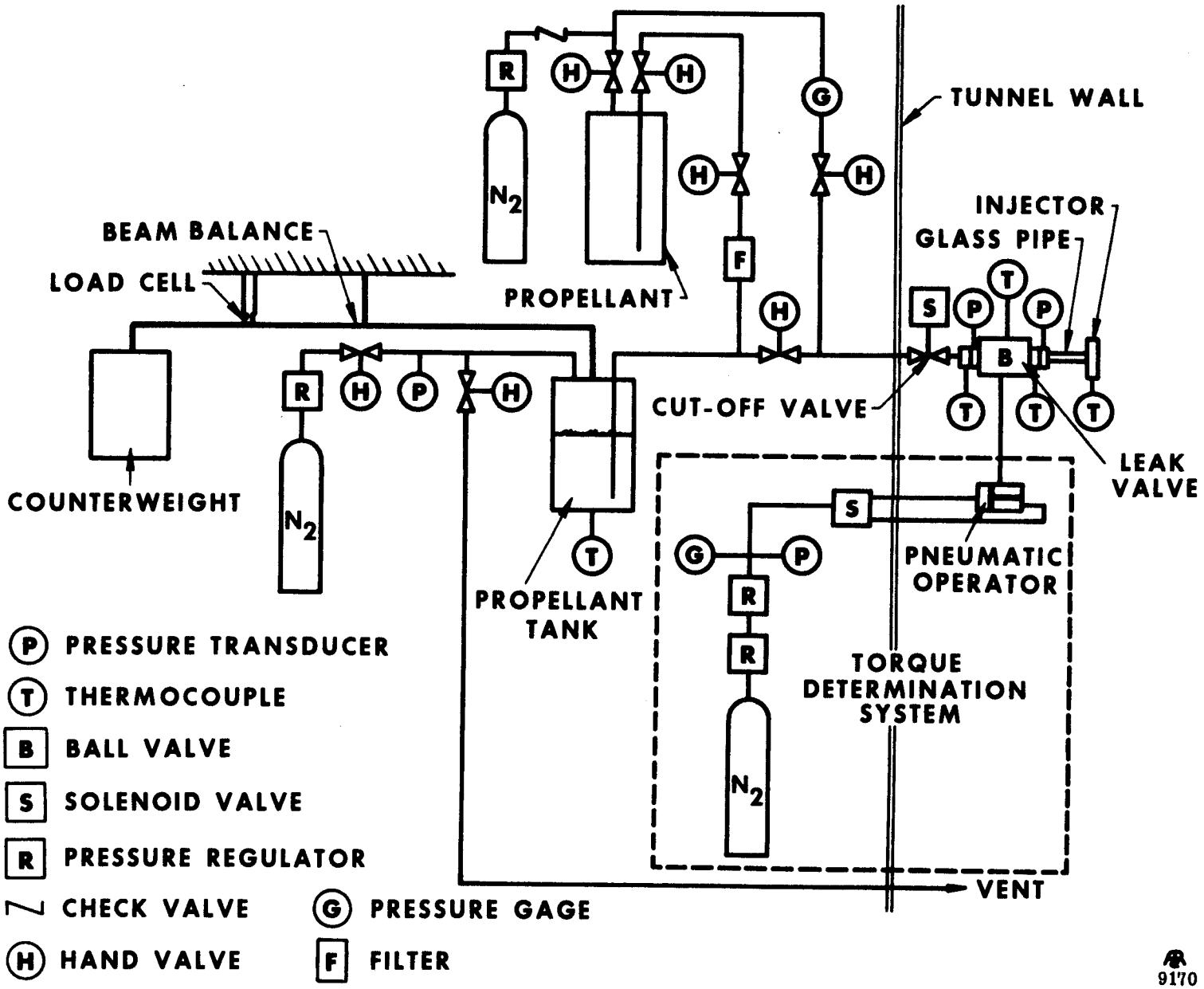

Figure 4-2. Schematic Diagram of Propellant Flow System for Leak Tests.

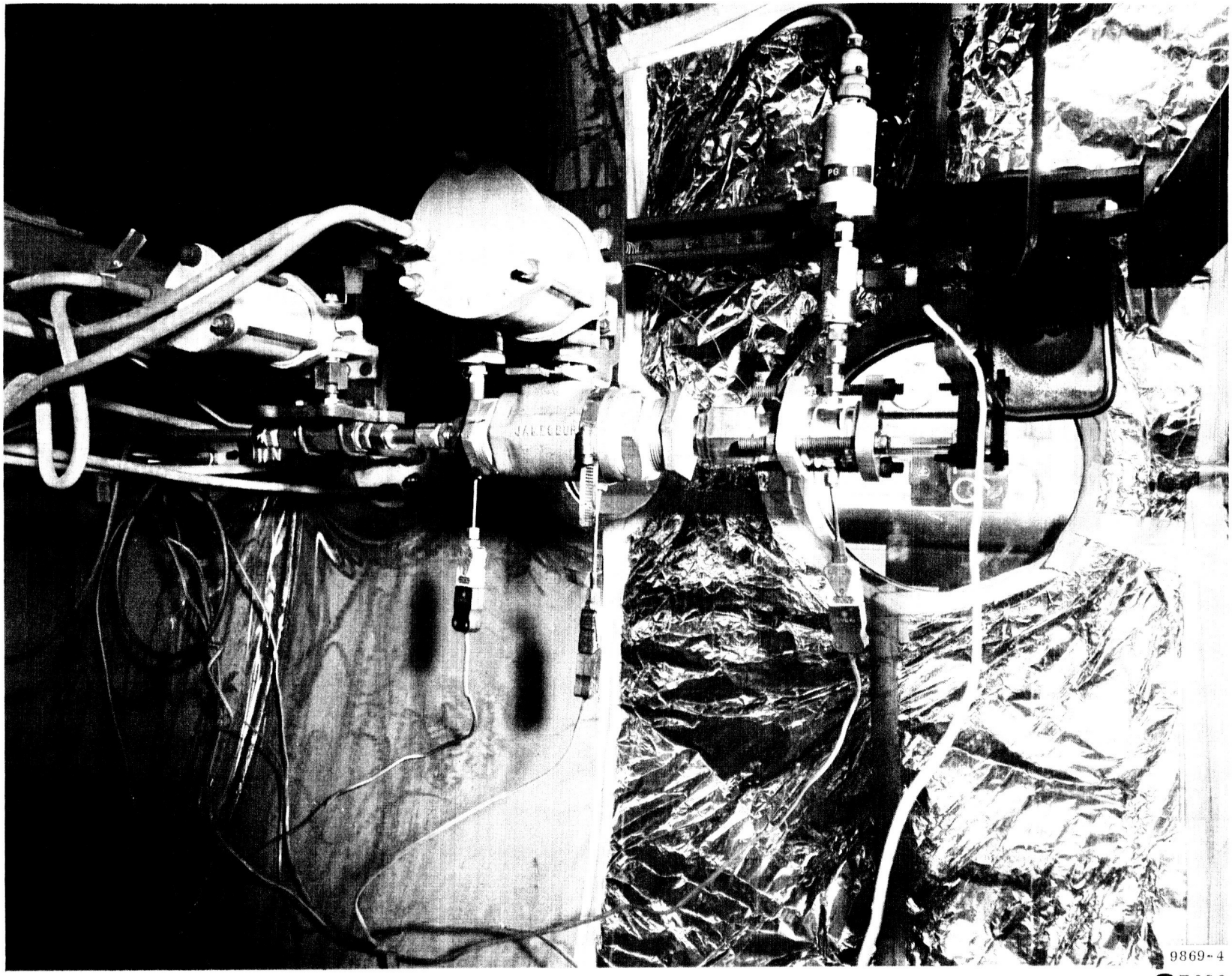

Figure 4.3. Two-Inch Leak Valve Located Inside of Vacuum Tunnel.

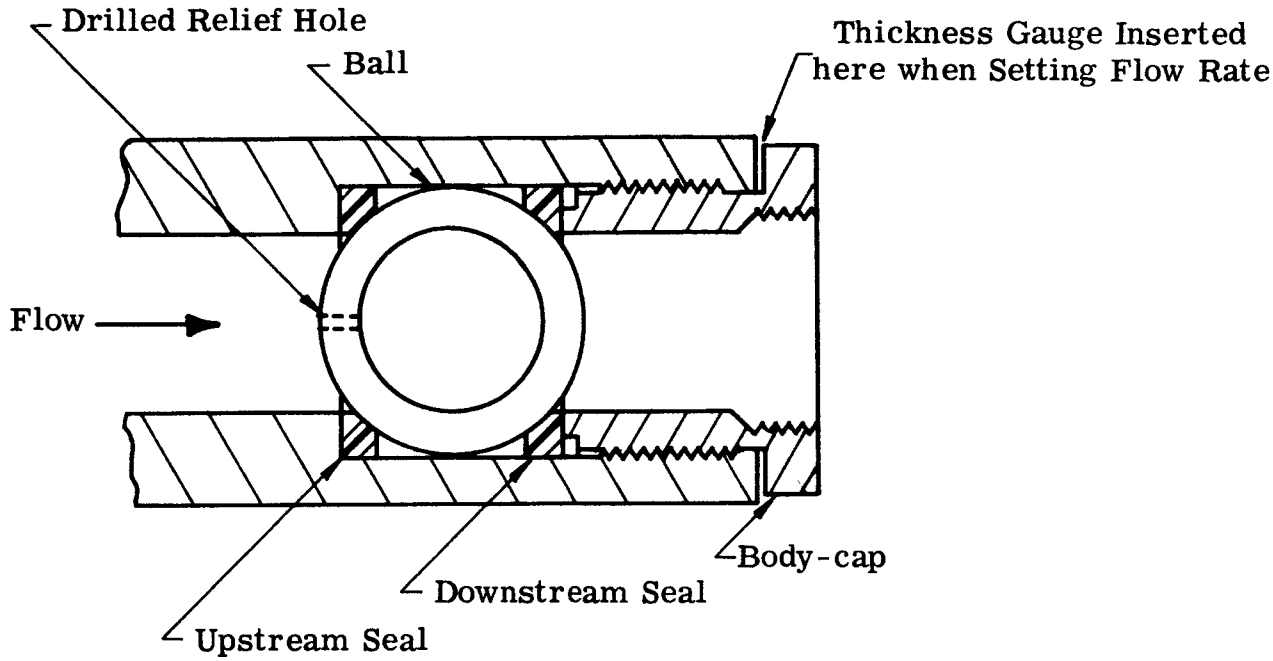

Figure 4-4. Schematic Cross Section of Test Valve.

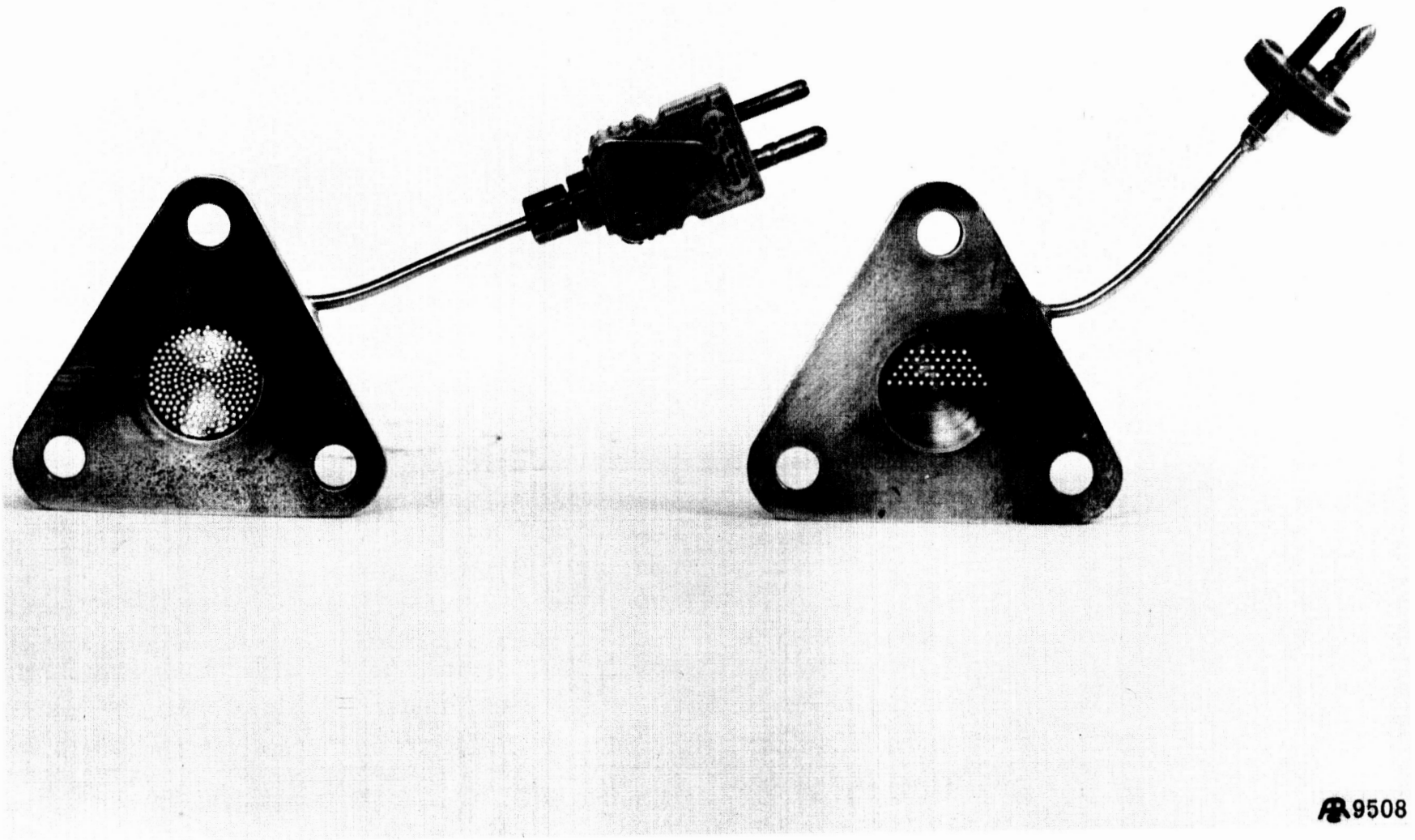

Figure 4-5. Injector Plate Configuration Used for Phase II Tests.

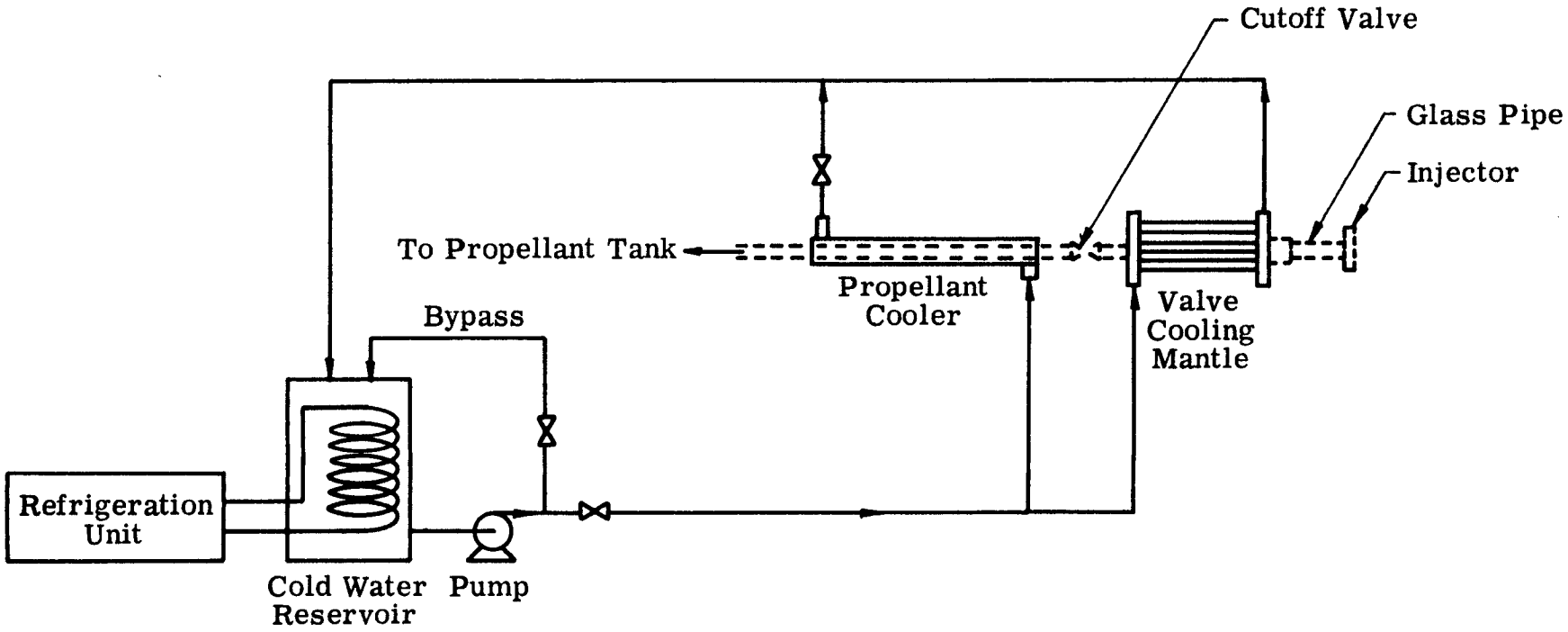

Figure 4-6. Coolant Flow Sheet.

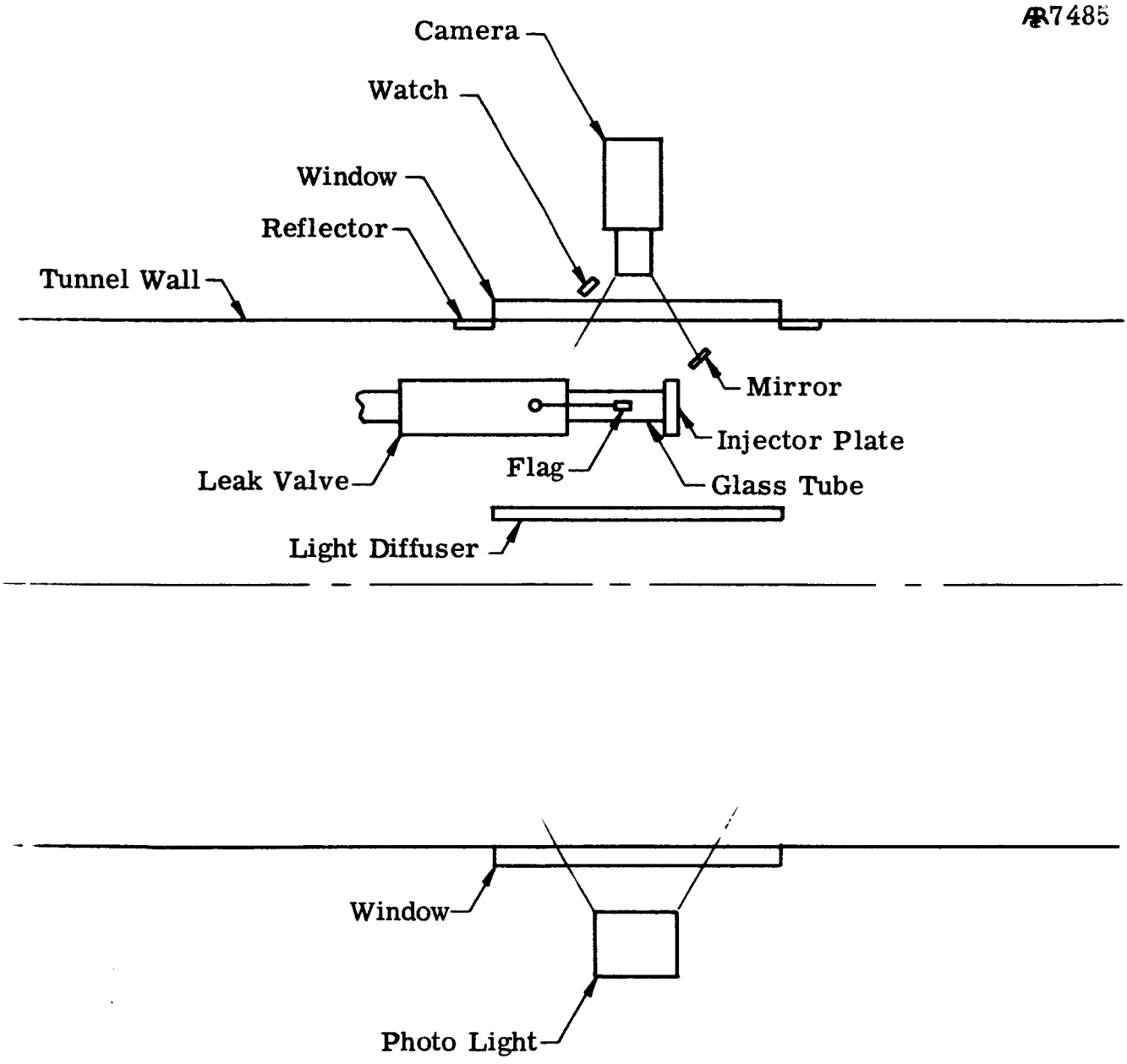

Figure 4-7. Photographic Setup.

5.0 PROGRAM STATUS

5.1 PROGRAM SCHEDULE AND MANPOWER EXPENDITURE

The program schedule, showing accomplishments up to the time of completion of the Phase II tests is shown in Figure 5-1. The test program continued directly into Phase III after the Phase II tests were completed.

Approximately 8,945 man-hours were expended to complete the work scheduled through Phase II. This expenditure represents about 79 per cent of the total program.

5.2 FUTURE WORK

The apparatus for conducting the Phase III tests has been completed and Phase III tests are underway. The purpose of these tests is to determine effects of propellant freezing on hypergolic ignition. Investigations of remedial techniques will also be made.

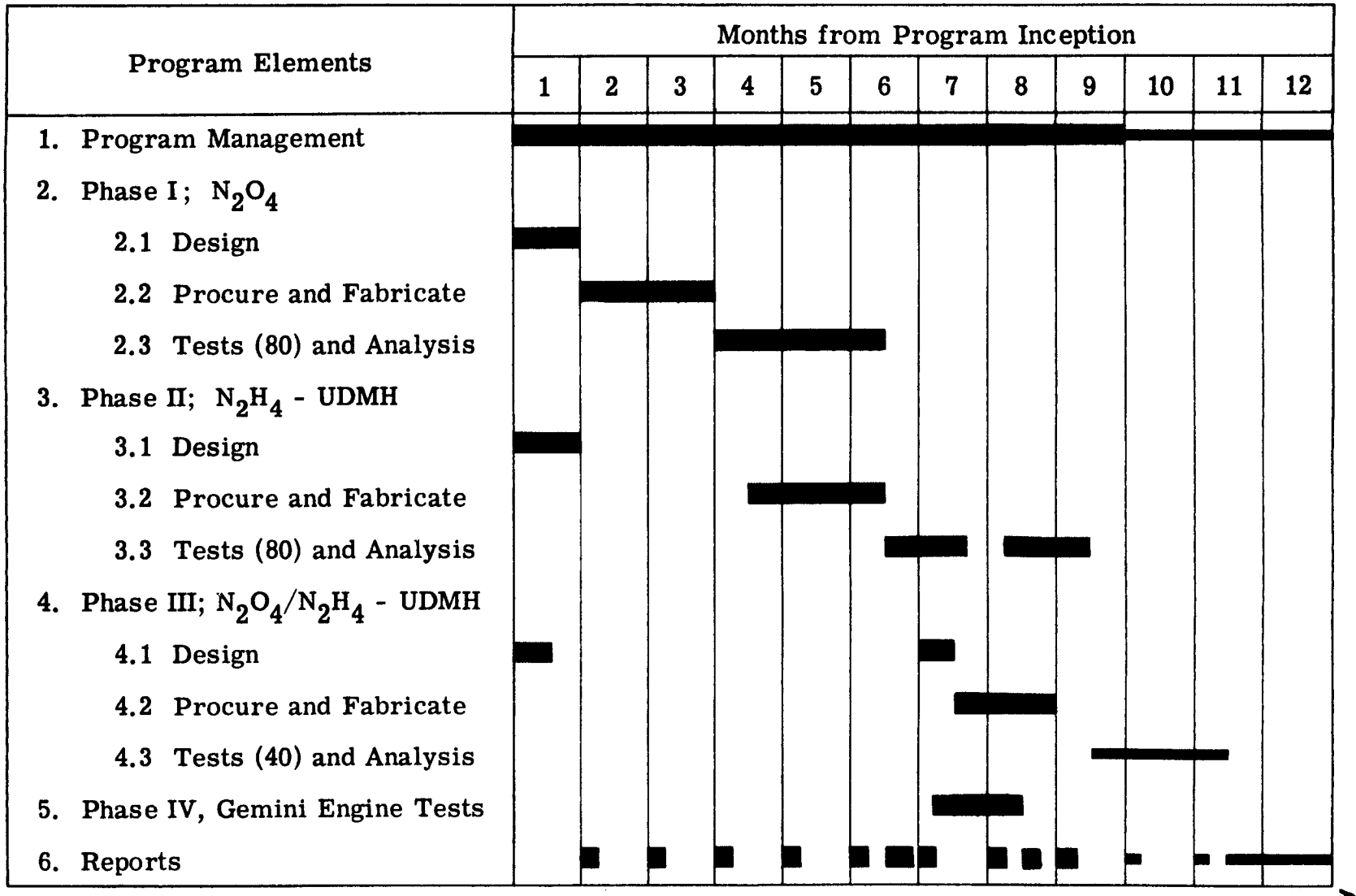

AR 8091

Figure 5-1. Program Schedule.

LITERATURE CITATIONS

1. Atlantic Research Corporation, "Study of Propellant Valve Leakage in a Vacuum", Phase I Report, June 7, 1965 to November 24, 1965, Contract No. NAS 9-4494.

2. Atlantic Research Corporation, "Study of Propellant Valve Leakage in a Vacuum", Phase IV Report, December 10, 1965 to January 14, 1966, Contract No. NAS 9-4494.

3. Bell Aerosystems Company, "Titan II Storable Propellant Handbook", AFFTC TR-61-32, Contract No. AF 04(611)-6079, June 1961.

APPENDIX A

TEST DATA

This appendix contains the pertinent run data obtained during the 81 tests conducted in Phase II. Because of the many fluctuations of the various parameters that were recorded versus time, it is necessary to present the data graphically to show the interdependence of some of the variables. The runs of major interest are those during which propellant freezing was achieved and during which no experimental difficulties were experienced. Accordingly, graphs for 53 tests are presented. Data for the other 28 tests have been analyzed but have not been plotted for one of the following reasons: (1) leak rate too slow, (2) leak rate too fast or (3) experimental difficulties.

Five of the variables recorded were plotted versus time for the runs during which these variables were measured.

1. Leak-rate, cc/sec
2. Downstream pressure, psia
3. Downstream temperature, ^{o}F
4. Injector temperature, ^{o}F
5. Leak valve surface temperature, ^{o}F.

Other measured quantities which were recorded but were not plotted are

1. Tank pressure, psia
2. Upstream pressure, psia
3. Upstream temperature, ^{o}F
4. Tunnel pressure.

The test configurations used for the 81 runs involved four variables: leak-valve size, injector port area, liquid temperature, and leak-valve temperature. The schedule of tests, in terms of combinations of these variables, is shown in Table A-1. These variables are discussed in detail in Section 4.2.2.

TABLE A-1

SCHEDULE OF TESTS

Run No.	Leak-Valve Size	No. of 0.04" I.D. Injector Ports	Liquid Temp.	Leak-Valve Temp.
1-14	2"	40	ambient	ambient
15-54	1"	212	cooled	cooled
55-81	1"	212	heated	cooled

Notes: ambient temperature ranged from 65 - 80°F
cooled temperatures were approximately 40°F
heated temperatures were approximately 135°F

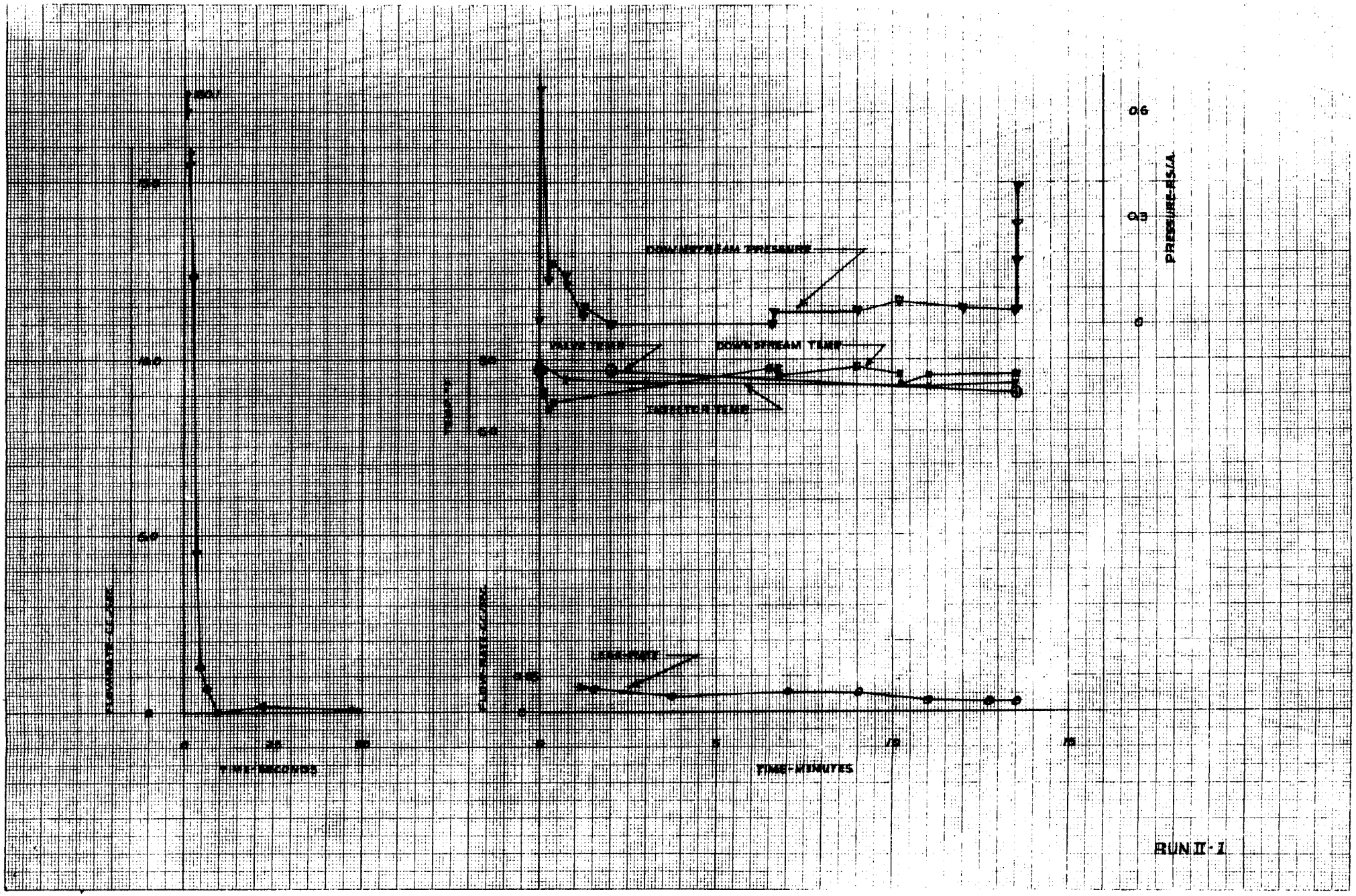
DOWNSTREAM PRESSURE
VALVE TEMP
DOWNSTREAM TEMP
INJECTOR TEMP
LOAD-KIPS
PRESSURE-PSIA
TEMP-DEGREES
TIME-SECONDS
TIME-MINUTES
RUN II-1

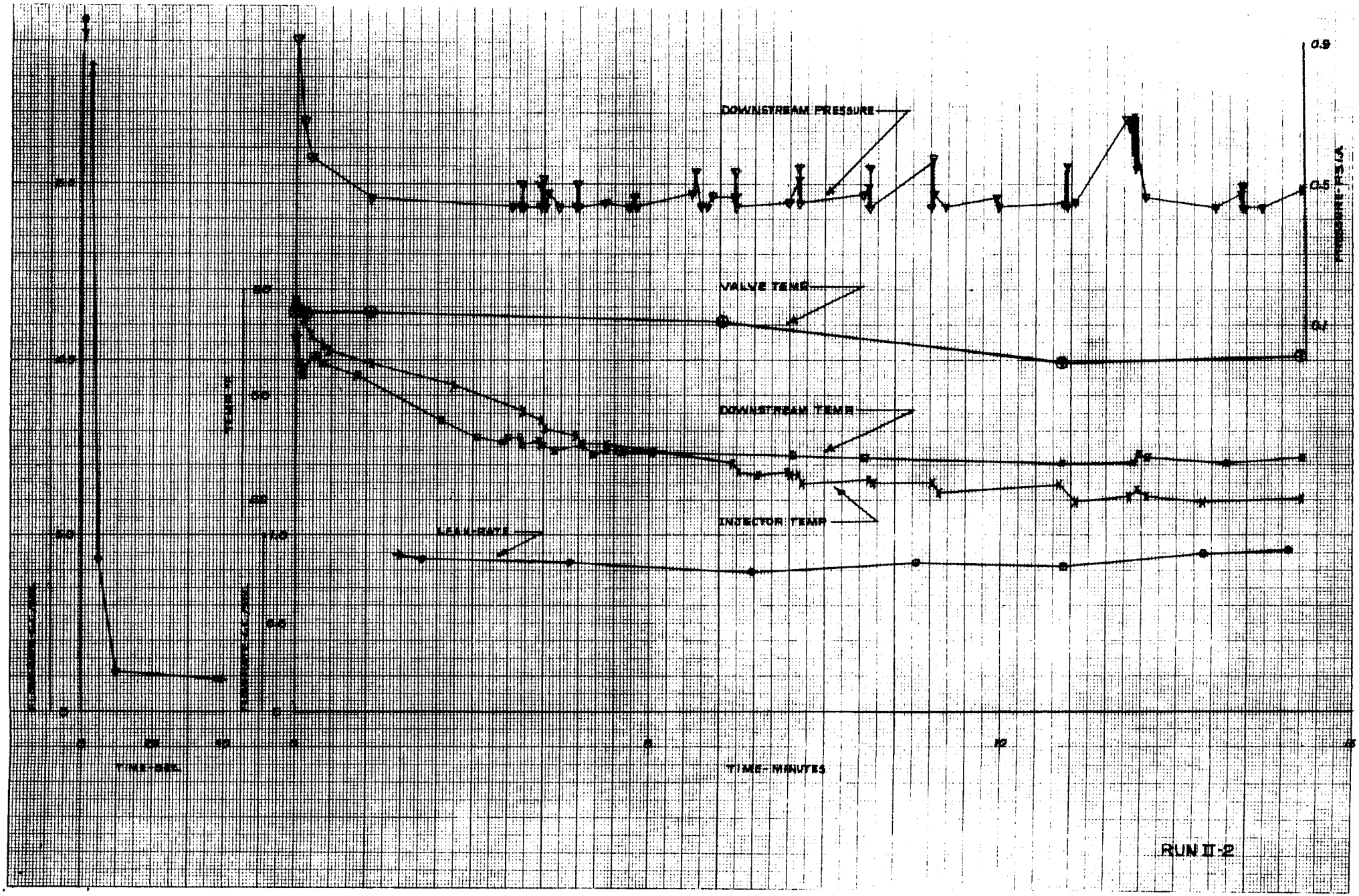
DOWNSTREAM PRESSURE
VALVE TEMP
DOWNSTREAM TEMP
INJECTOR TEMP
LEAK-RATE
PRESSURE - P.S.I.A.
TEMP °F
TIME - SEC.
TIME - MINUTES
RUN II-2

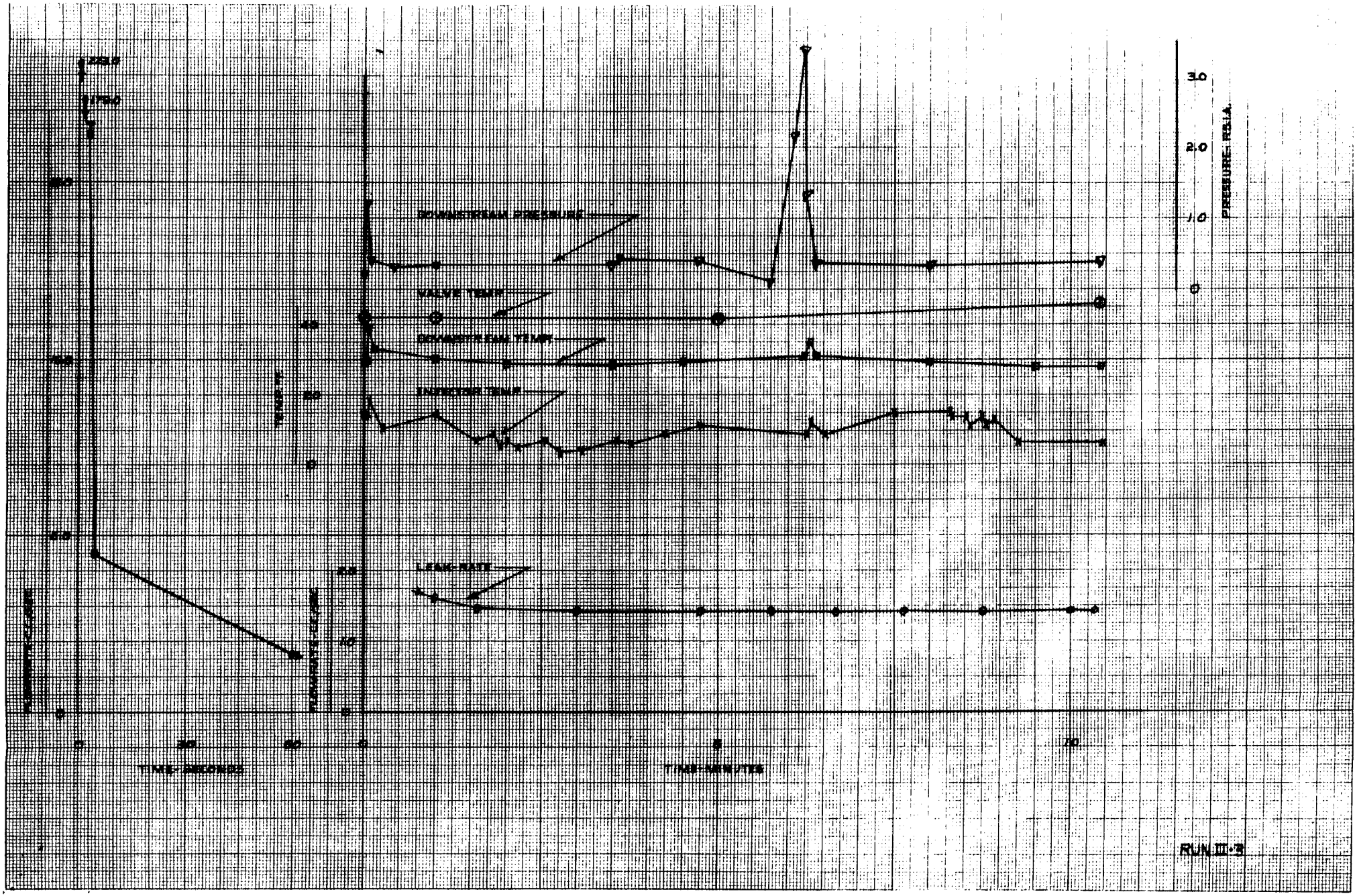
DOWNSTREAM PRESSURE
VALVE TEMP
DOWNSTREAM TEMP
INJECTOR TEMP
LEAK-RATE
PRESSURE - P.S.I.A.
TIME - SECONDS
TIME - MINUTES
RUN III-3

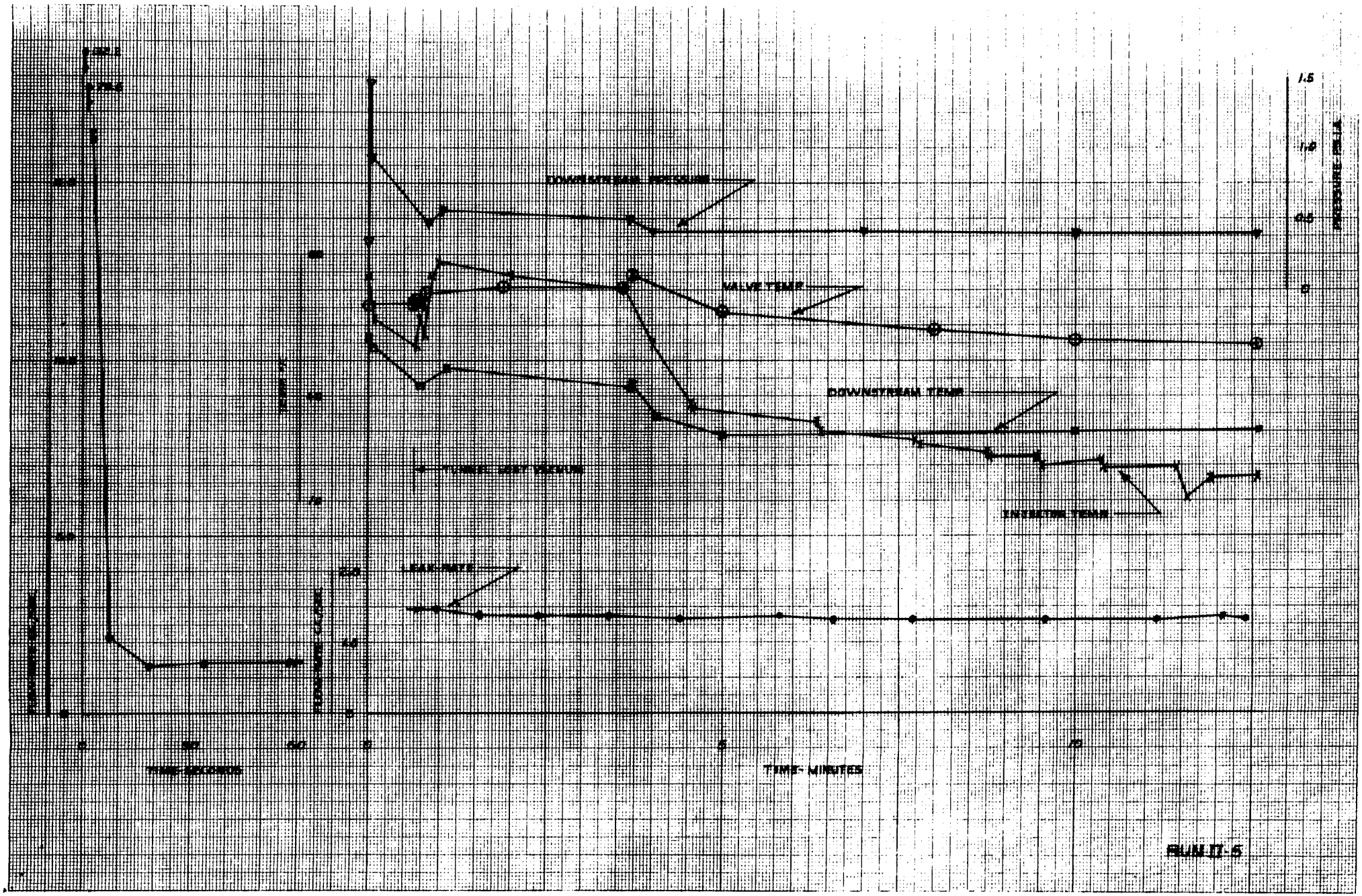
DOWNSTREAM PRESSURE
VALVE TEMP
DOWNSTREAM TEMP
INJECTOR TEMP
LEAK RATE
TIME-SECONDS
TIME- MINUTES
PRESSURE-PSIA
RUN II-5

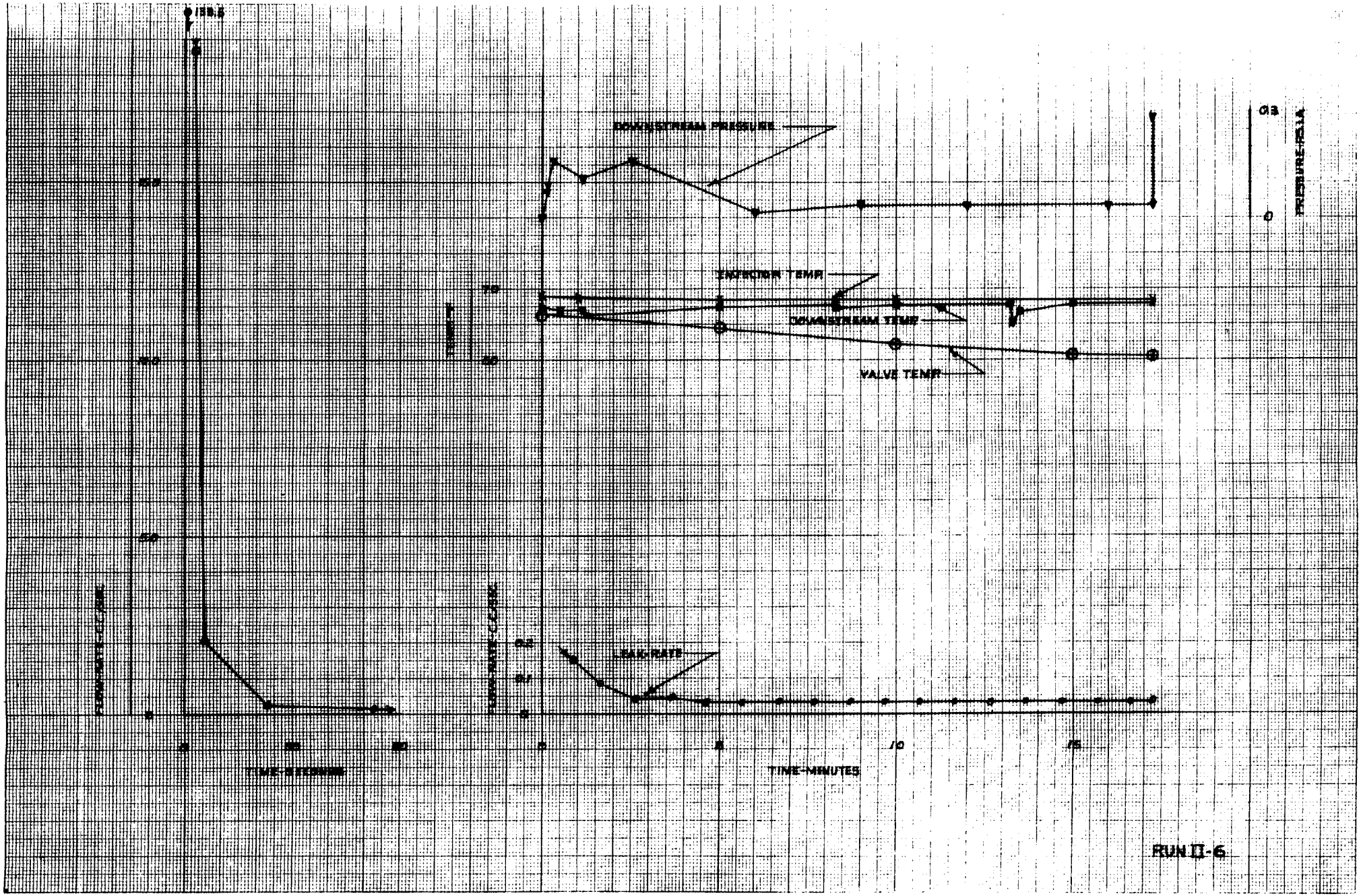
DOWNSTREAM PRESSURE
INTERIOR TEMP
DOWNSTREAM TEMP
VALVE TEMP
LEAK RATE
TIME-MINUTES
TIME-MINUTES
RUN II-6

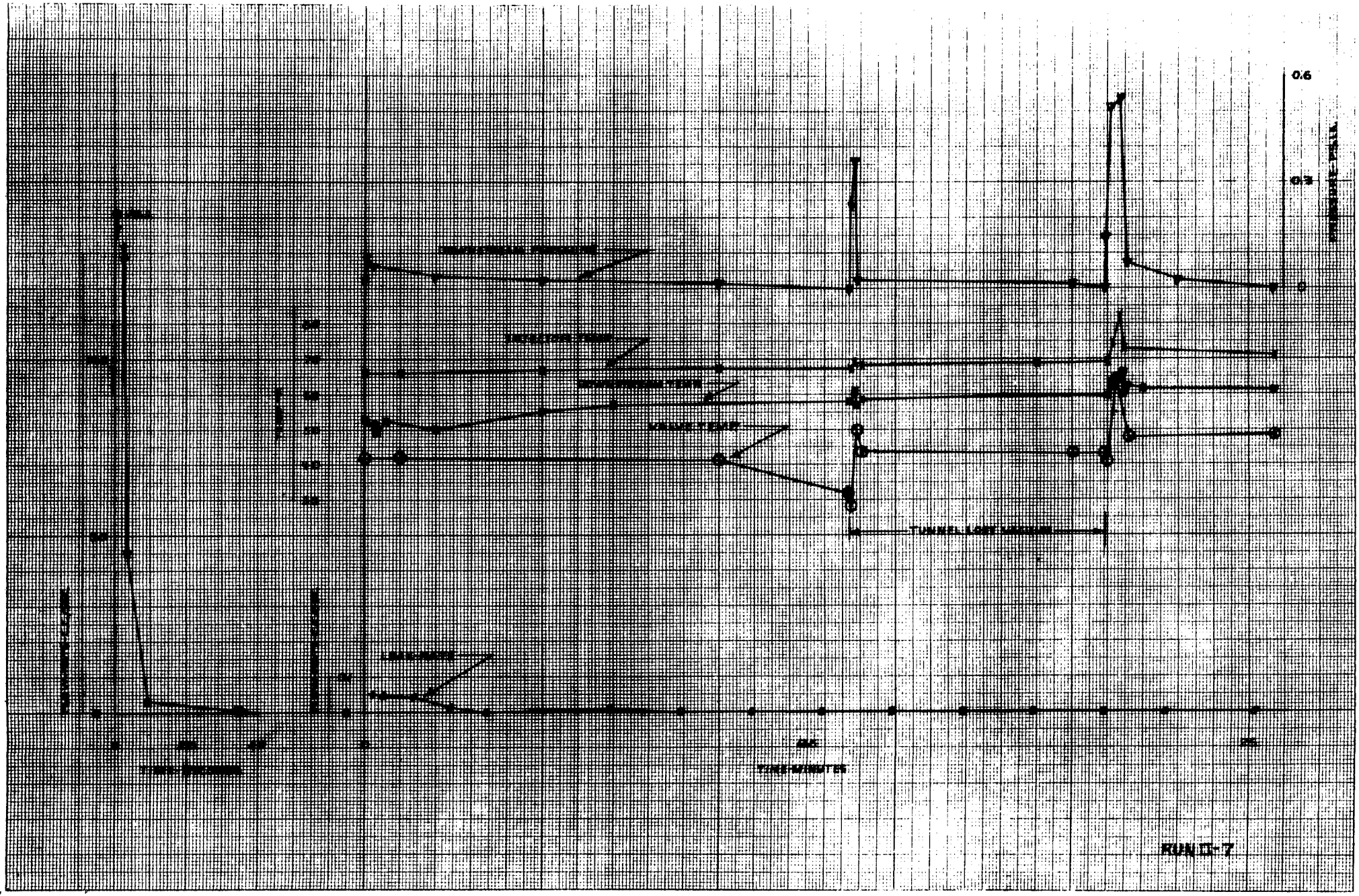
0.6
0.3
0
TIME-MINUTES
RUN C-7

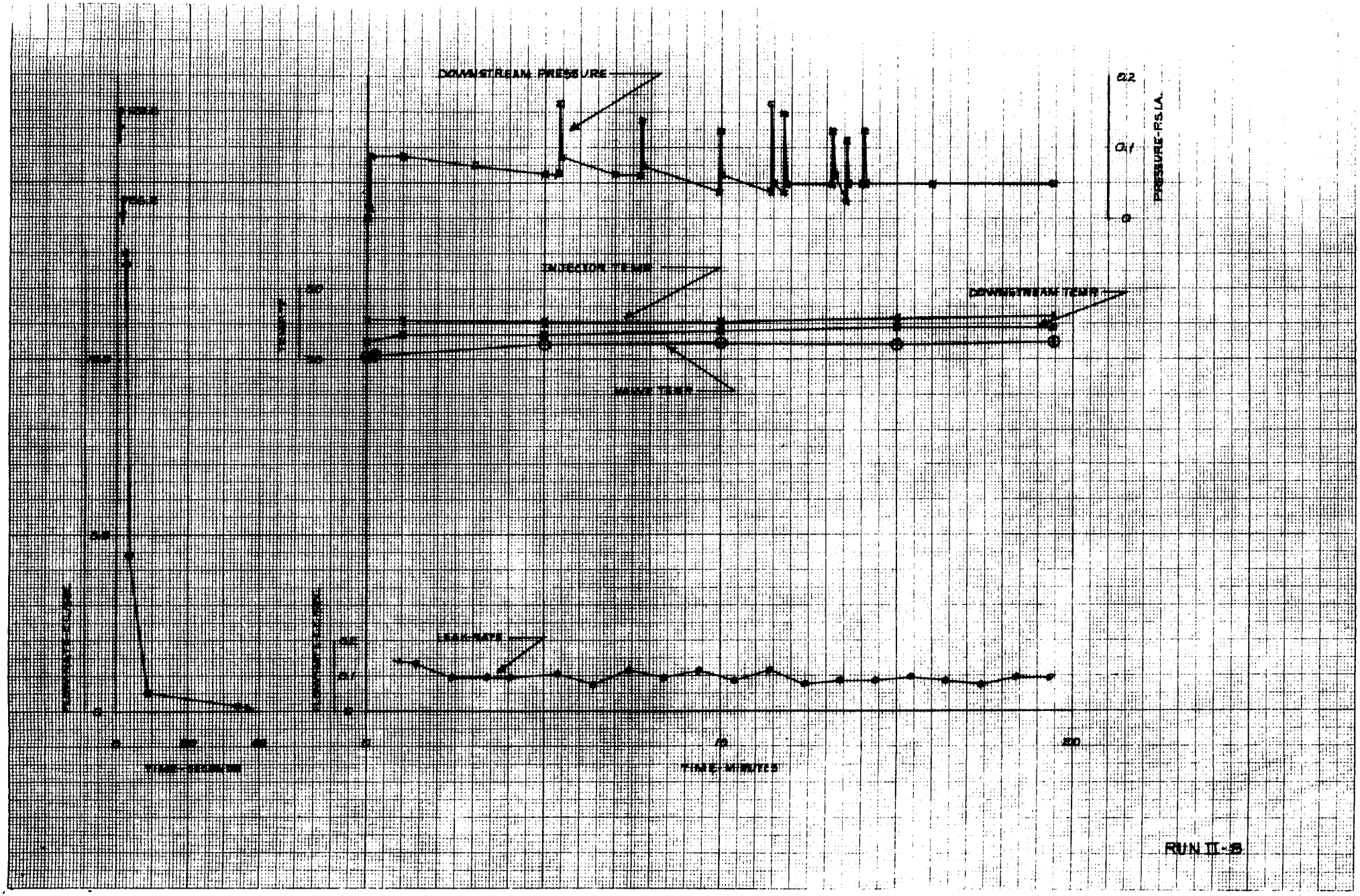
DOWNSTREAM PRESSURE
INJECTION TEMP
DOWNSTREAM TEMP
VALVE TEMP
LEAK-RATE
PRESSURE-P.S.I.A.
0.2
0.1
0
TIME-MINUTES
RUN II-B

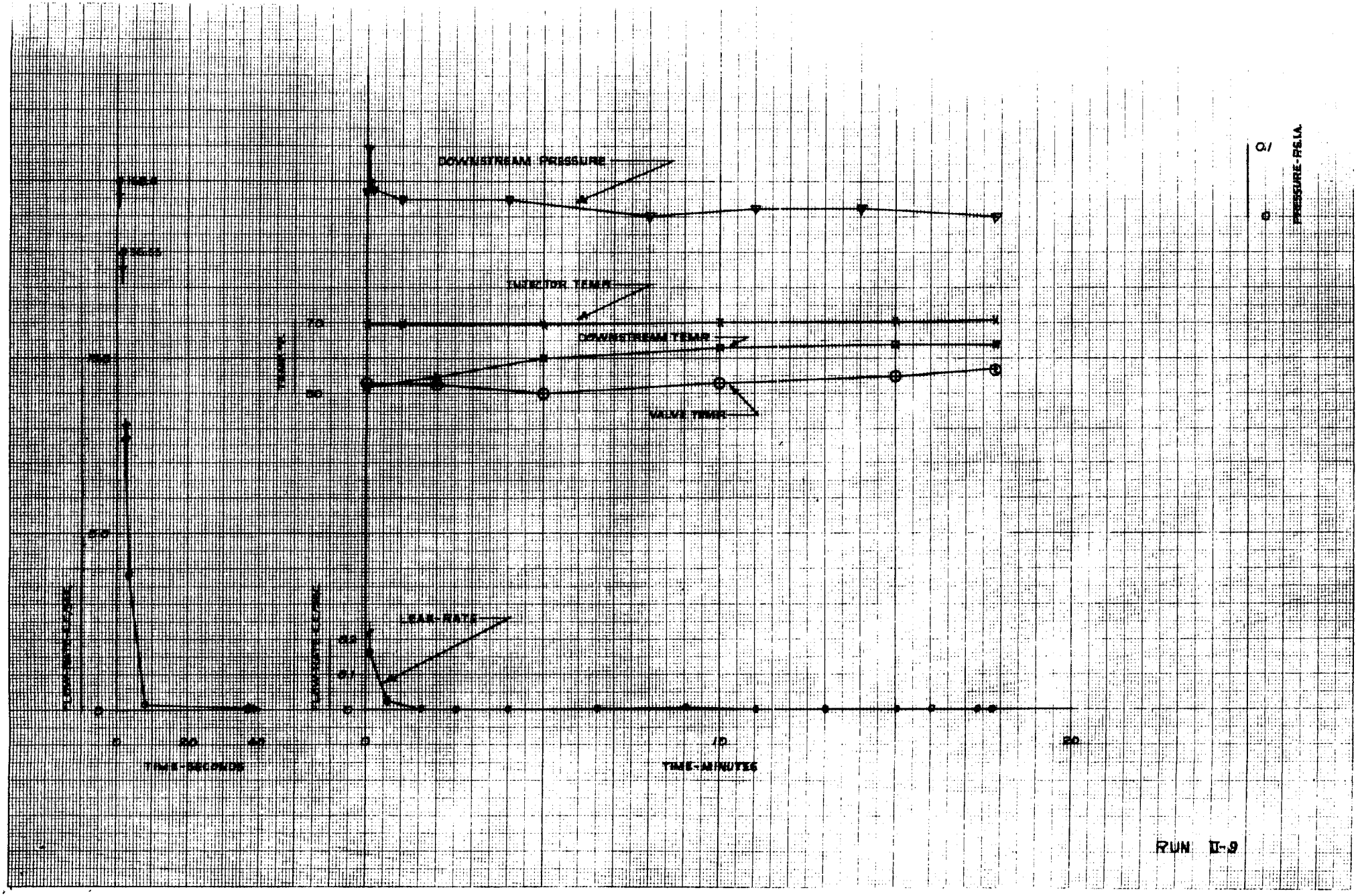
DOWNSTREAM PRESSURE
INJECTOR TEMP.
DOWNSTREAM TEMP.
VALVE TEMP.
LEAK-RATE
PRESSURE-P.S.I.A.
TEMPERATURE-°F
LEAK-RATE-CC/SEC
TIME-SECONDS
TIME-MINUTES
RUN D-9

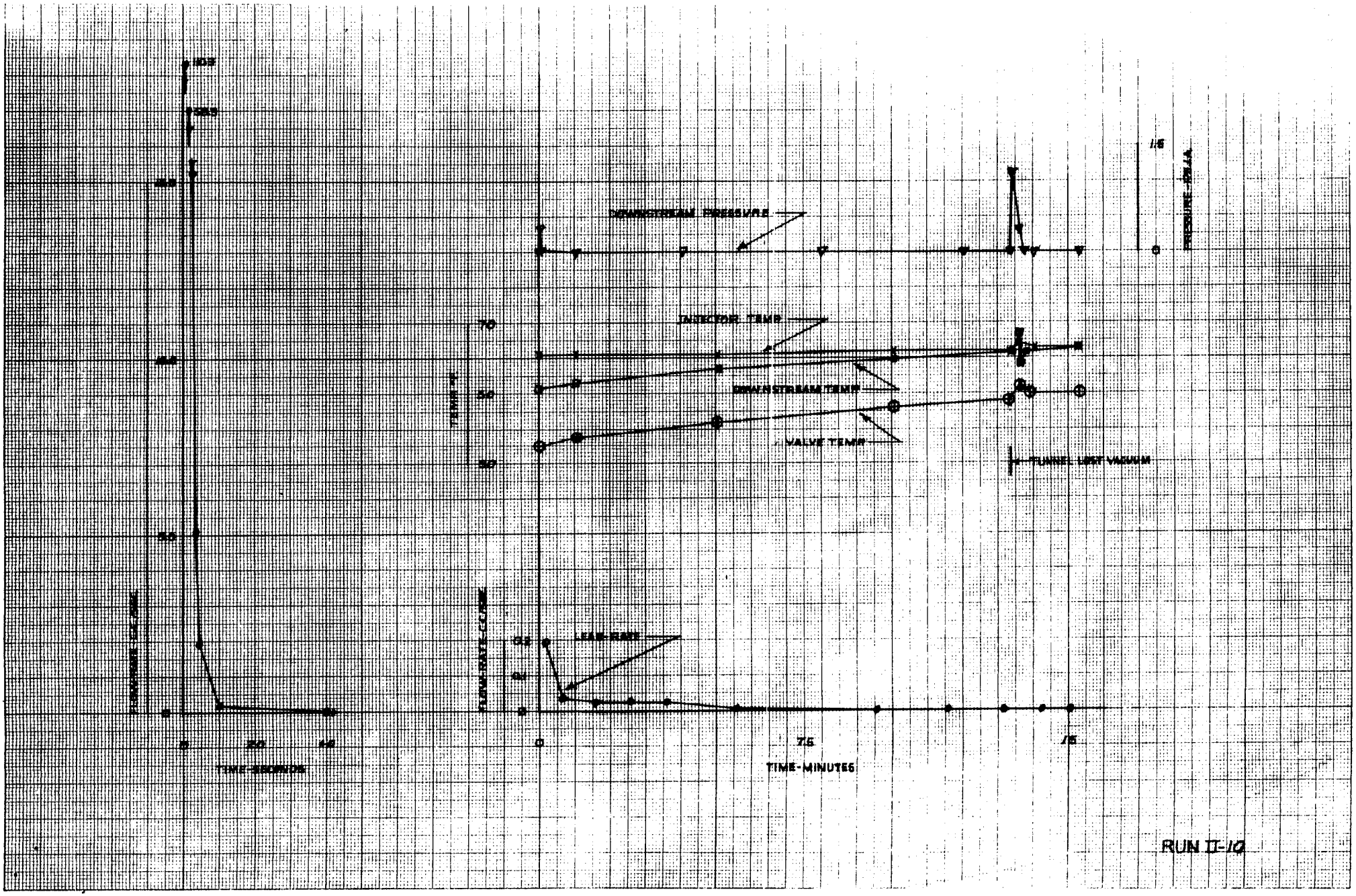
DOWNSTREAM PRESSURE
INJECTOR TEMP
DOWNSTREAM TEMP
VALVE TEMP
TUNNEL LOST VACUUM
PRESSURE - PSIA
TEMP °F
FLOW RATE - SCFM
LEAK RATE
TIME - SECONDS
TIME - MINUTES
RUN II-10

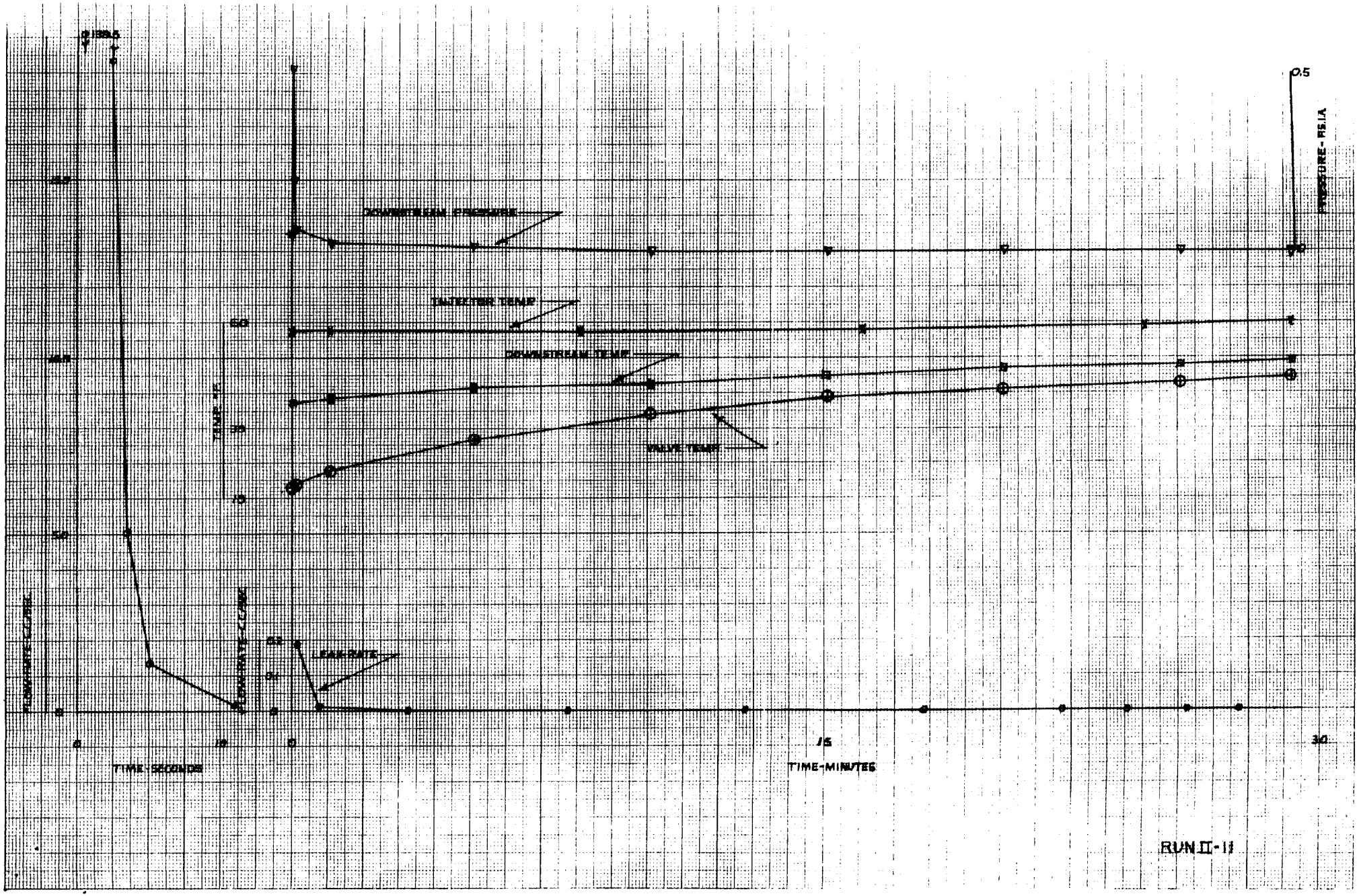
DOWNSTREAM PRESSURE
INJECTOR TEMP
DOWNSTREAM TEMP
VALVE TEMP
LEAK RATE
TEMP °C
PRESSURE - MM Hg
PRESSURE - PSI A
LEAK RATE - CC/SEC
TIME - SECONDS
TIME - MINUTES
RUN II - 11

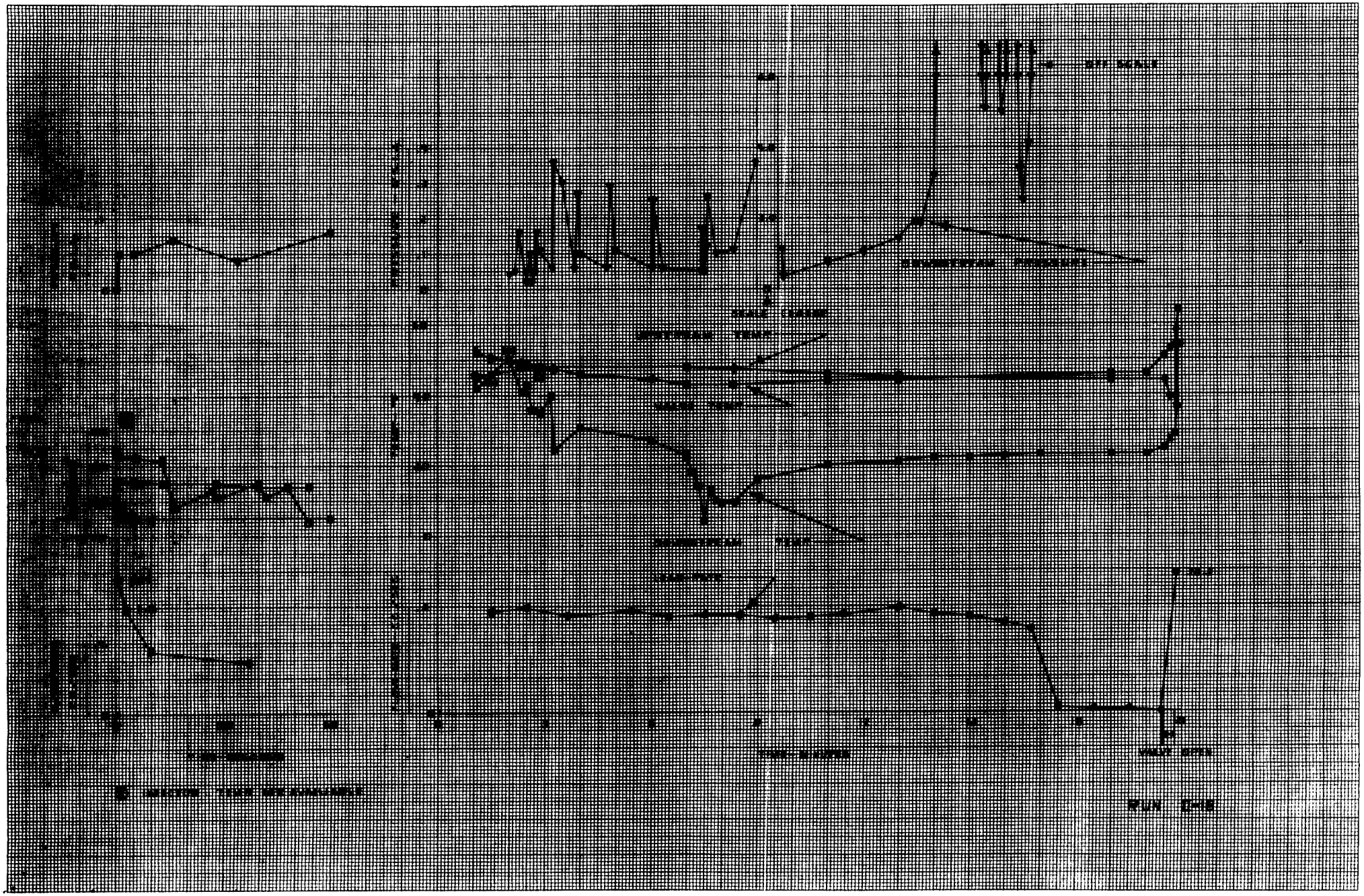

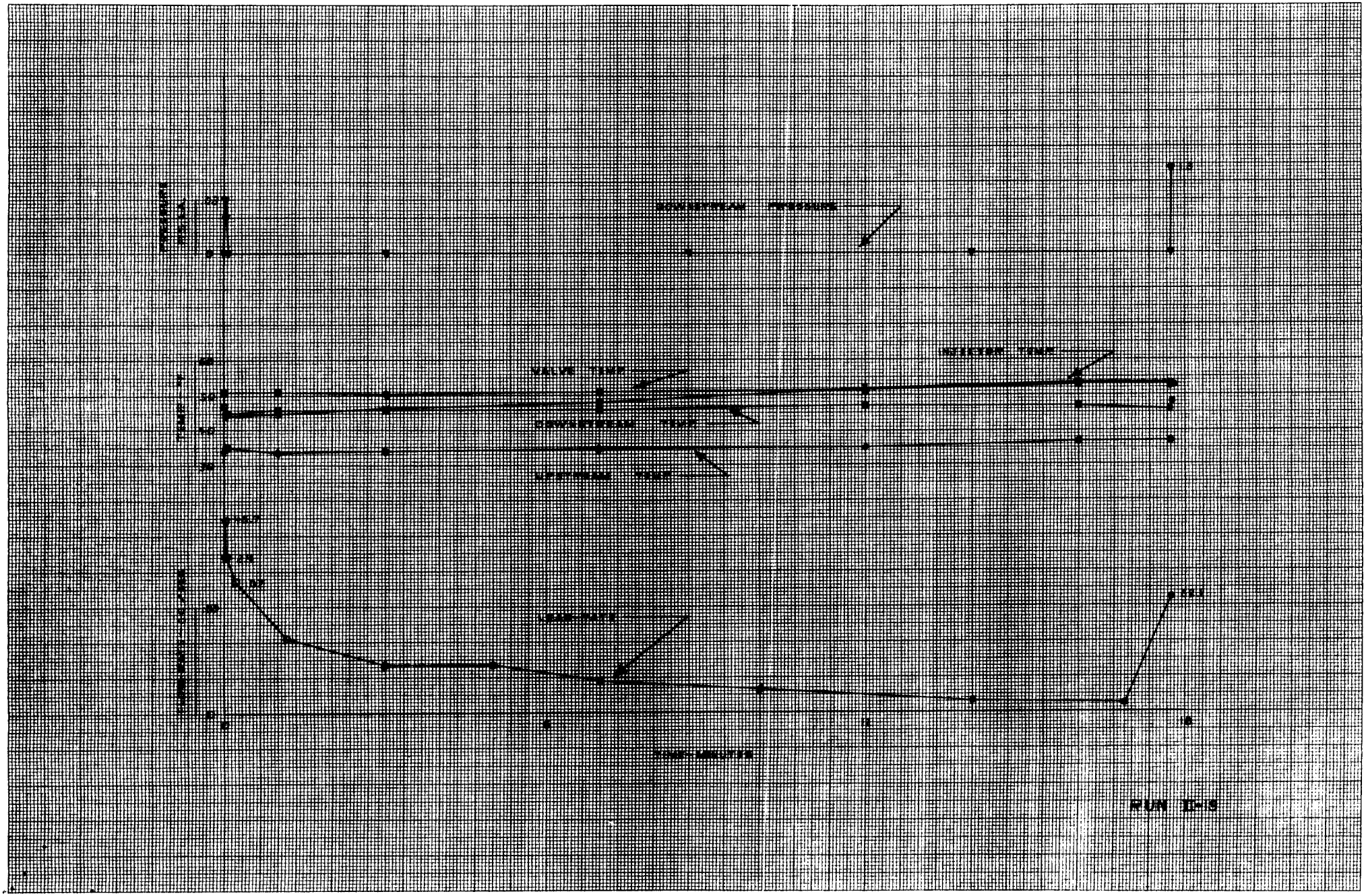
VALVE TEMP
WATER TEMP
DOWNSTREAM TEMP
UPSTREAM TEMP
RUN II-15

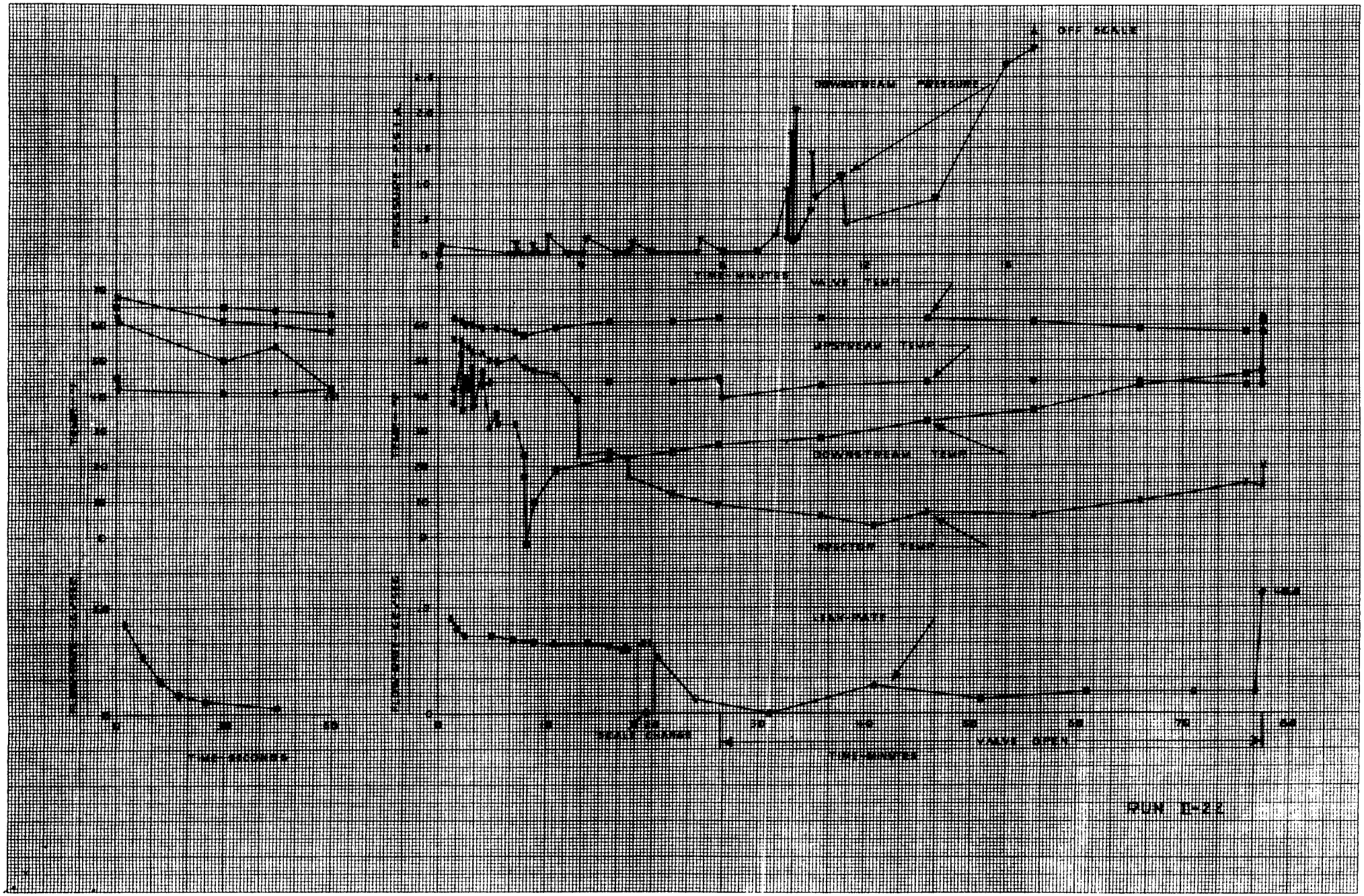
OFF SCALE
DOWNSTREAM PRESSURE
TIME MINUTES
VALVE TEMP
UPSTREAM TEMP
DOWNSTREAM TEMP
INJECTION TEMP
GAS RATE
SCALE CHANGE
TIME MINUTES
VALVE OPEN
TIME SECONDS
RUN E-22

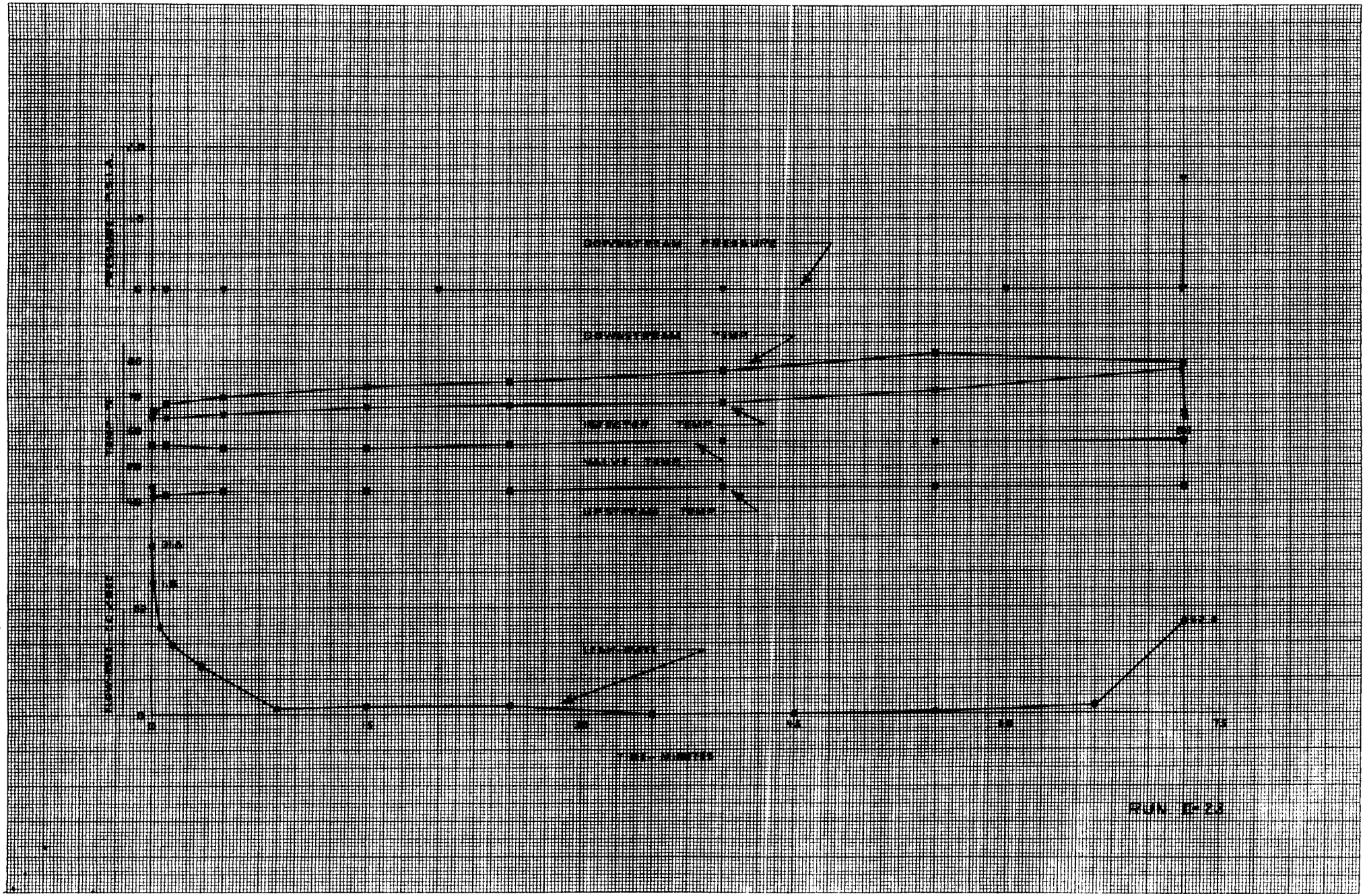
DOWNSTREAM PRESSURE
DOWNSTREAM TEMP
INTAKE TEMP
VALVE TEMP
UPSTREAM TEMP
LEAK RATE
TIME-MINUTES
RUN 8-23

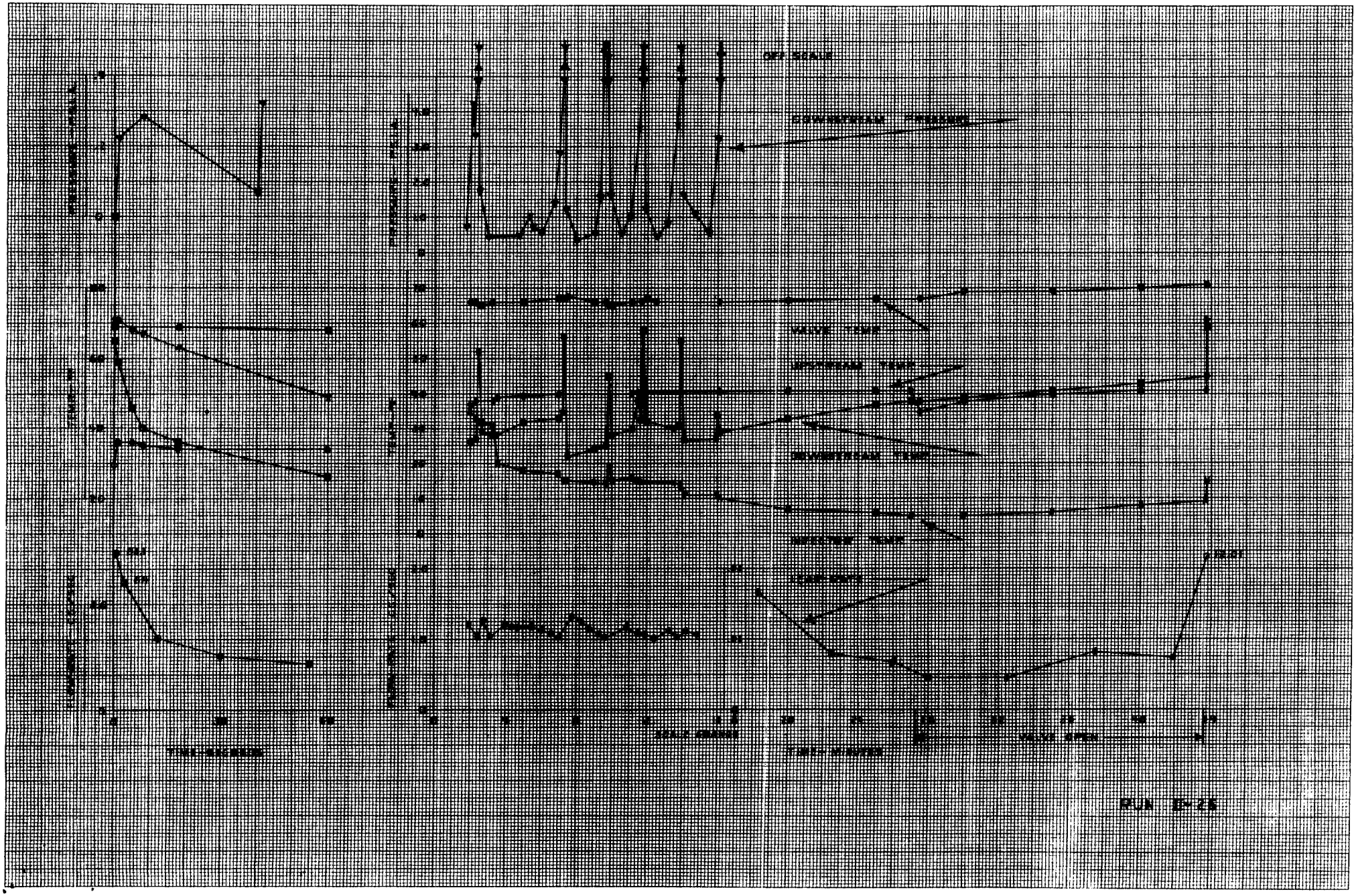
OFF SCALE
RUN 25

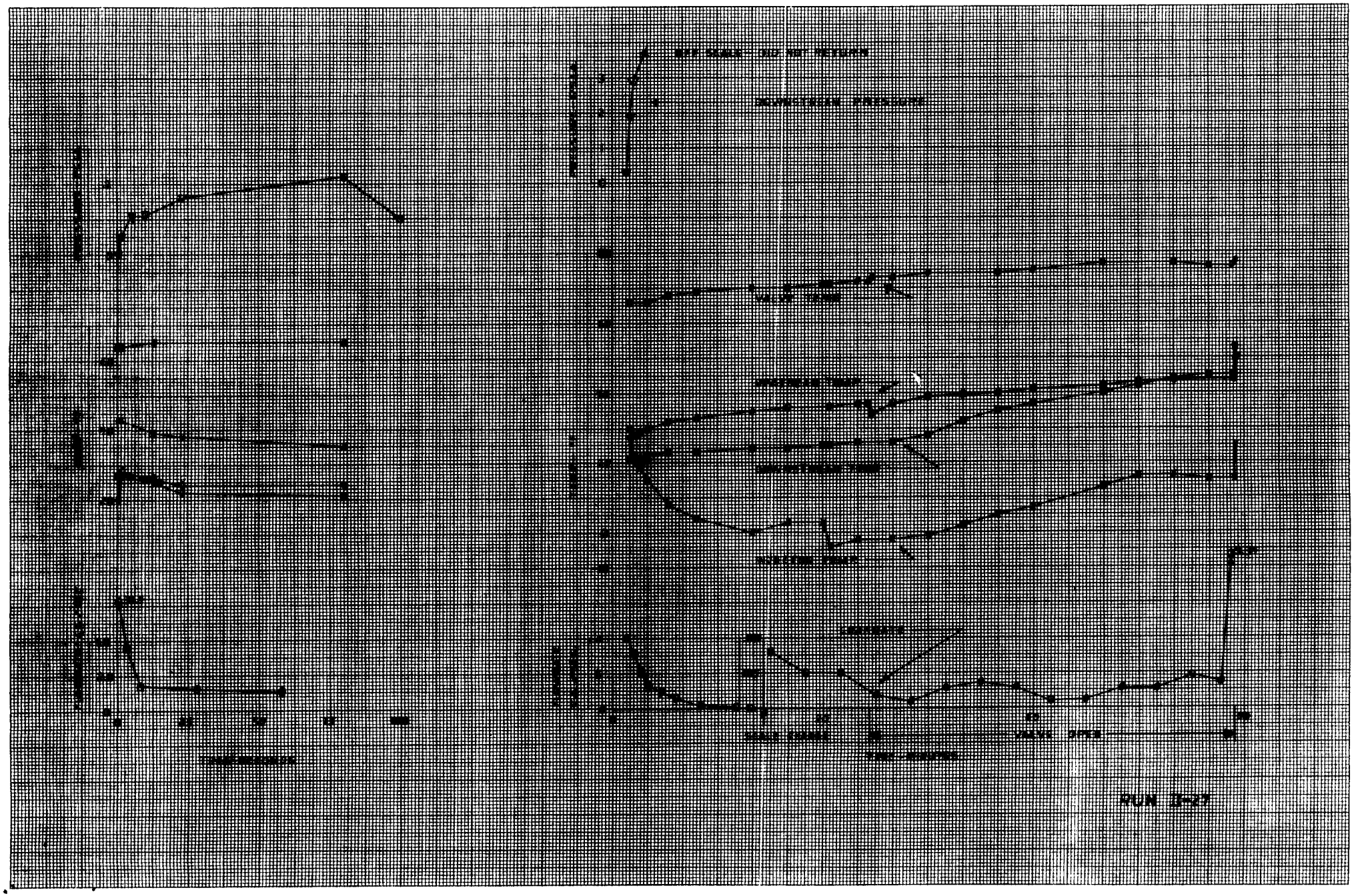
RUN B-27

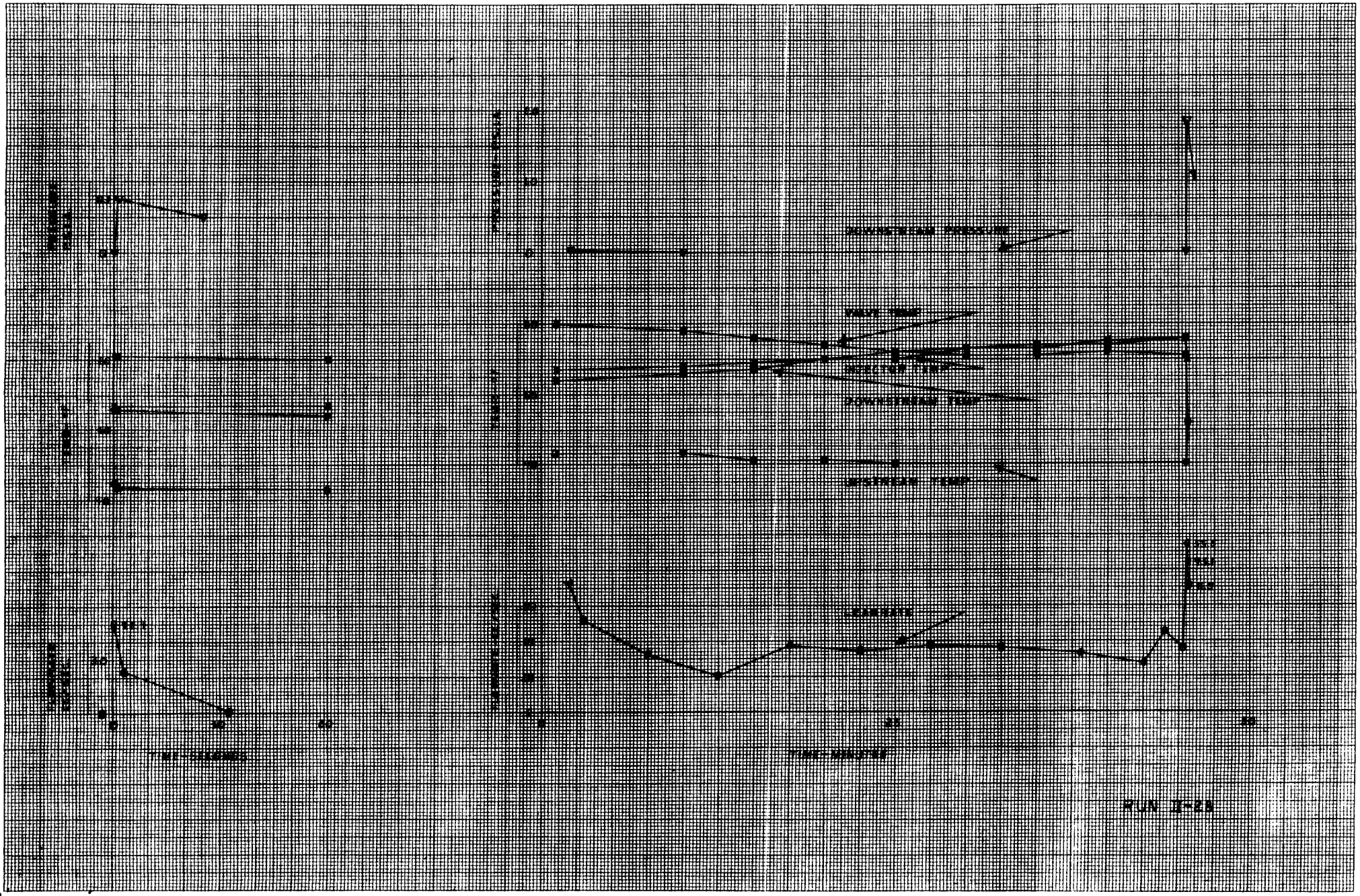
DOWNSTREAM PRESSURE
VALVE TEMP
INJECTOR TEMP
DOWNSTREAM TEMP
UPSTREAM TEMP
LEAKRATE
TIME-MINUTES
RUN B-28

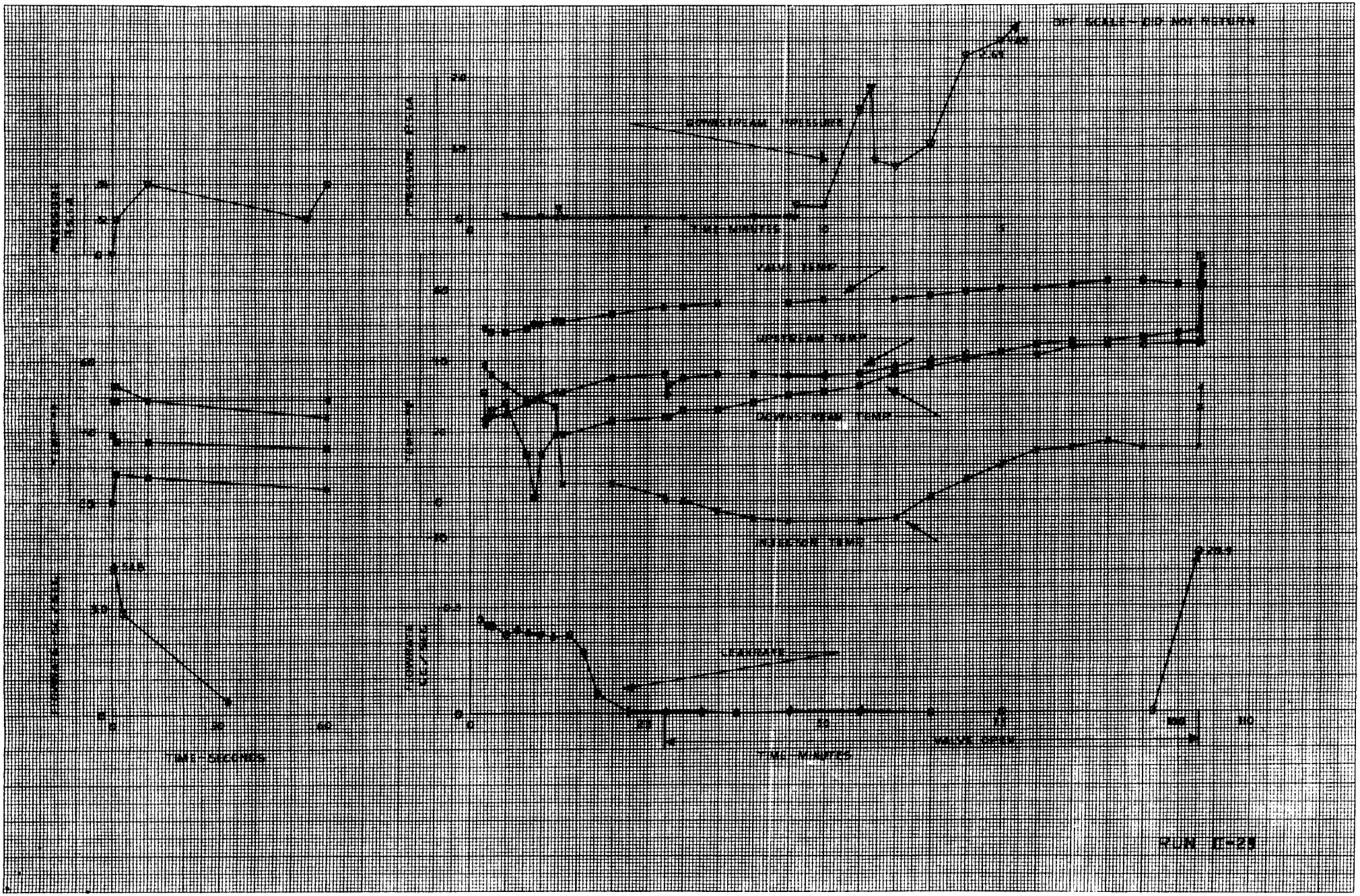
OFF SCALE - DID NOT RETURN
2.0X
UPSTREAM PRESSURE
TIME-MINUTES
VALVE TEMP
DOWNSTREAM TEMP
DOWNSTREAM TEMP
INJECTOR TEMP
LEAKRATE
VALVE OPEN
TIME-MINUTES
2.0X
TIME-SECONDS
RUN E-25

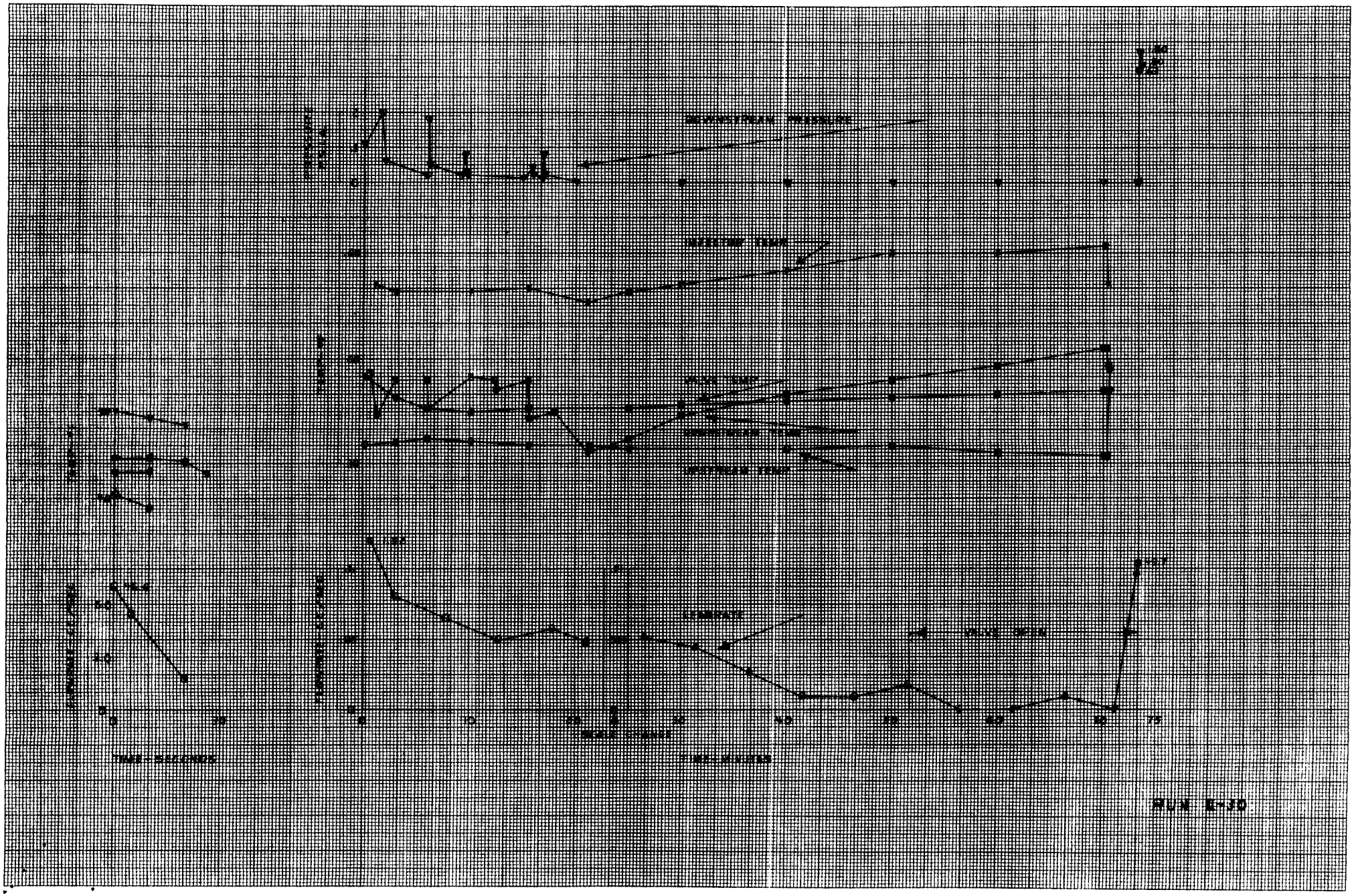
TIME-SECONDS
TIME-MINUTES
RUN E-30

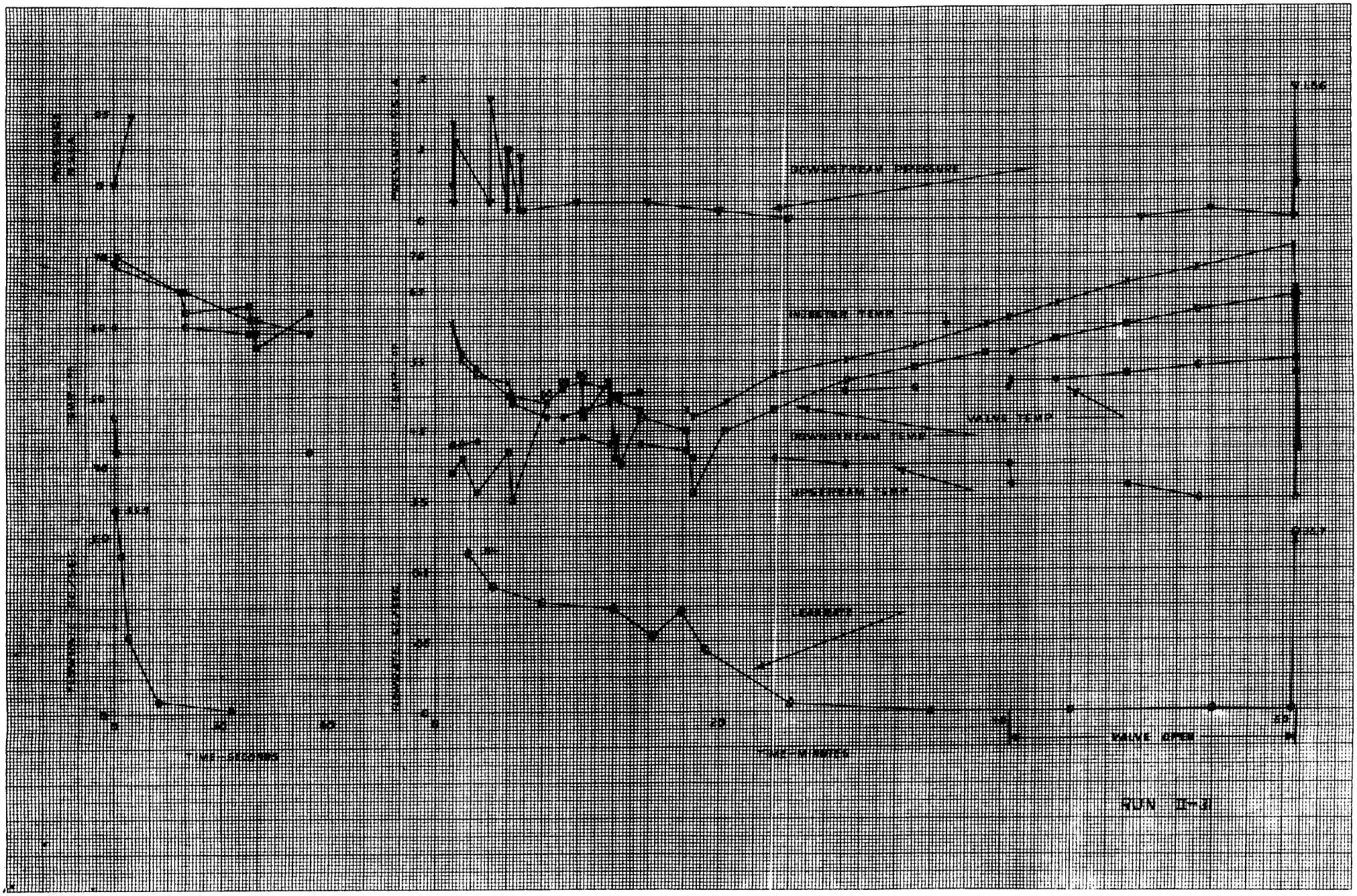
DOWNSTREAM PRESSURE
UPSTREAM PRESSURE
VALVE TORQUE
DOWNSTREAM FLOW
UPSTREAM FLOW
CAVITY
VALVE OPEN
TIME-SECONDS
TIME-MINUTES
RUN II-31

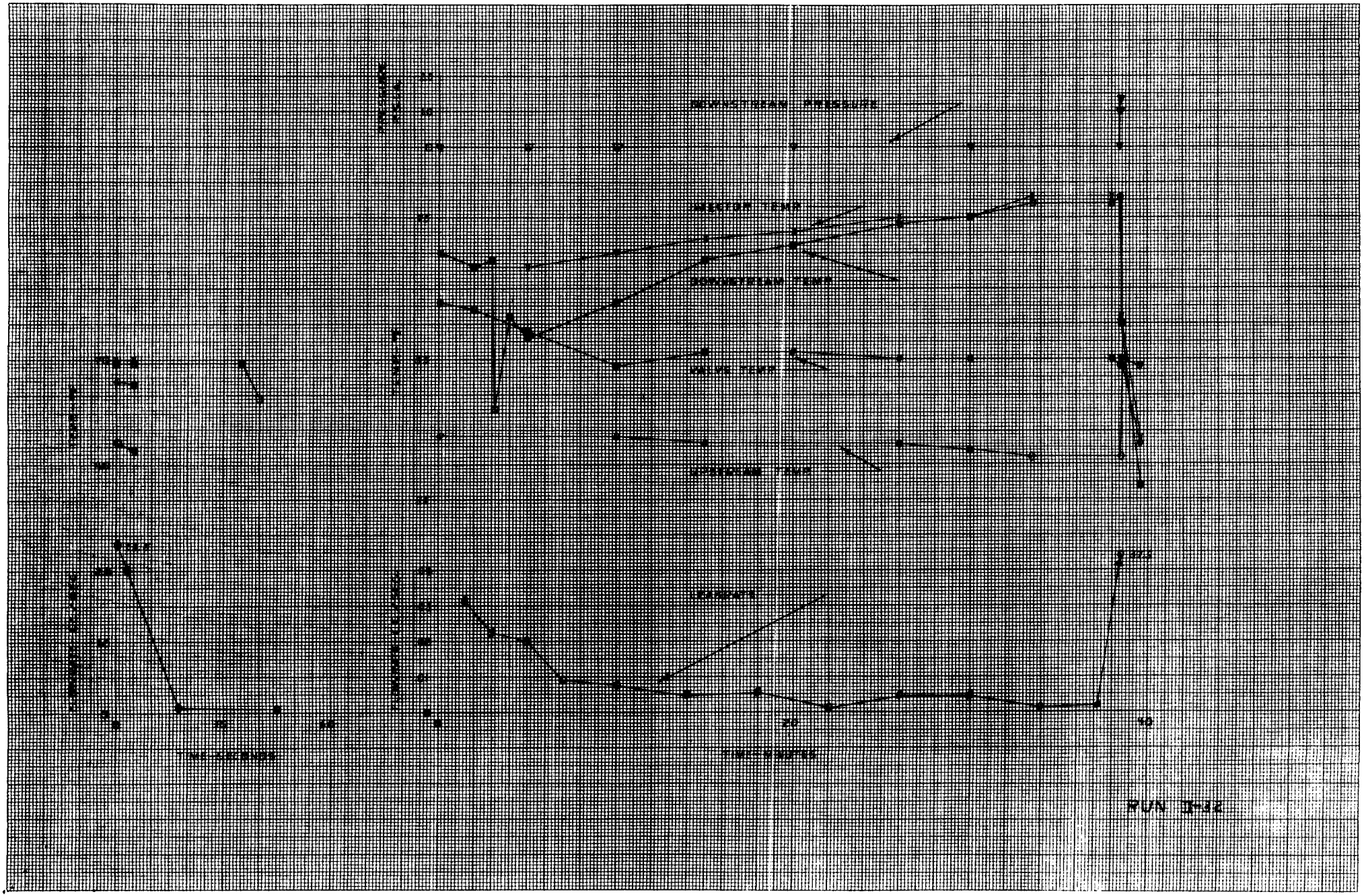
DOWNSTREAM PRESSURE
INJECTOR TEMP
DOWNSTREAM TEMP
VALVE TEMP
UPSTREAM TEMP
CHAMBER
TIME-MINUTES
TIME-MINUTES
RUN II-32

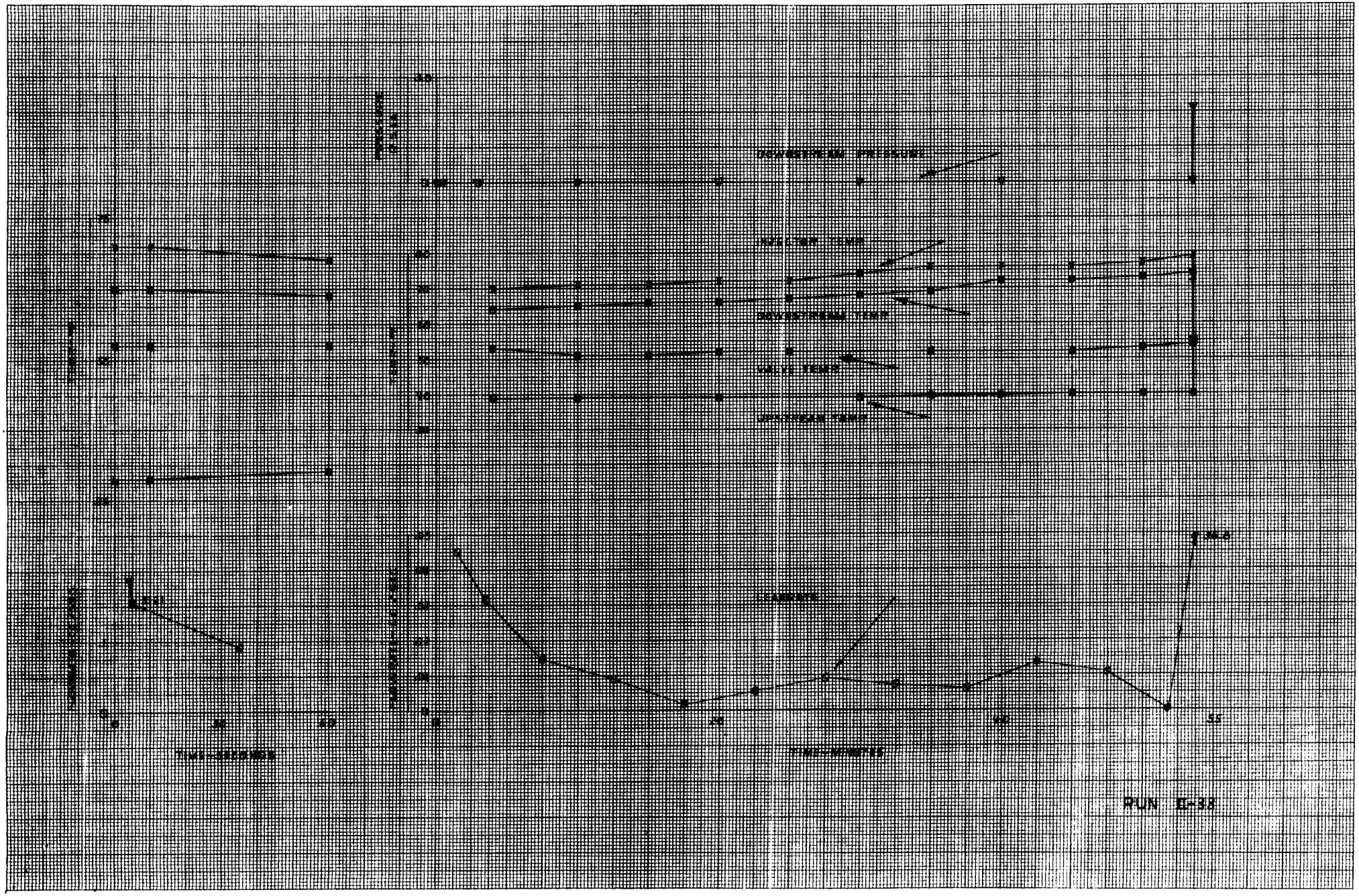
RUN 11-38

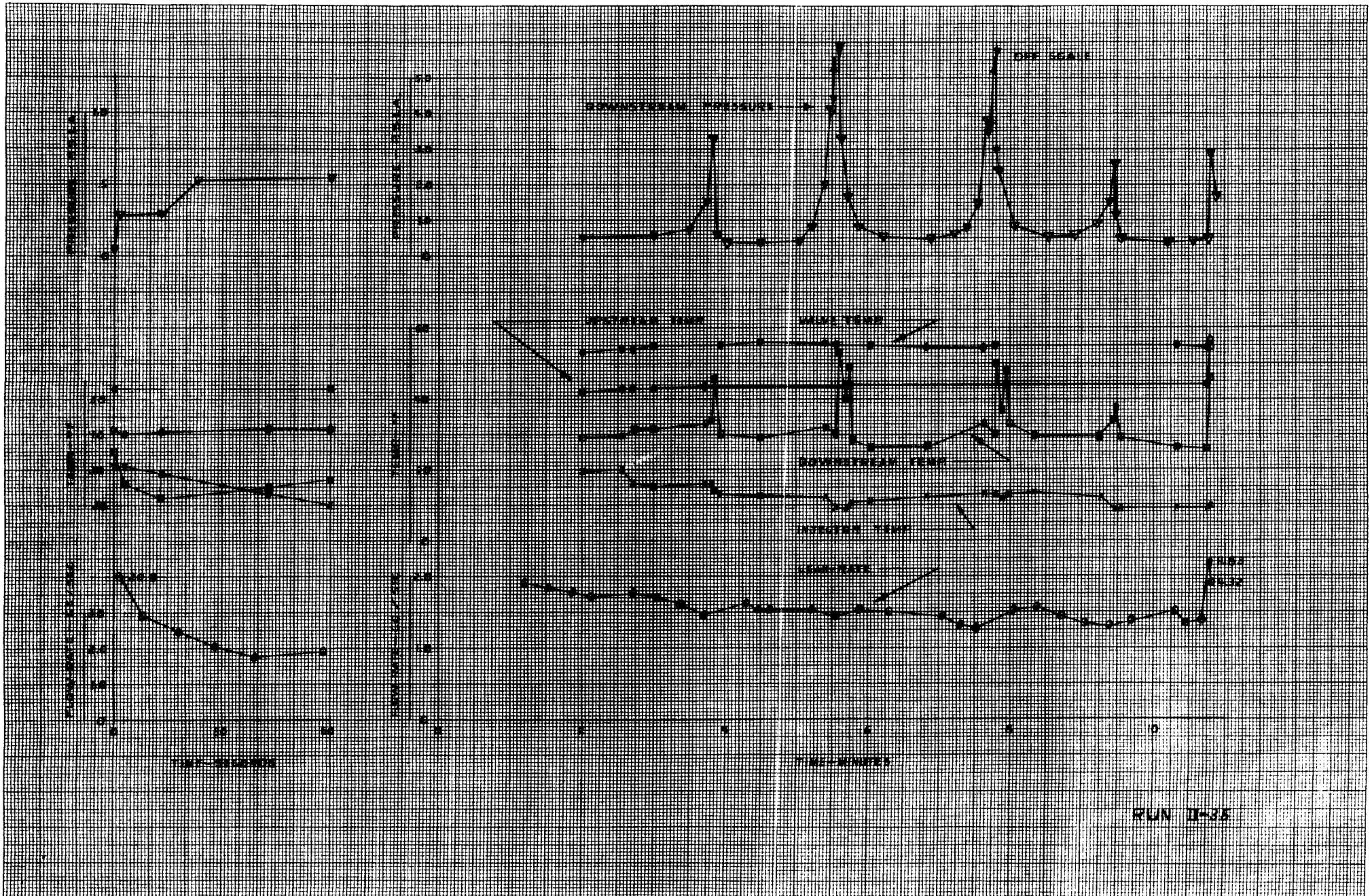
DOWNSTREAM PRESSURE
DOT SCALE
UPSTREAM TEMP
VALVE TEMP
DOWNSTREAM TEMP
INTERIOR TEMP
LEAK RATE
PULSE HEIGHT
TIME-SECONDS
TIME-MINUTES
RUN II-35

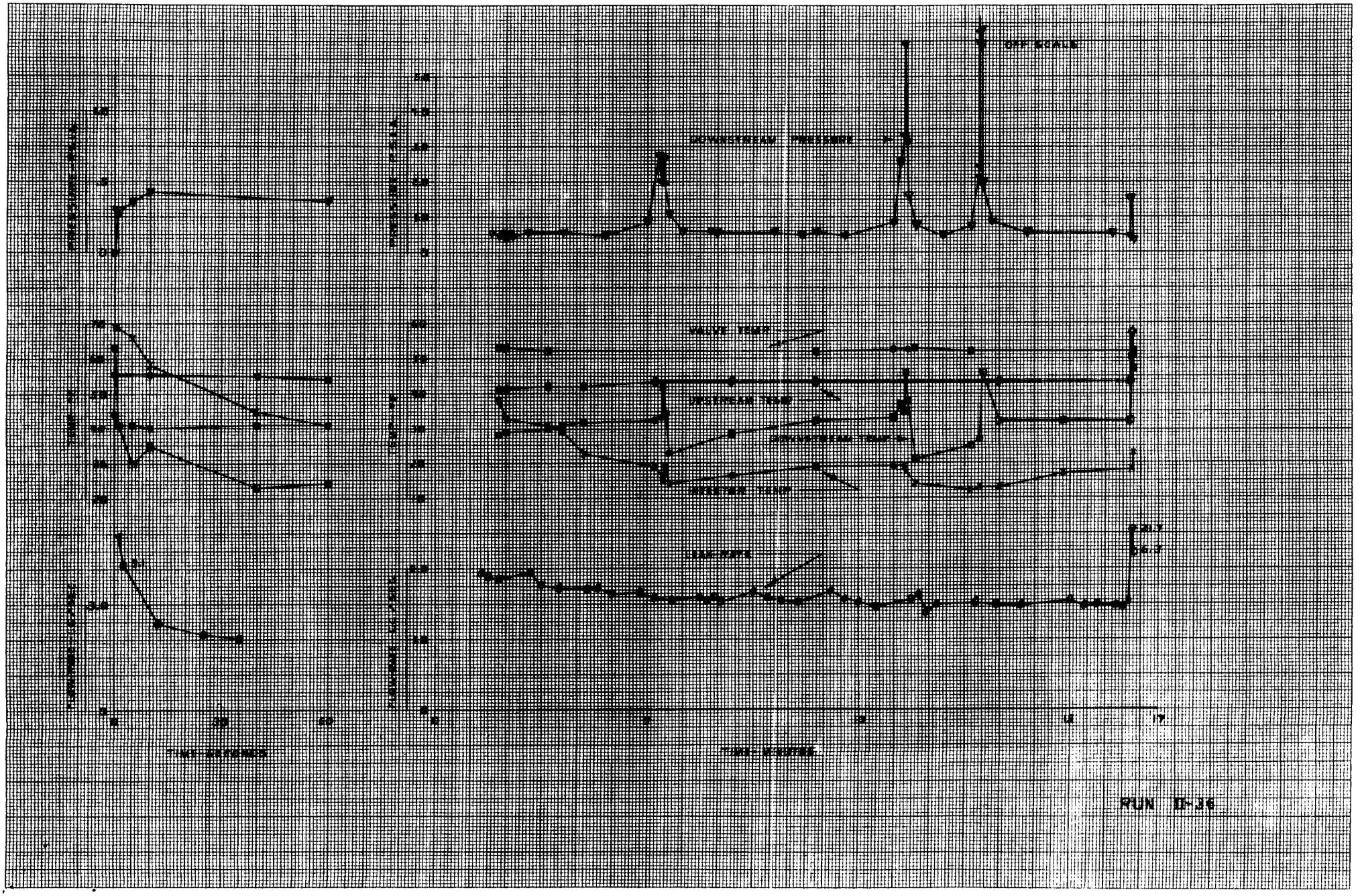
OFF SCALE
DOWNSTREAM PRESSURE
VALVE TEMP
UPSTREAM TEMP
DOWNSTREAM TEMP
HEATER TEMP
LEAK RATE
TIME BETWEEN
TIME HEATER
RUN ID-36

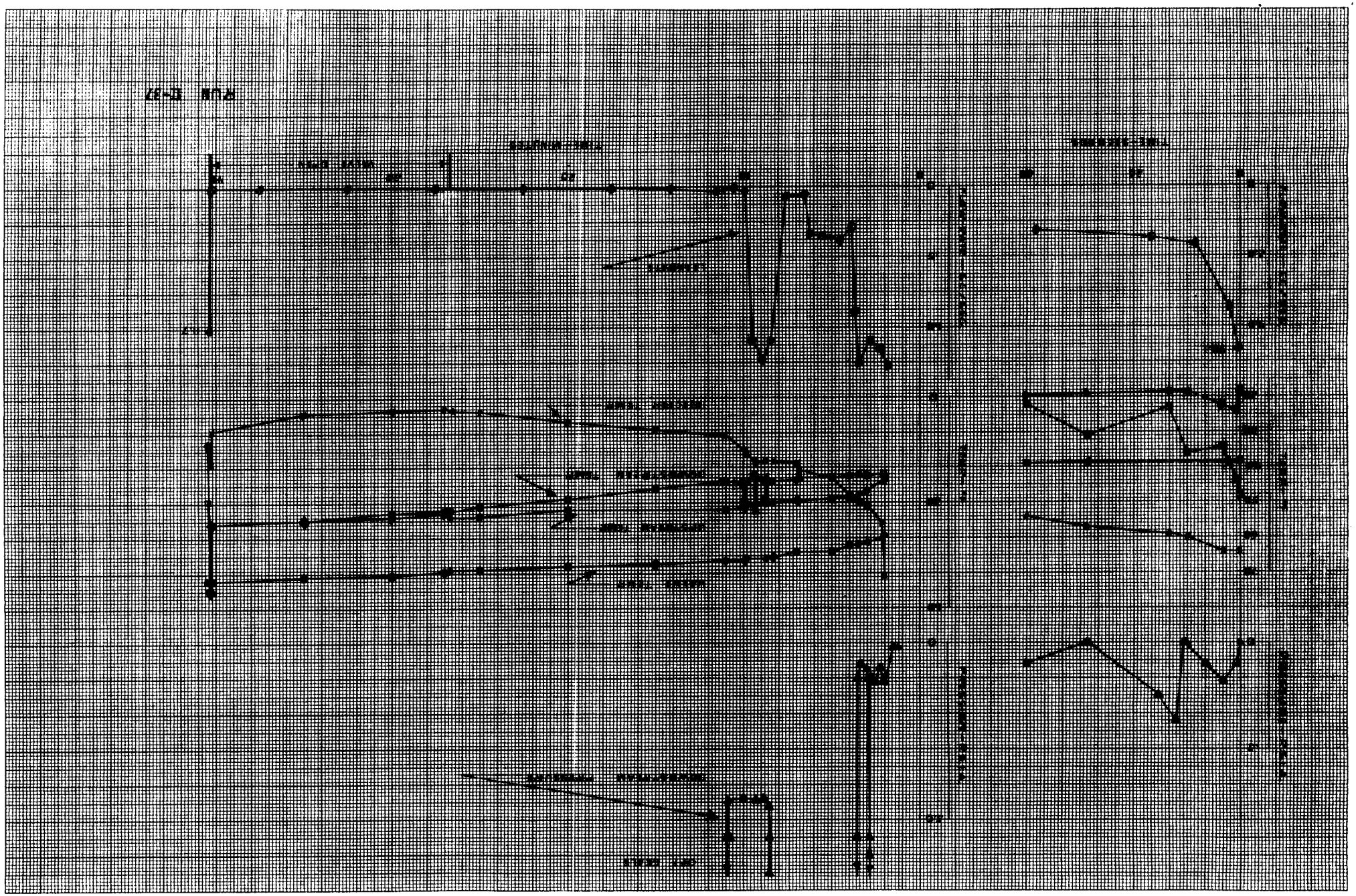

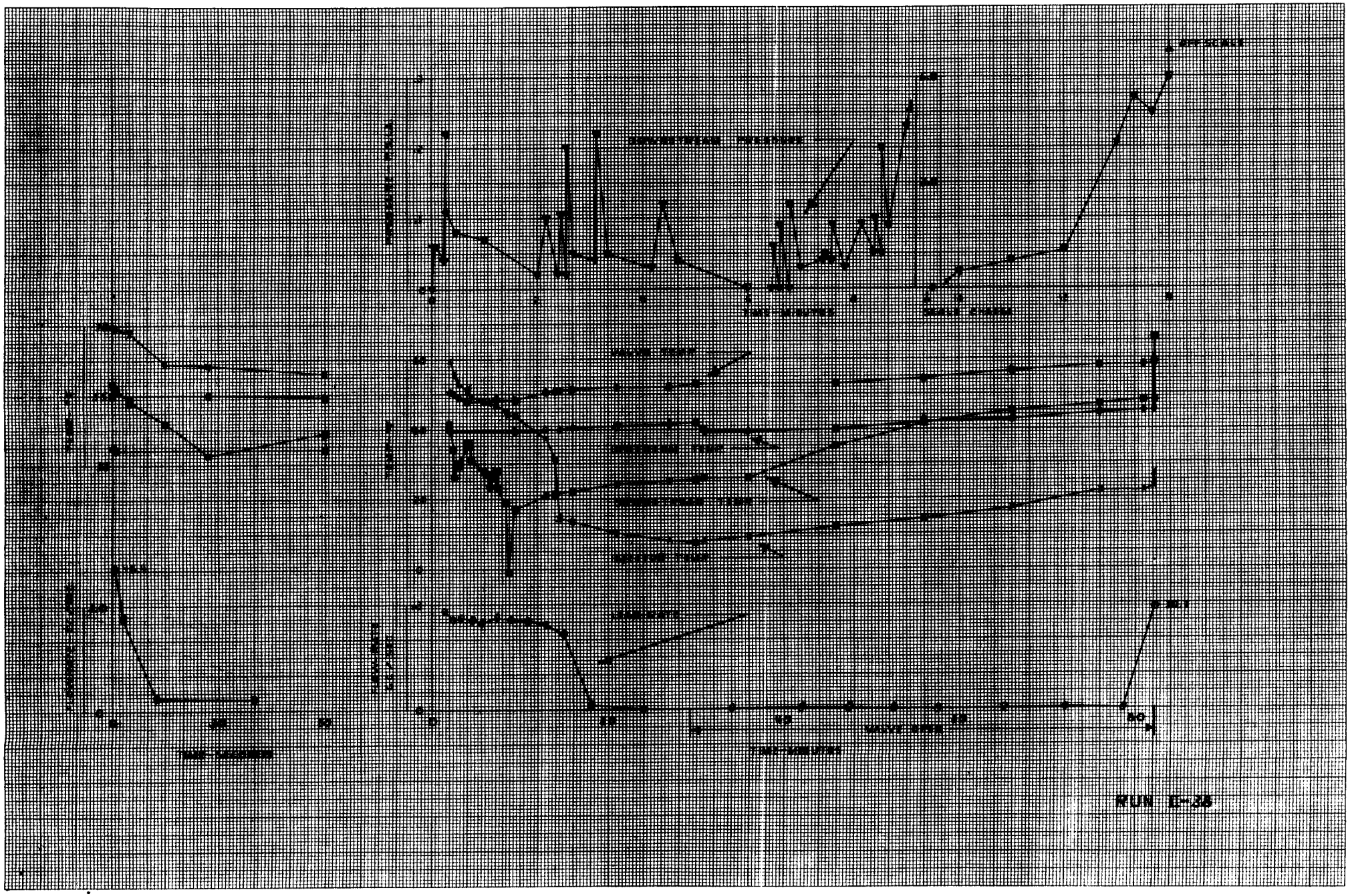
RUN E-28

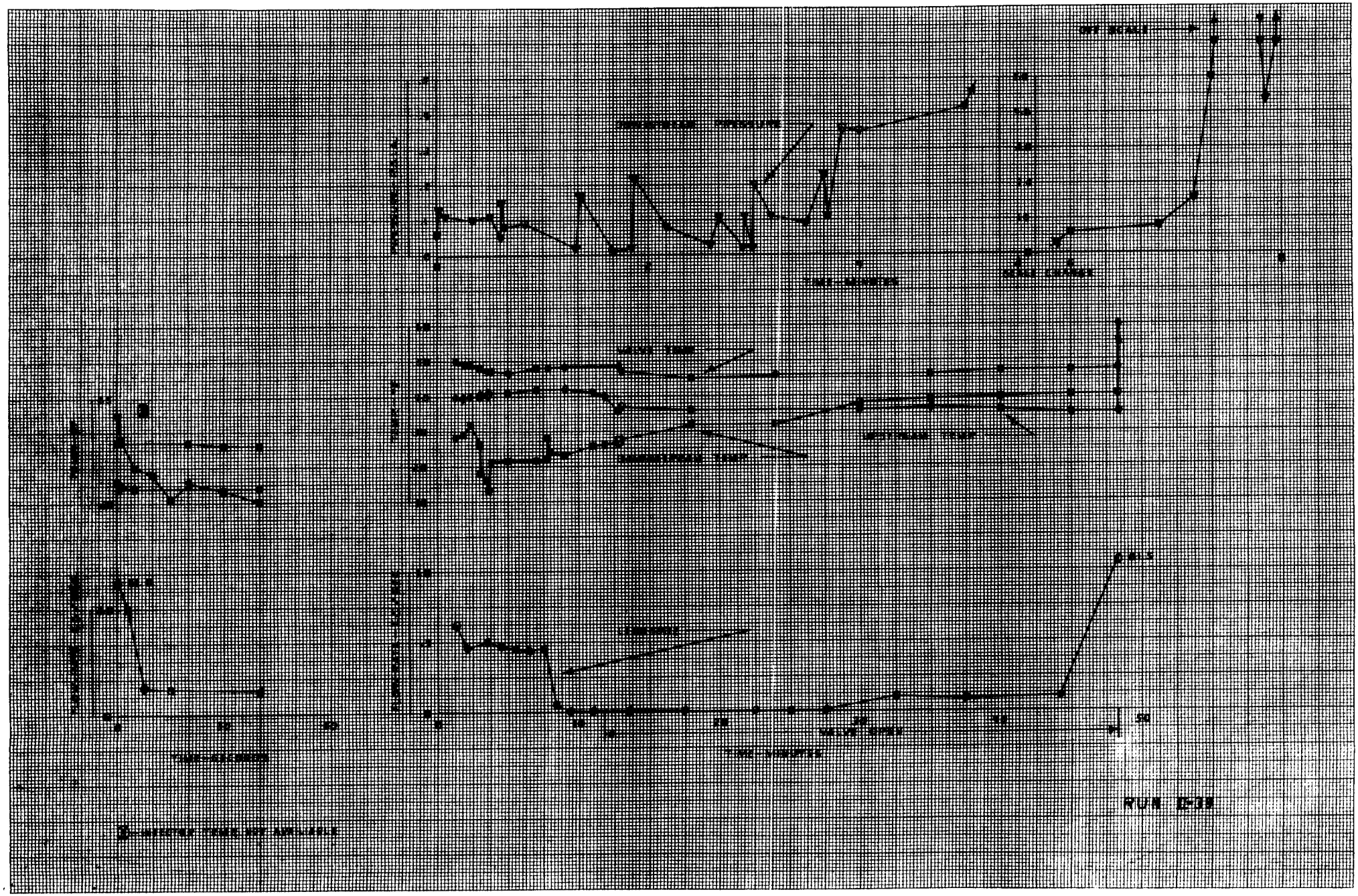
OFF SCALE
RUN E-38

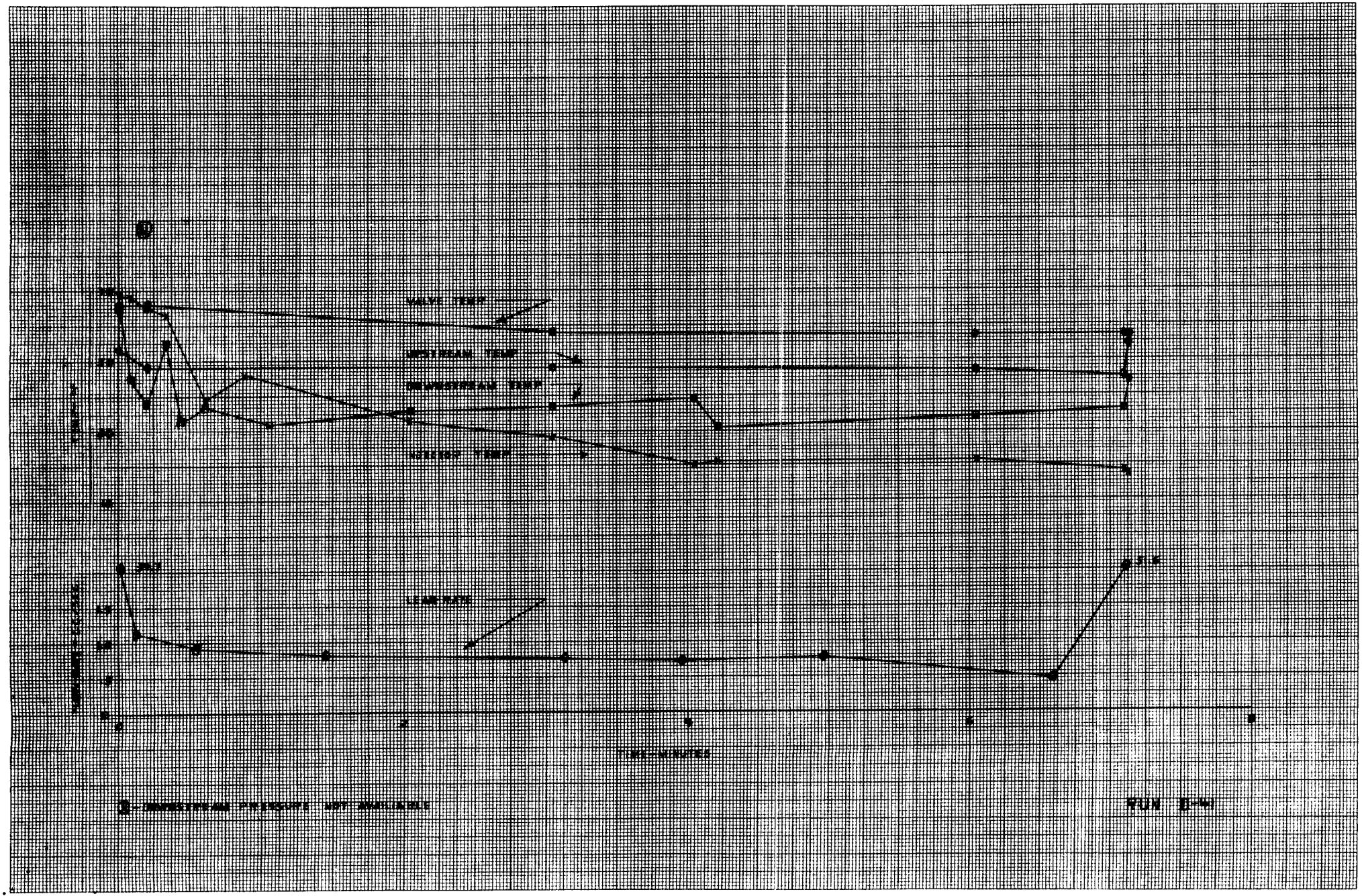
VALVE TEMP
UPSTREAM TEMP
DOWNSTREAM TEMP
ADAPTOR TEMP
LEAK RATE
TIME-MINUTES
RUN E-41

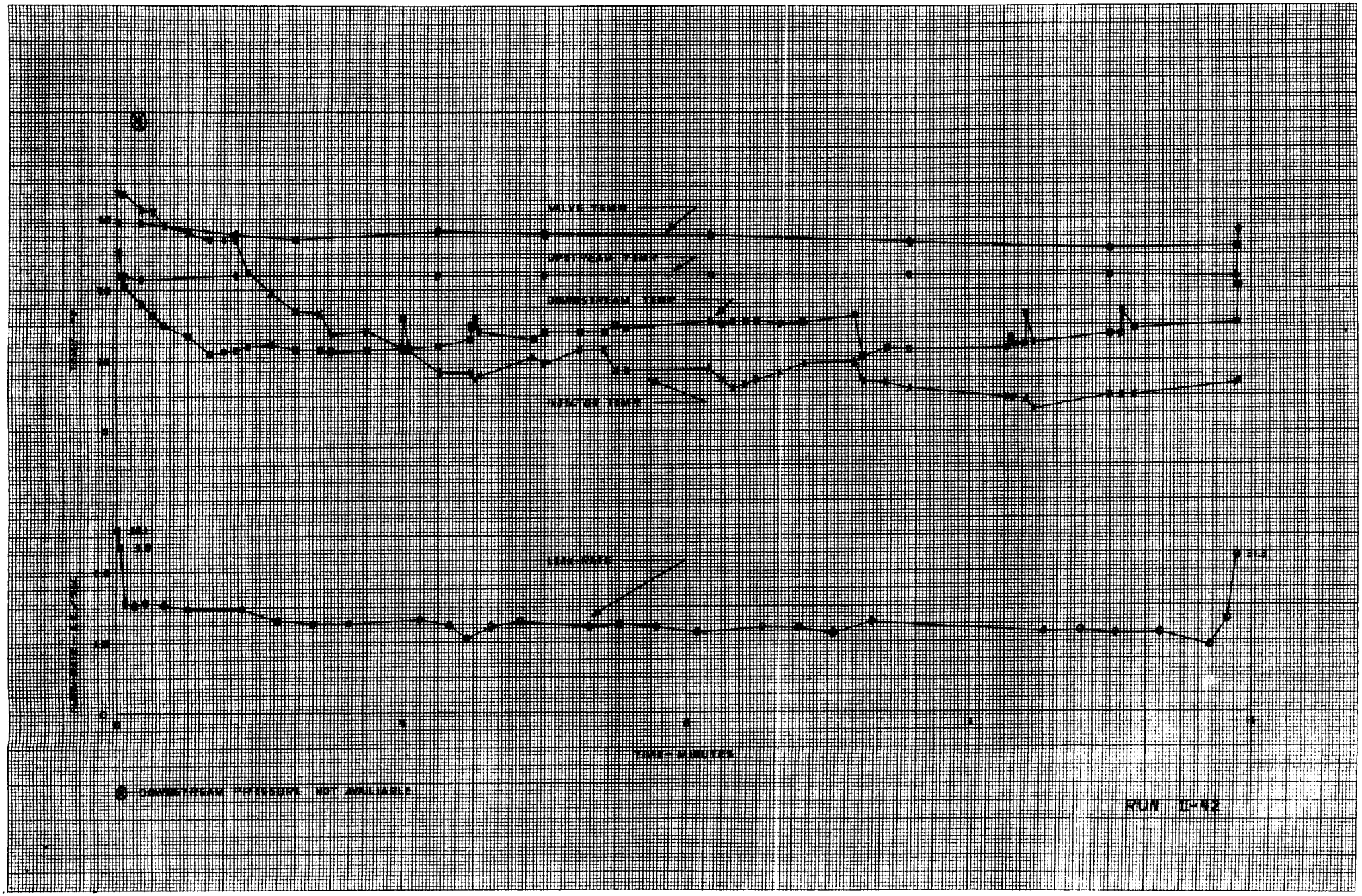
VALVE TEMP
UPSTREAM TEMP
DOWNSTREAM TEMP
INJECTOR TEMP
PEAK-RATE
TIME-MINUTES
RUN K-42

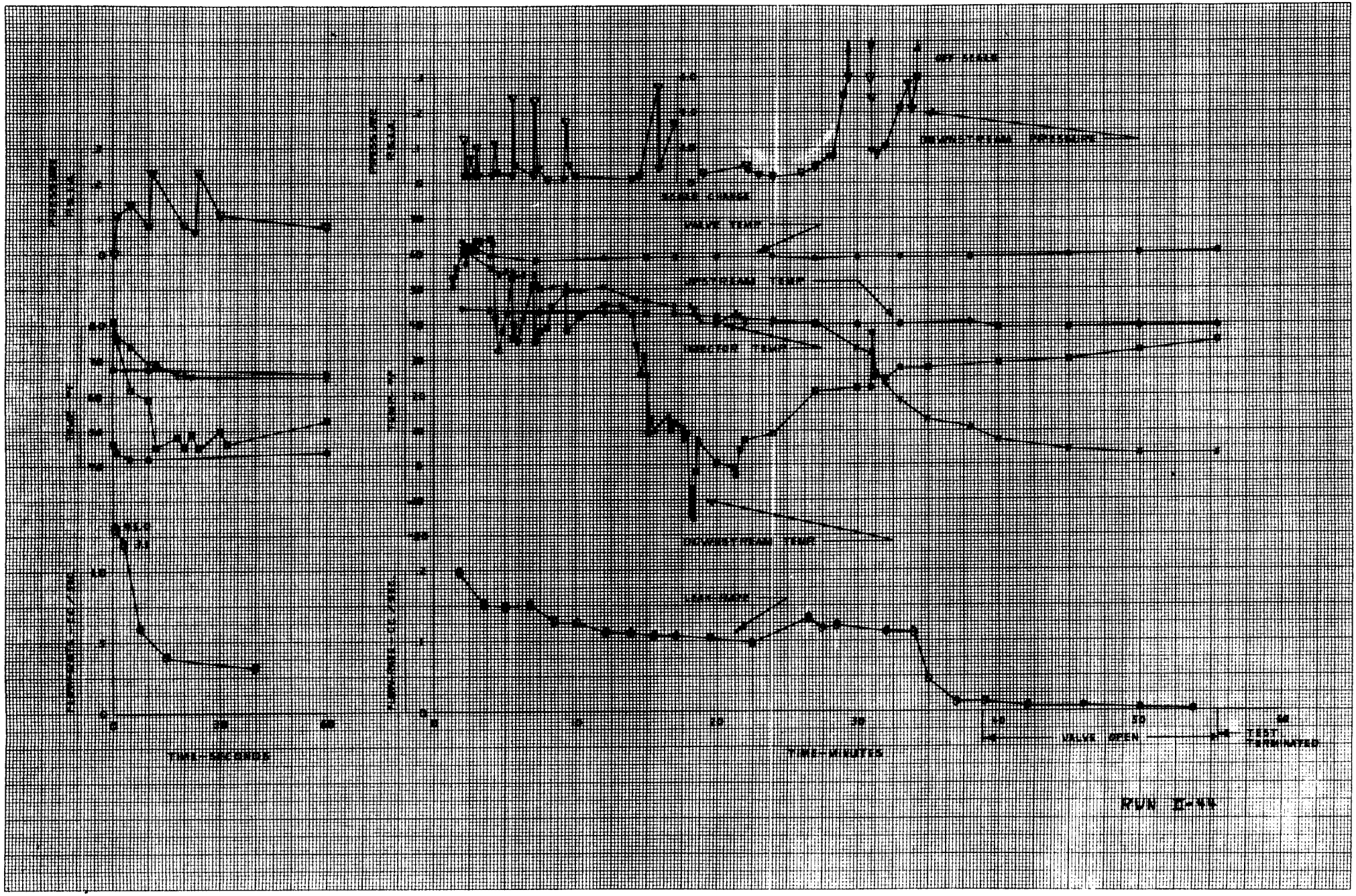
OFF SCALE
MANIFOLD PRESSURE
NOZZLE COOLANT
VALVE TEMP
MANIFOLD TEMP
INJECTOR TEMP
POWERSTRAM TEMP
THRUST
VALVE OPEN
TEST TERMINATED
TIME-SECONDS
TIME-MINUTES
RUN II-44

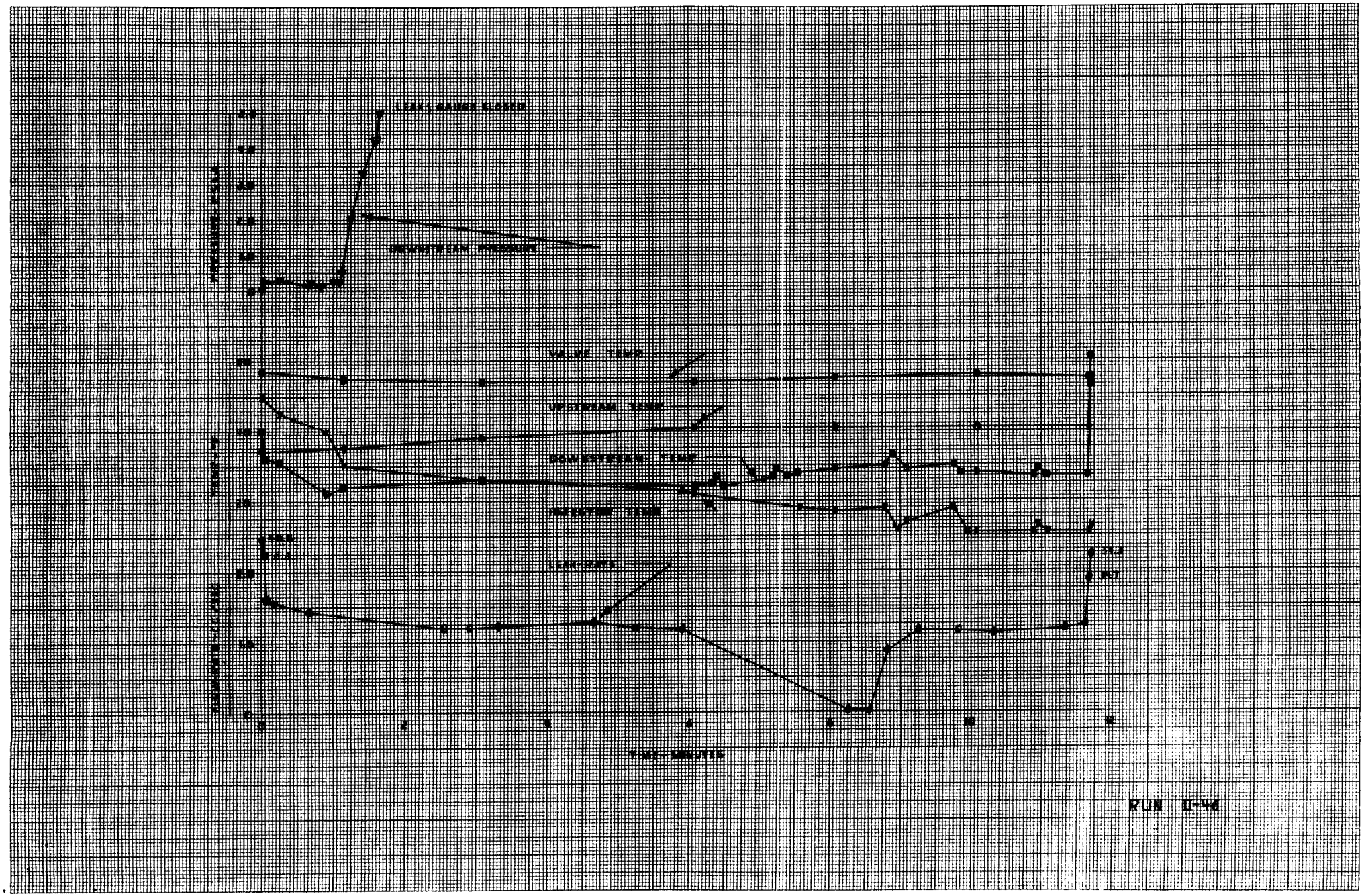
VALVE TIME
RUN D-46

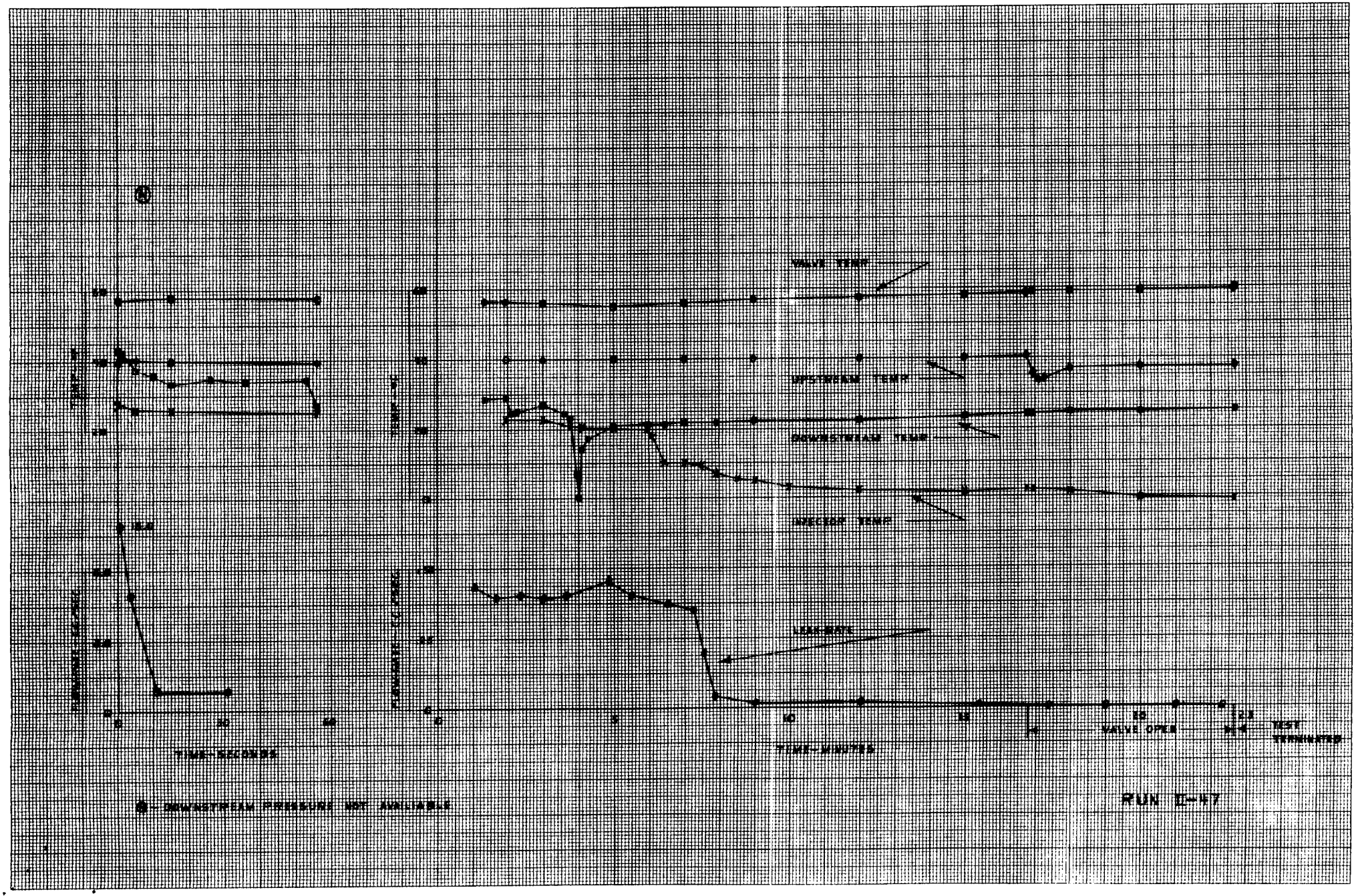

(B) - DOWNSTREAM PRESSURE NOT AVAILIABLE

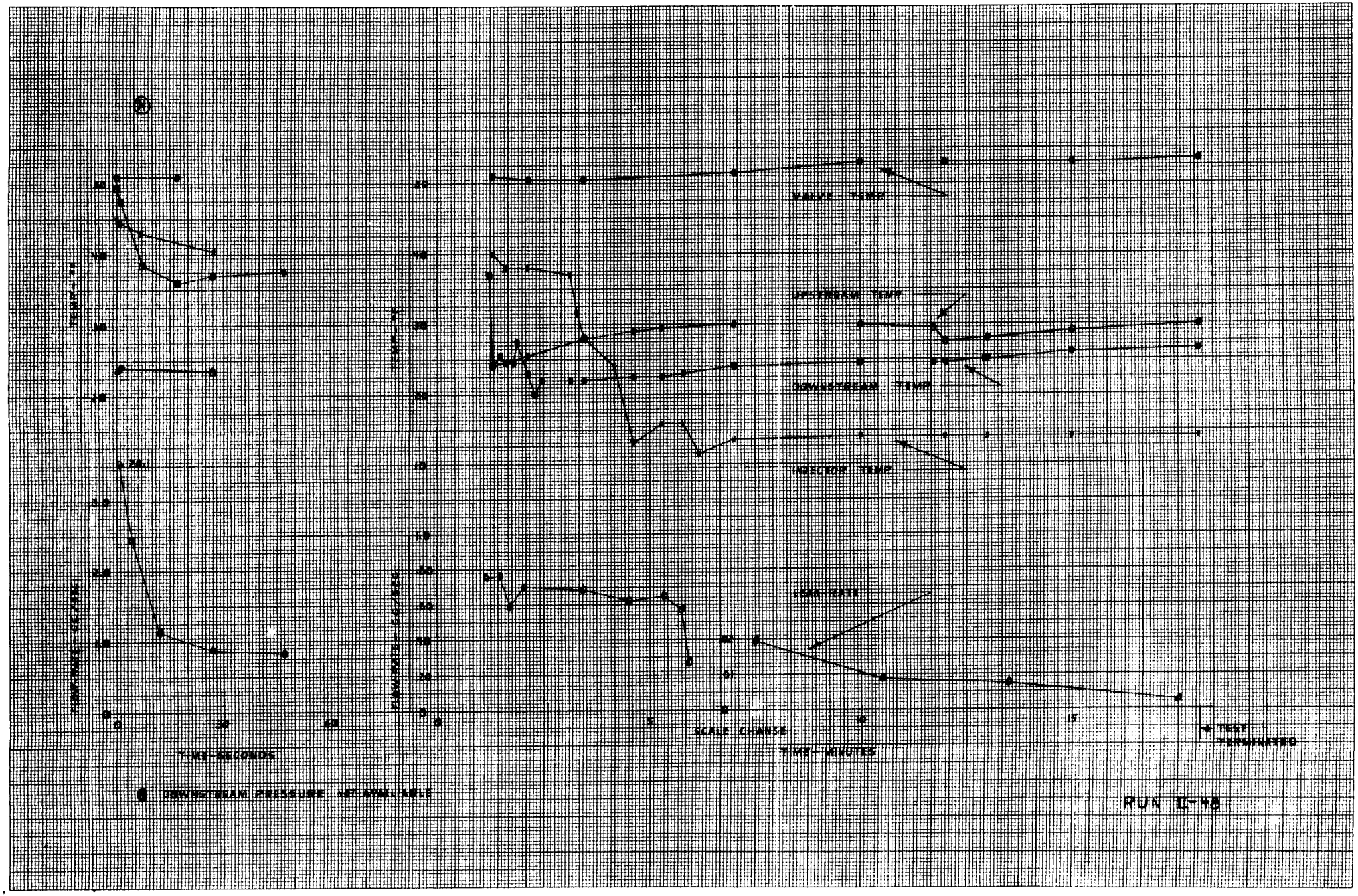
VALVE TEMP
UPSTREAM TEMP
DOWNSTREAM TEMP
INJECTOR TEMP
SCALE CHANGE
TIME - MINUTES
TEST TERMINATED
TIME - SECONDS
DOWNSTREAM PRESSURE NOT AVAILABLE
RUN E-48

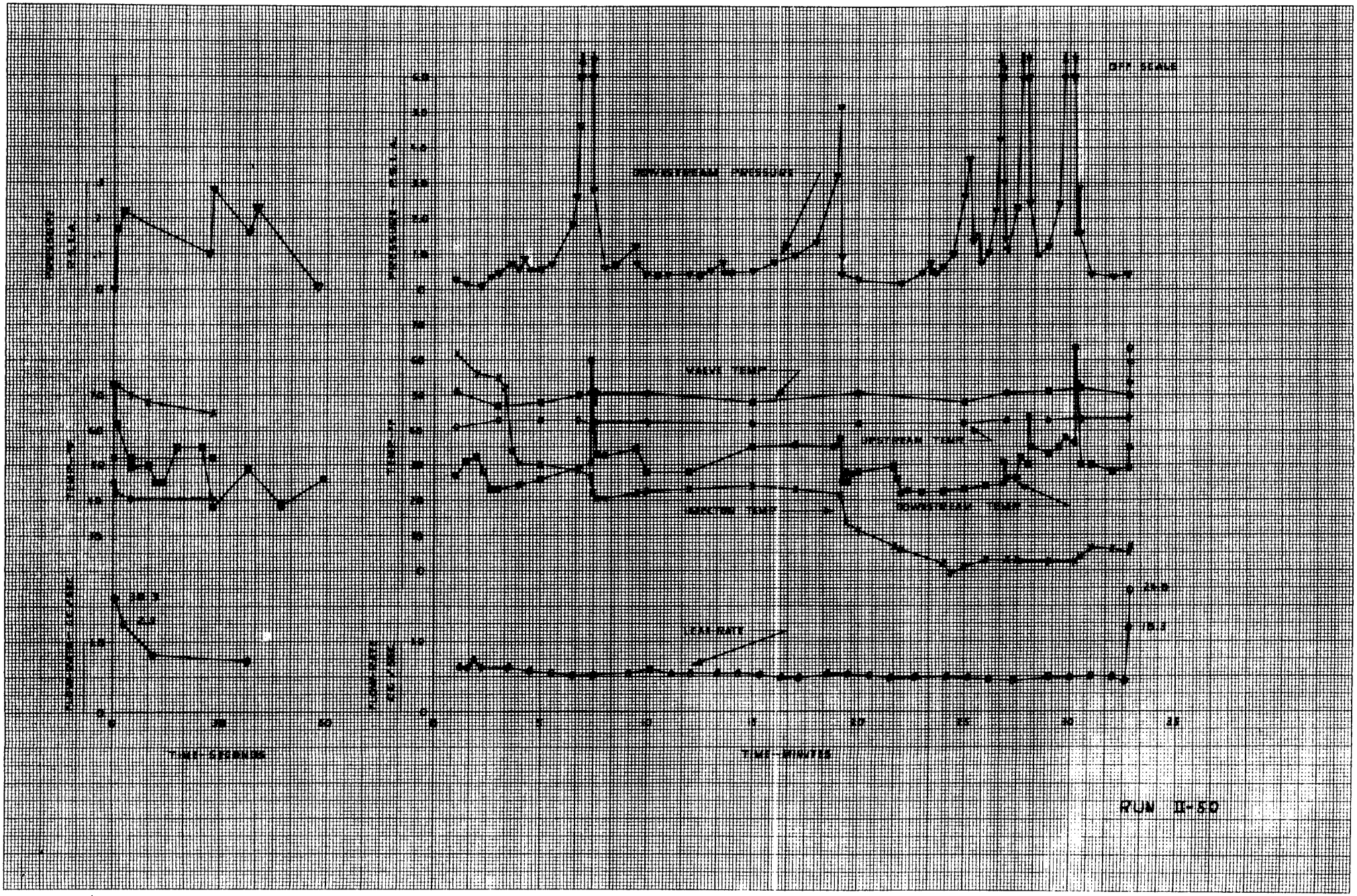
OFF SCALE
TIME-SECONDS
TIME-MINUTES
RUN II-50

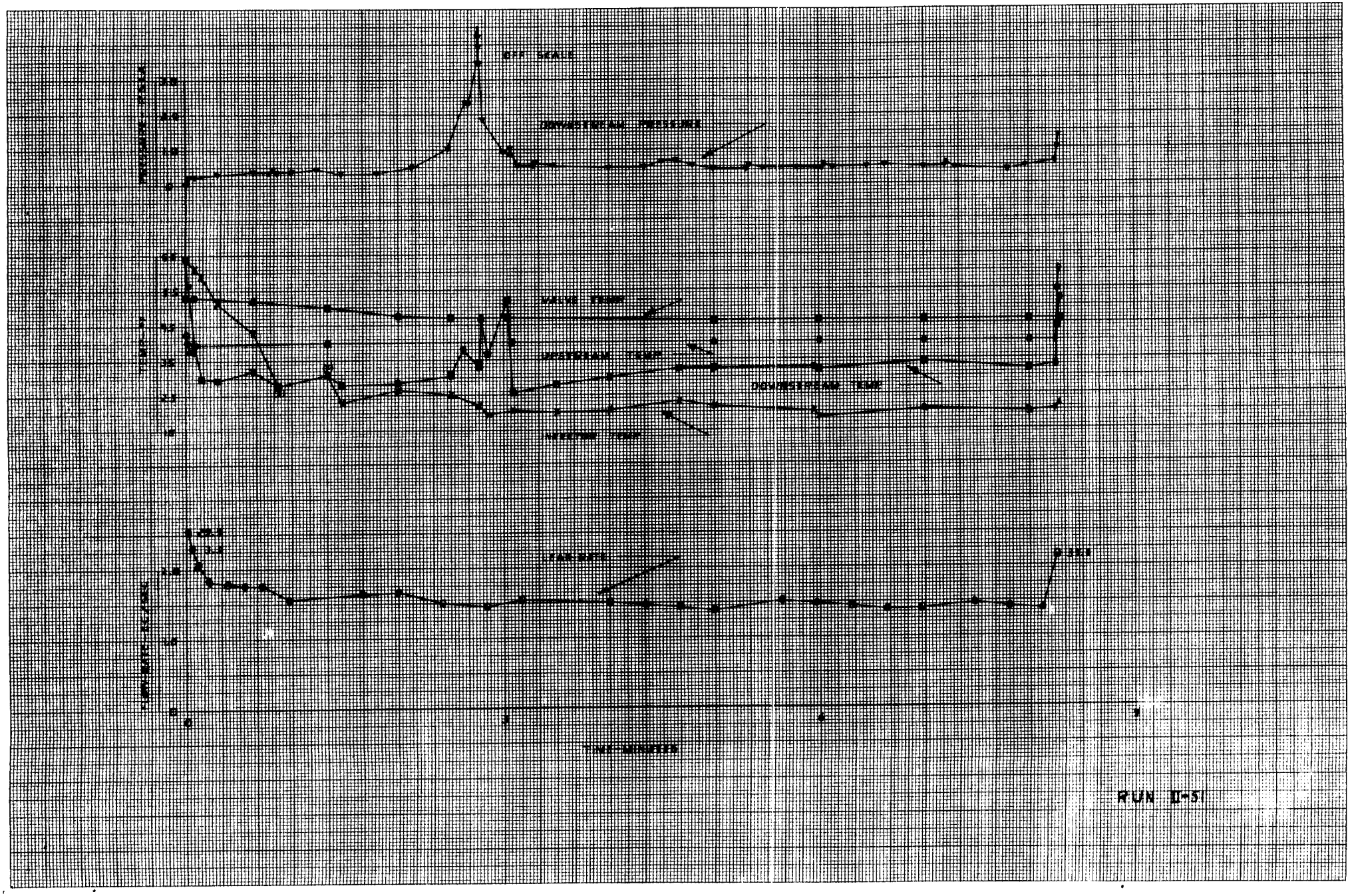
OFF SCALE
DOWNSTREAM PRESSURE
VALVE TEMP
UPSTREAM TEMP
DOWNSTREAM TEMP
INLET TEMP
FAN RATE
TIME-MINUTES
RUN II-51

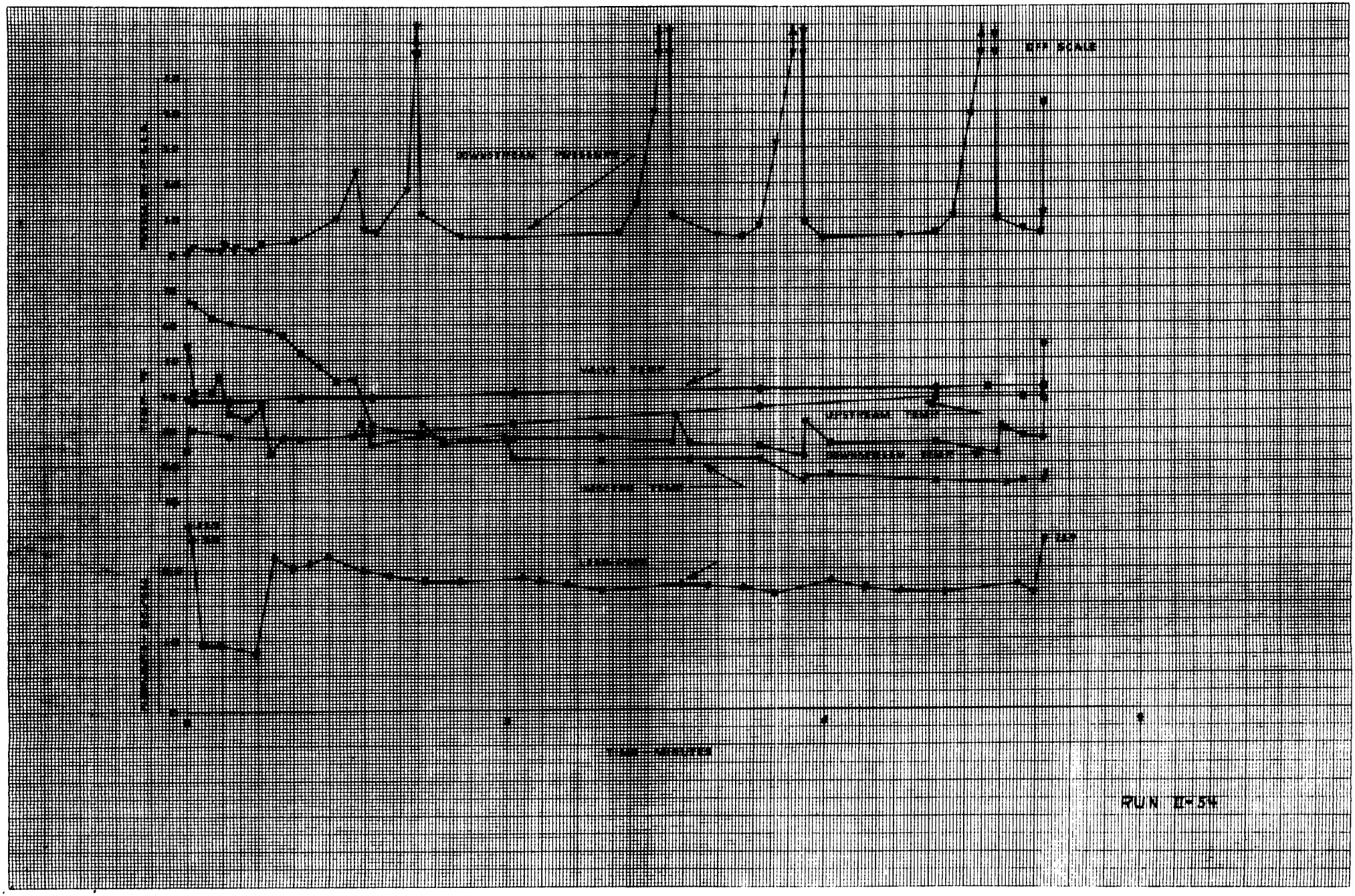
OFF SCALE
DOWNSTREAM TEMPERATURE °F
WATER TEMP
UPSTREAM TEMP
DOWNSTREAM TEMP
AIR TEMP
TIME - MINUTES
RUN II-54

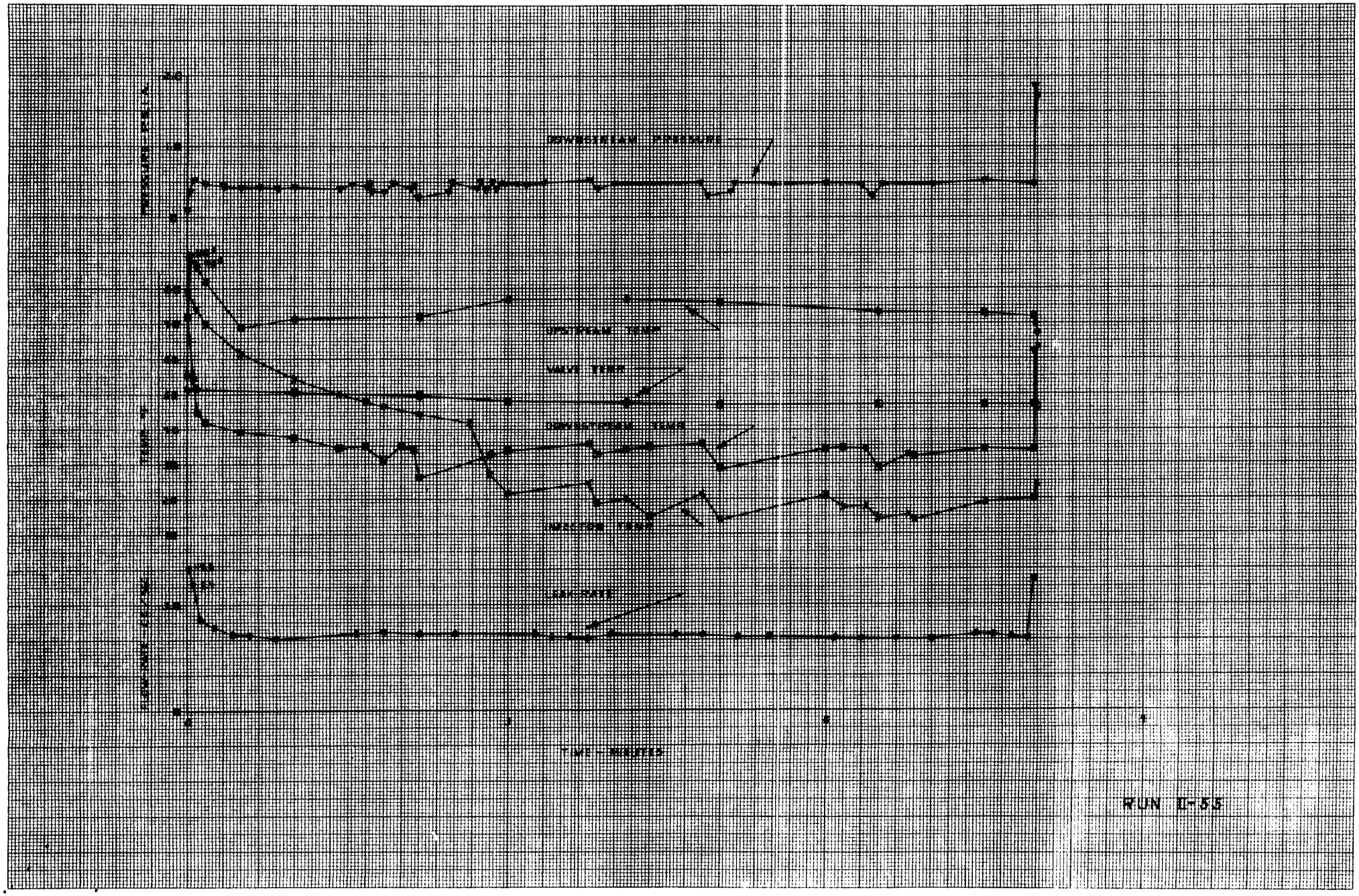
DOWNSTREAM PRESSURE
UPSTREAM TEMP
VALVE TEMP
DOWNSTREAM TEMP
INJECTOR TEMP
LEAK RATE
TIME - MINUTES
RUN II-55

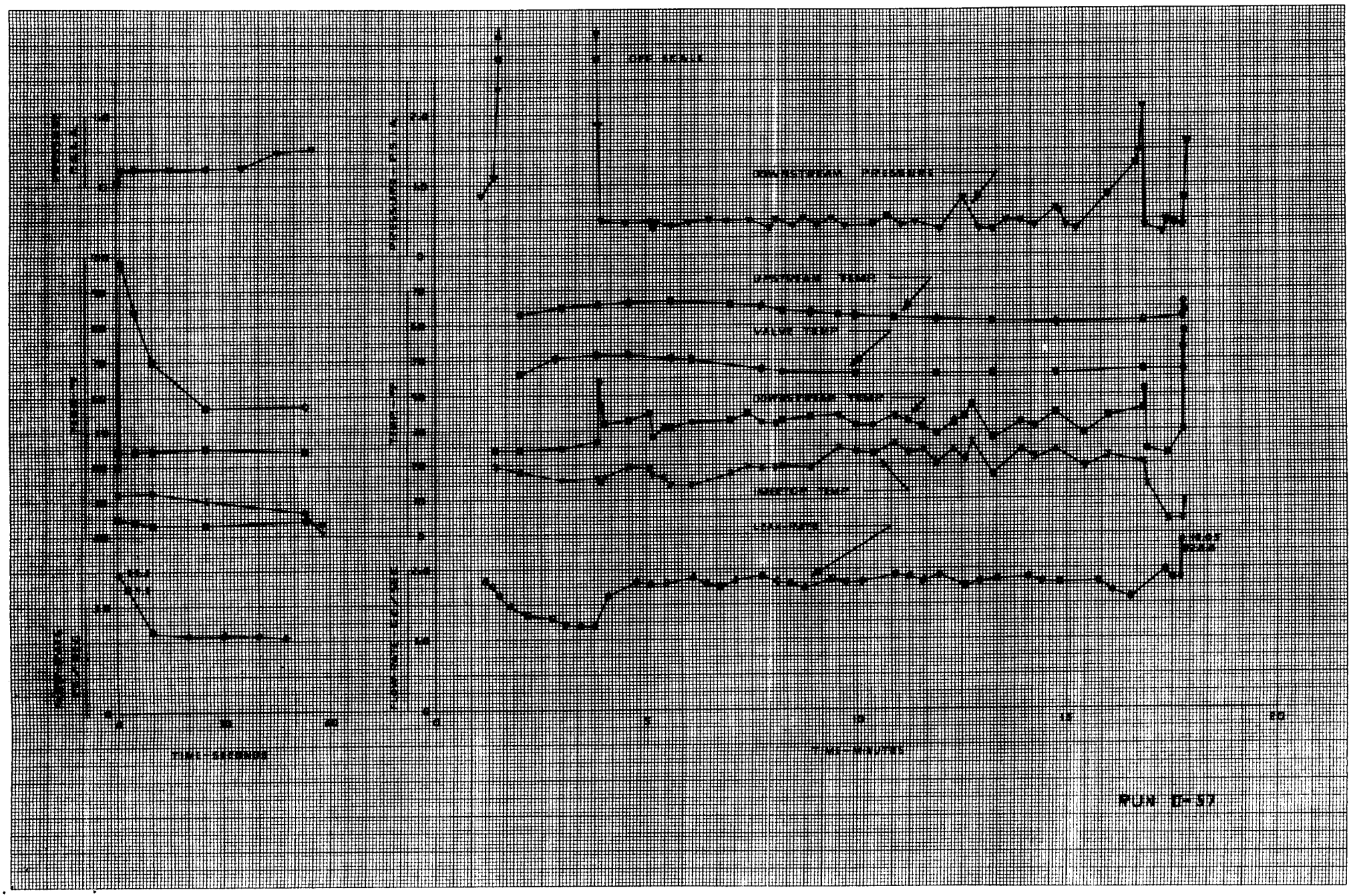
RUN E-57

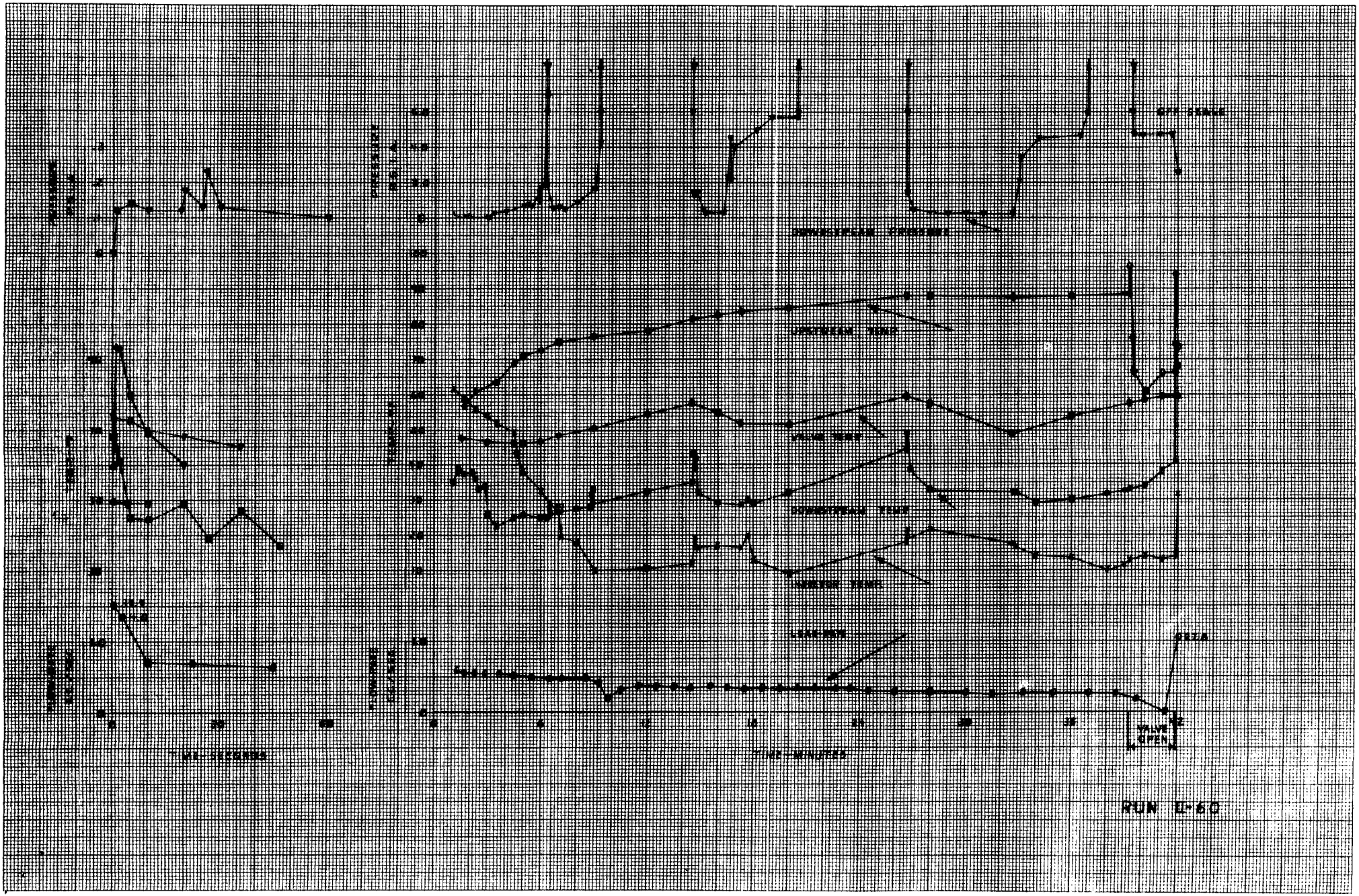
TIME-SECONDS
TIME-MINUTES
VALVE OPEN
RUN D-60

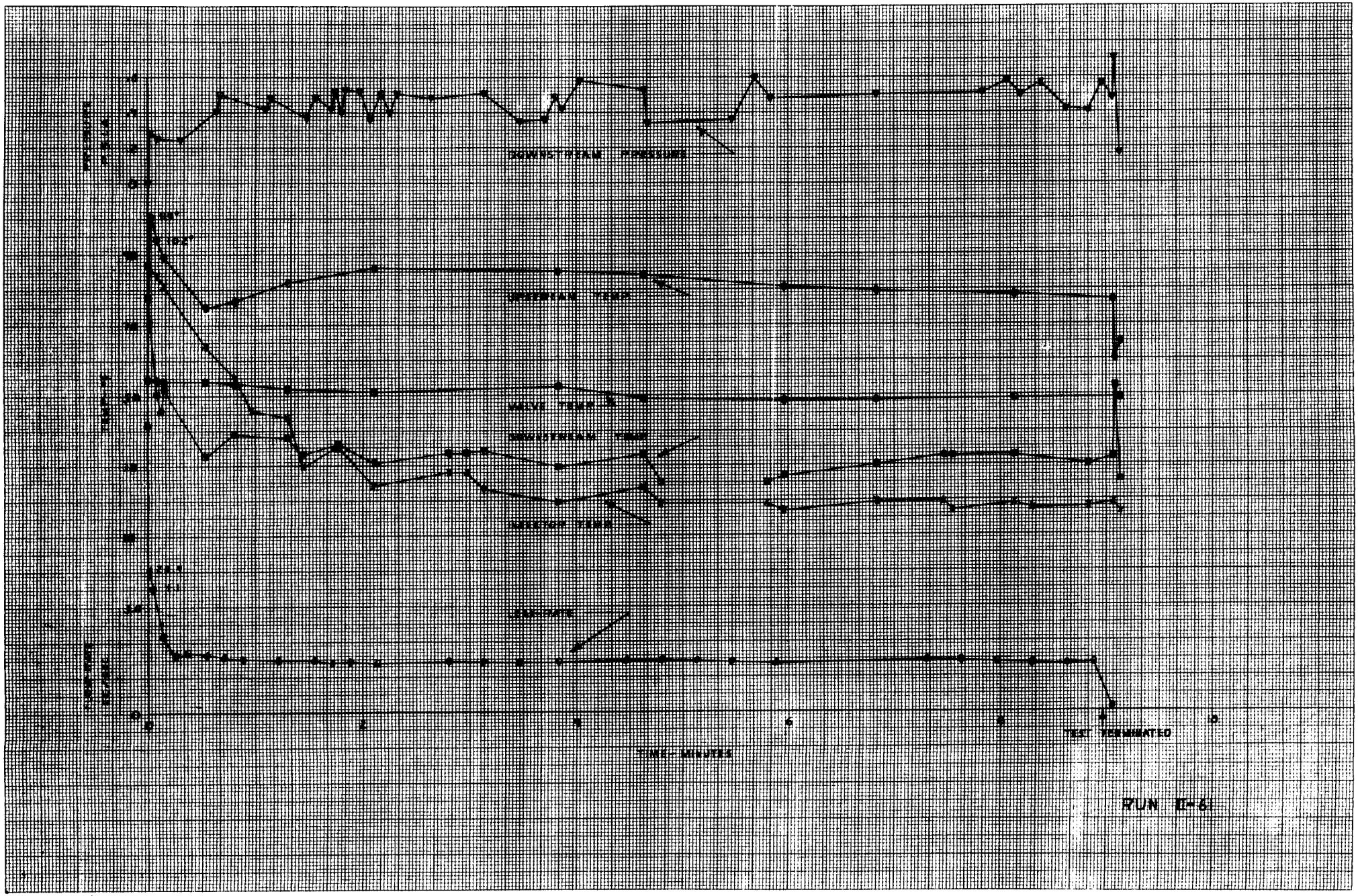
DOWNSTREAM PRESSURE
UPSTREAM TEMP
VALVE TEMP
DOWNSTREAM TEMP
ORIFICE TEMP
ORIFICE
TIME- MINUTES
TEST TERMINATED
RUN E-61

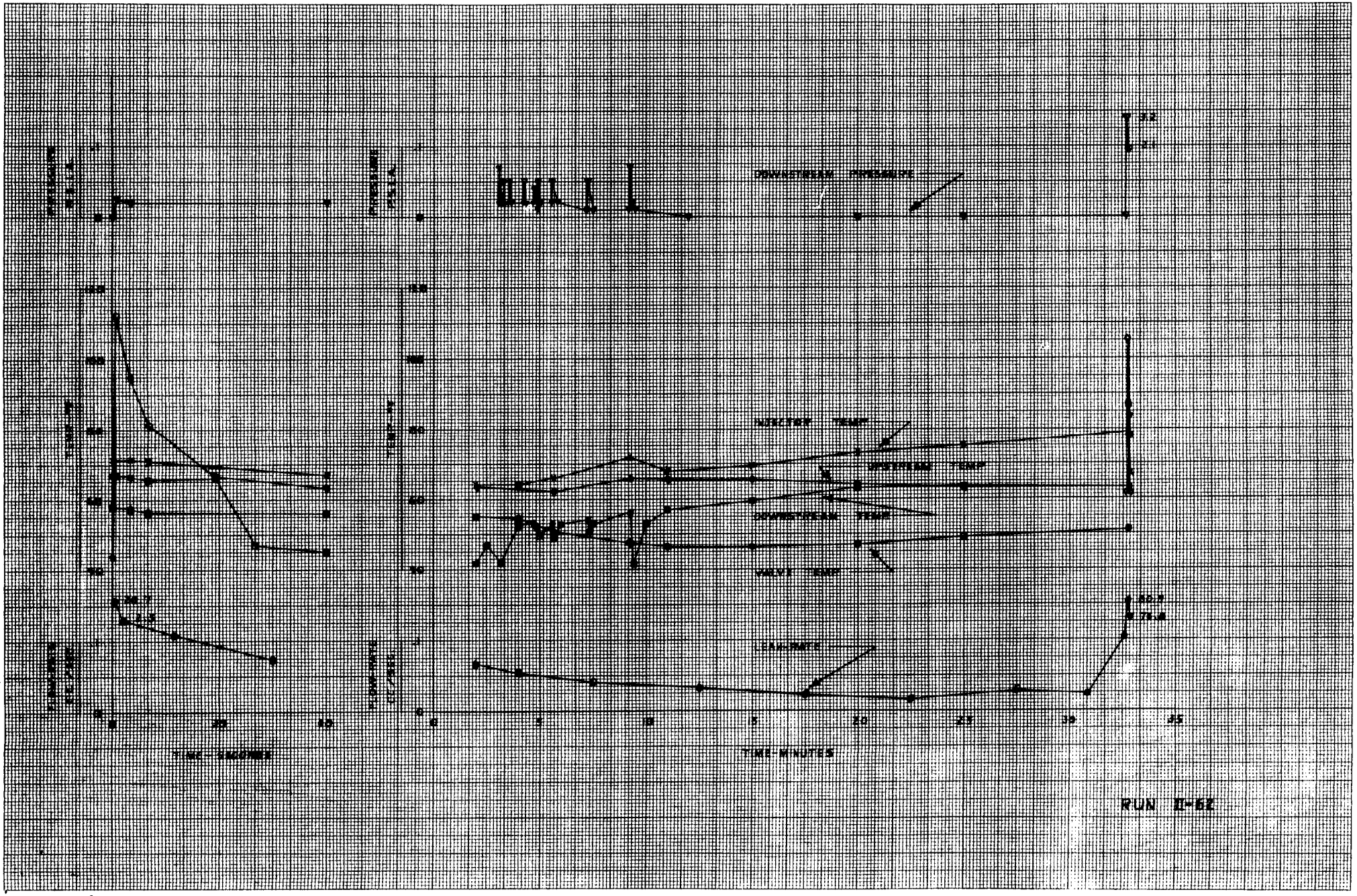
DOWNSTREAM PRESSURE
INJECTOR TEMP
UPSTREAM TEMP
DOWNSTREAM TEMP
VALVE TEMP
LEAK-RATE
TIME-SECONDS
TIME-MINUTES
RUN II-62

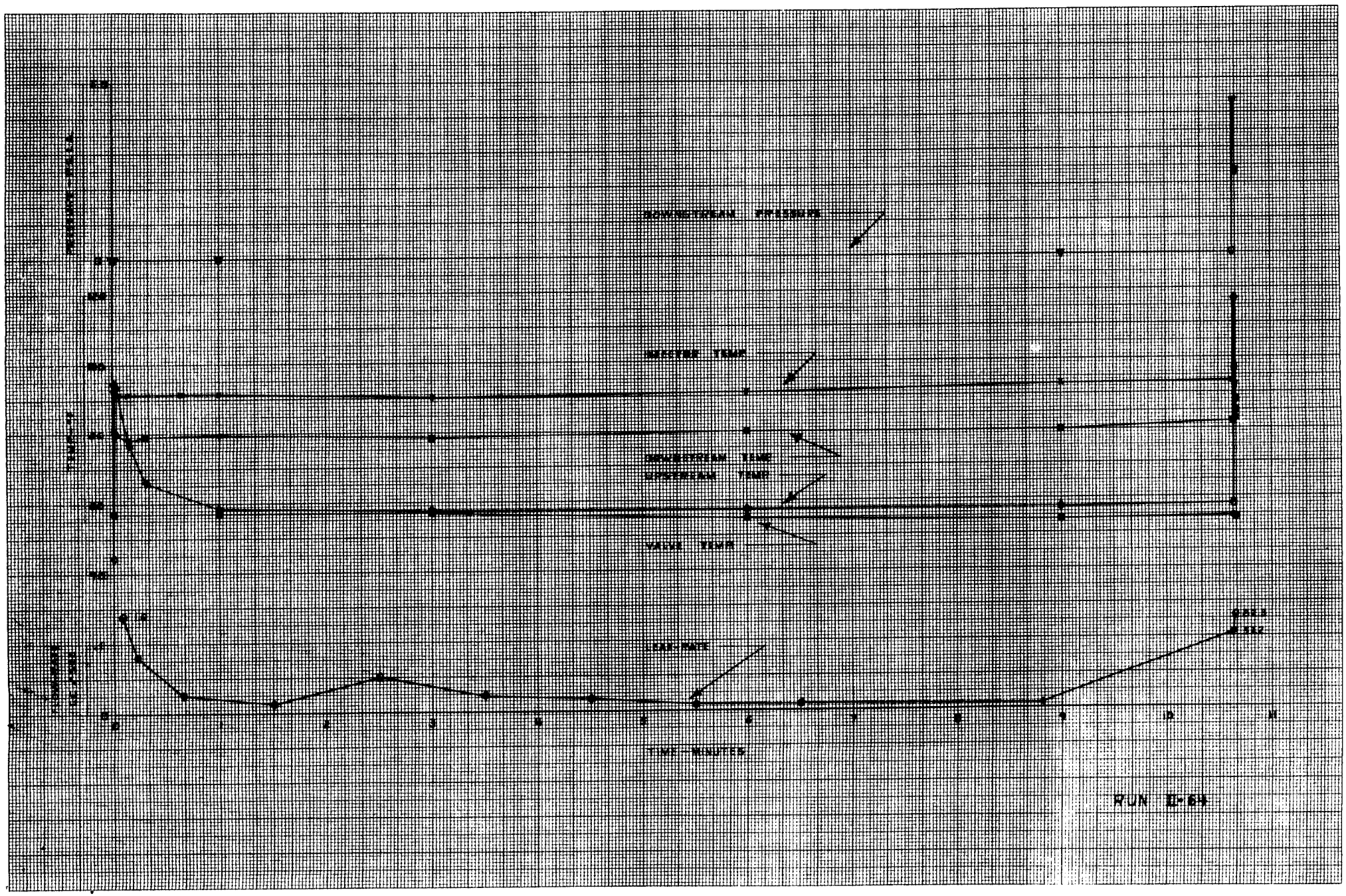
DOWNSTREAM PRESSURE
RECEIVER TEMP
DOWNSTREAM TEMP
UPSTREAM TEMP
VALVE TEMP
LEAK-RATE
TIME - MINUTES
RUN E-63

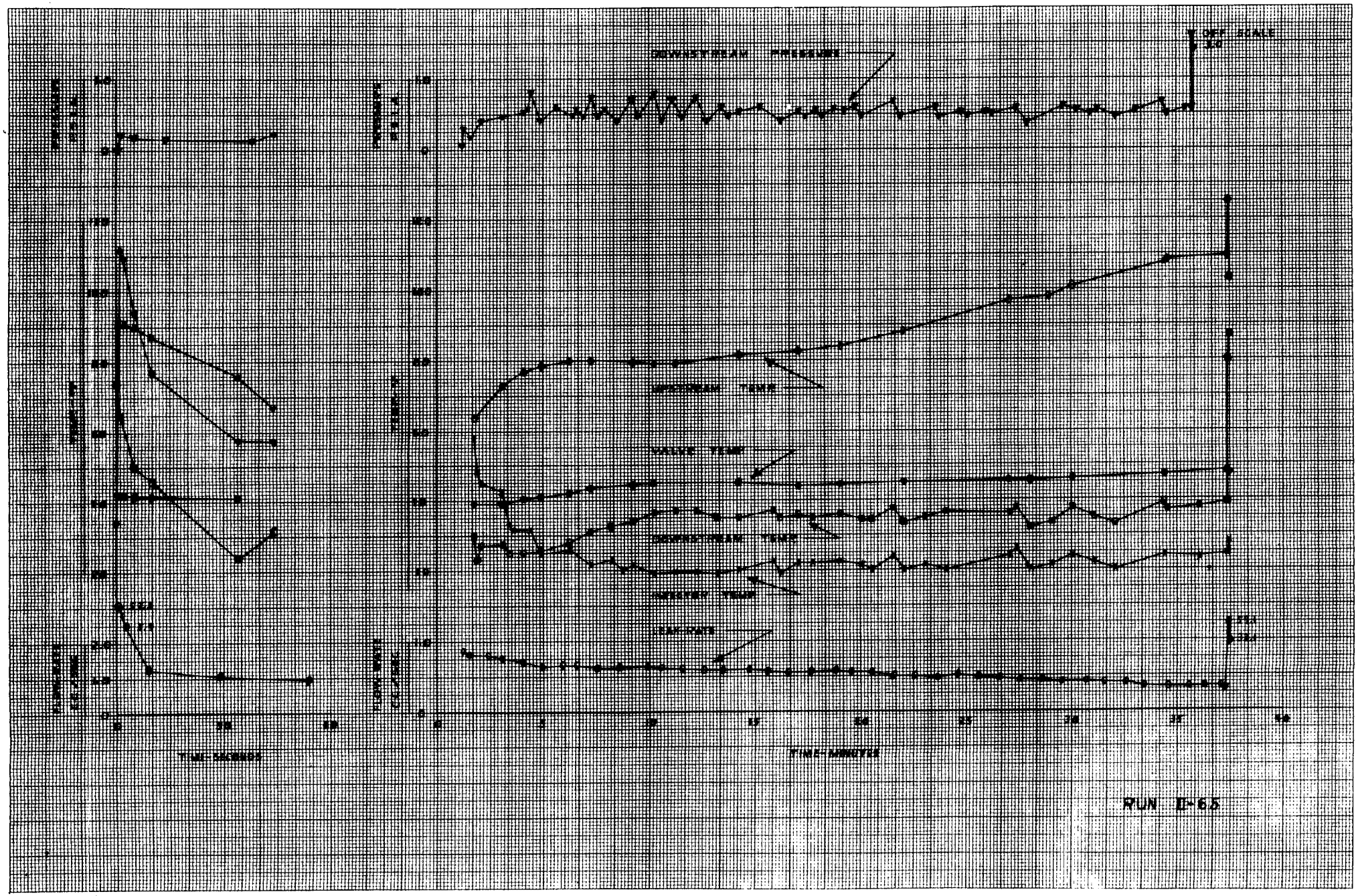
DOWNSTREAM PRESSURE
OFF SCALE
UPSTREAM TEMP
VALVE TEMP
DOWNSTREAM TEMP
INTERIOR TEMP
LEAK RATE
TIME-SECONDS
TIME-MINUTES
RUN E-6.5

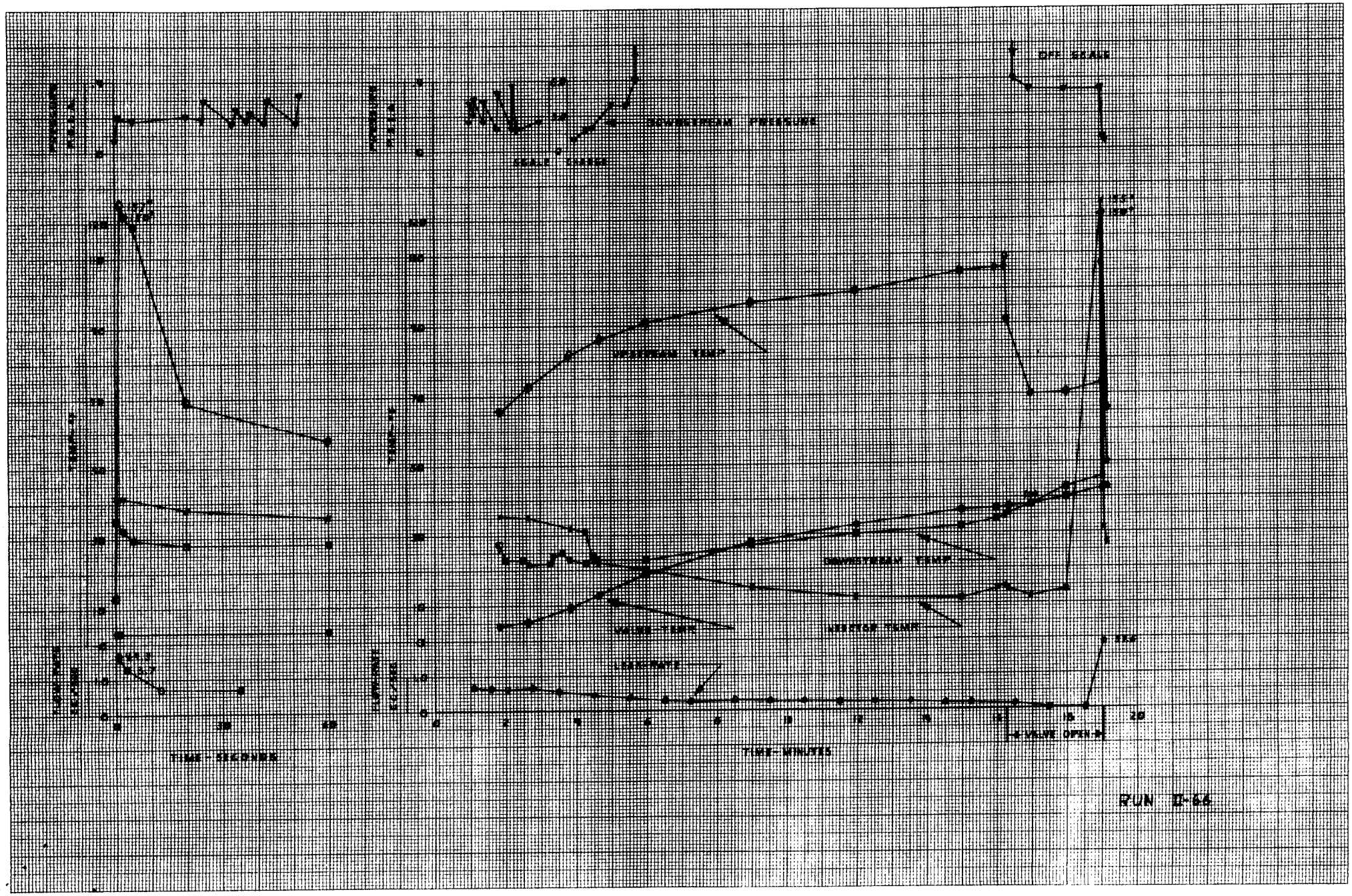
OFF SCALE
DOWNSTREAM PRESSURE
SCALE 0 - 5000 PSIG
UPSTREAM TEMP
DOWNSTREAM TEMP
VALVE TEMP
HEATER TEMP
FLOW RATE
TIME - SECONDS
TIME - MINUTES
RUN II-66

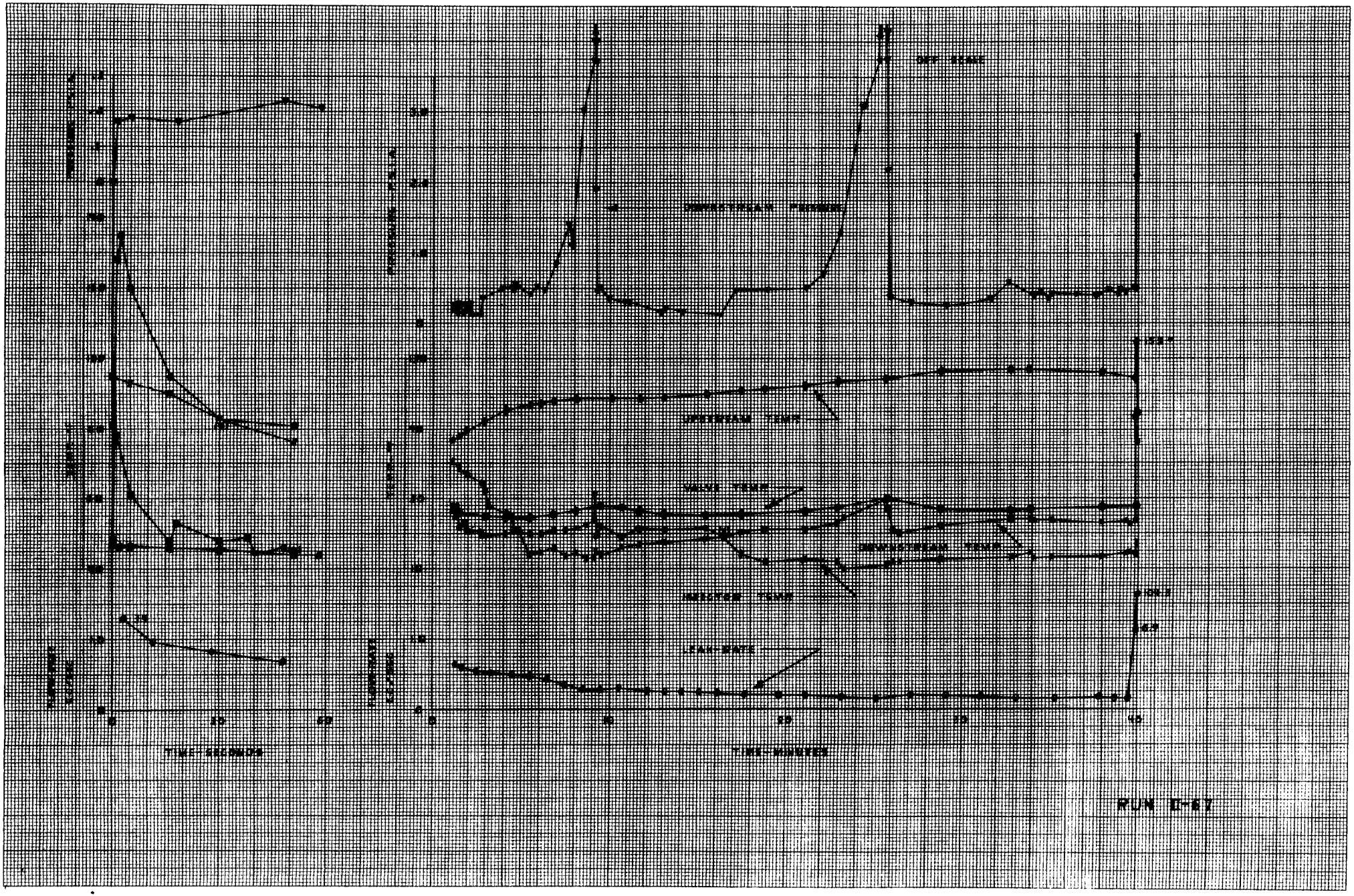
TIME-SECONDS
TIME-MINUTES
OFF GRADE
DOWNSTREAM PRESSURE
DOWNSTREAM TEMP
VALVE TEMP
UPSTREAM TEMP
INJECTOR TEMP
FLAME-RATE
RUN E-67

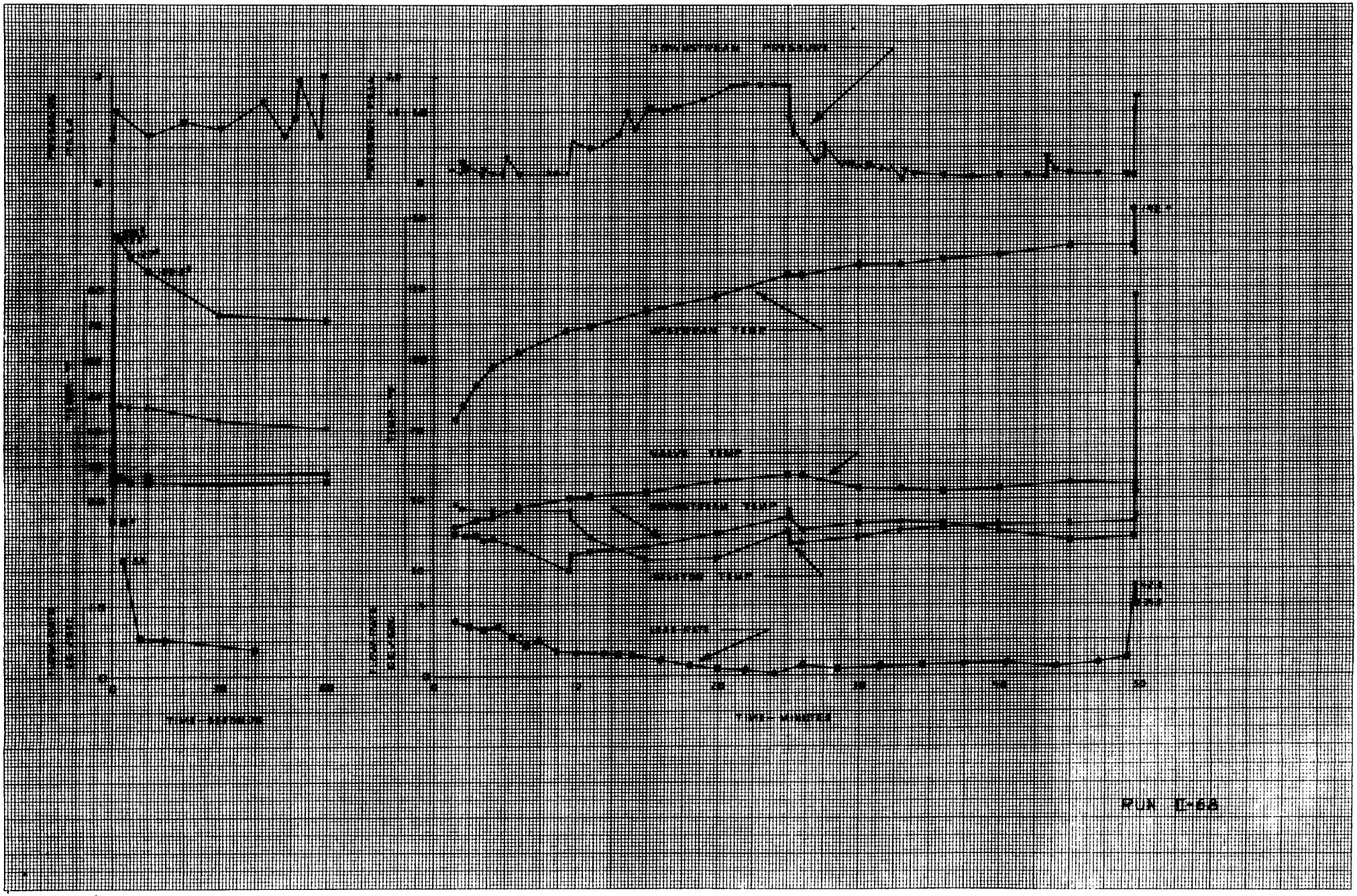
RUN E-6A

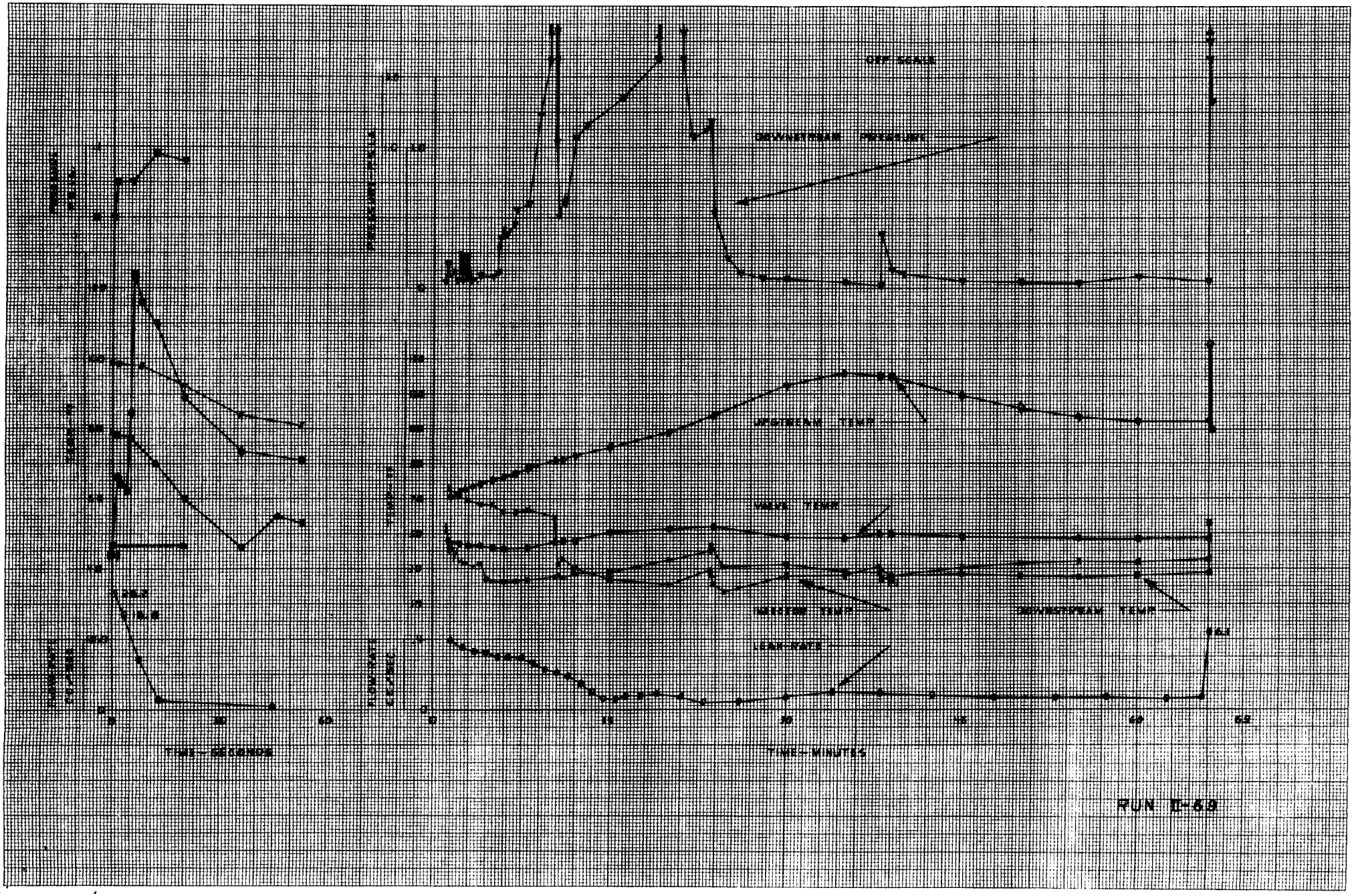
OFF SCALE
DOWNSTREAM PRESSURE
UPSTREAM TEMP
VALVE TEMP
WEIR TEMP
DOWNSTREAM TEMP
LEAK RATE
TIME - SECONDS
TIME - MINUTES
RUN II-69

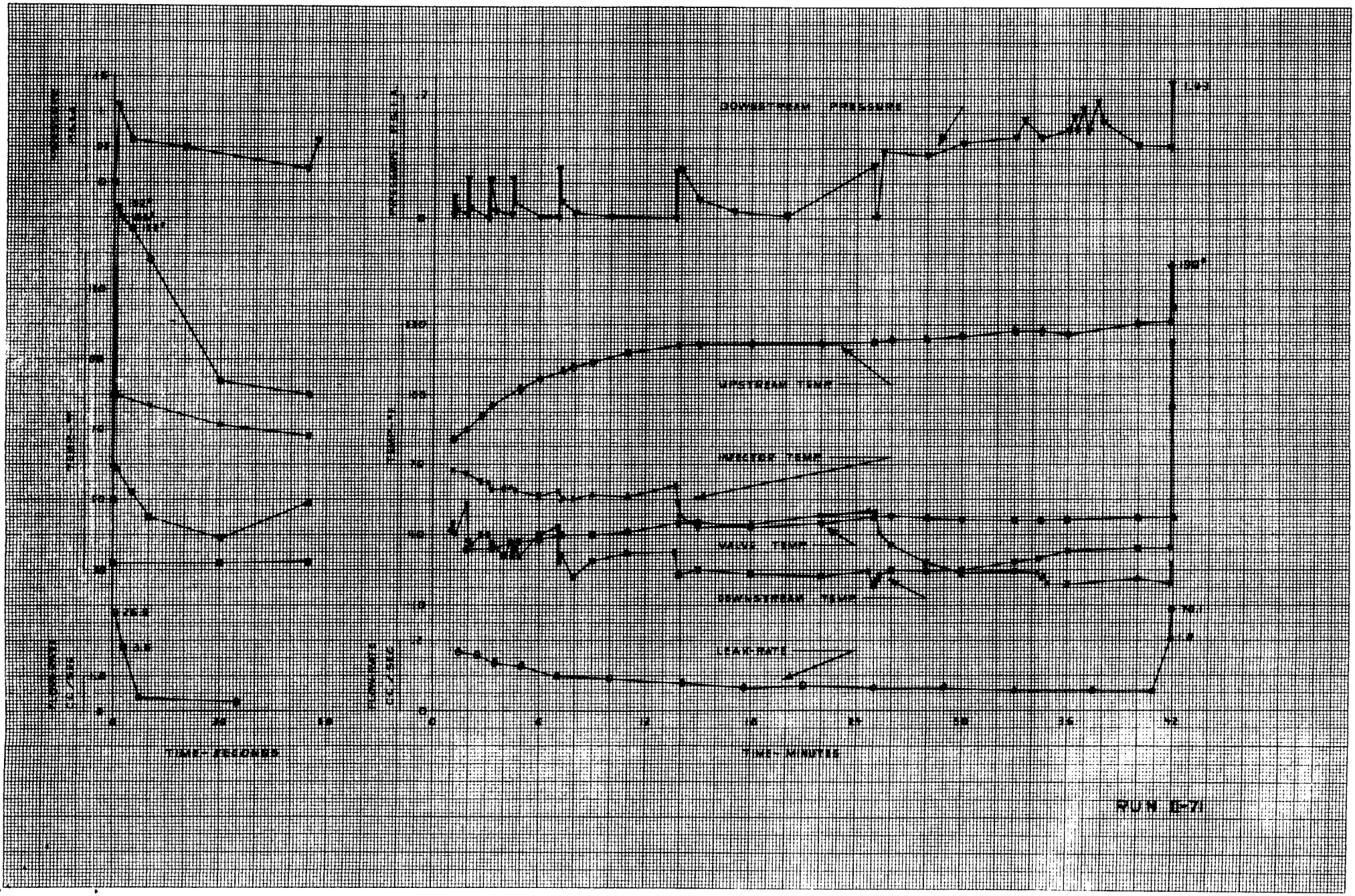
DOWNSTREAM PRESSURE
UPSTREAM TEMP
INLETER TEMP
VALVE TEMP
DOWNSTREAM TEMP
LEAK-RATE
TIME-SECONDS
TIME-MINUTES
RUN E-71

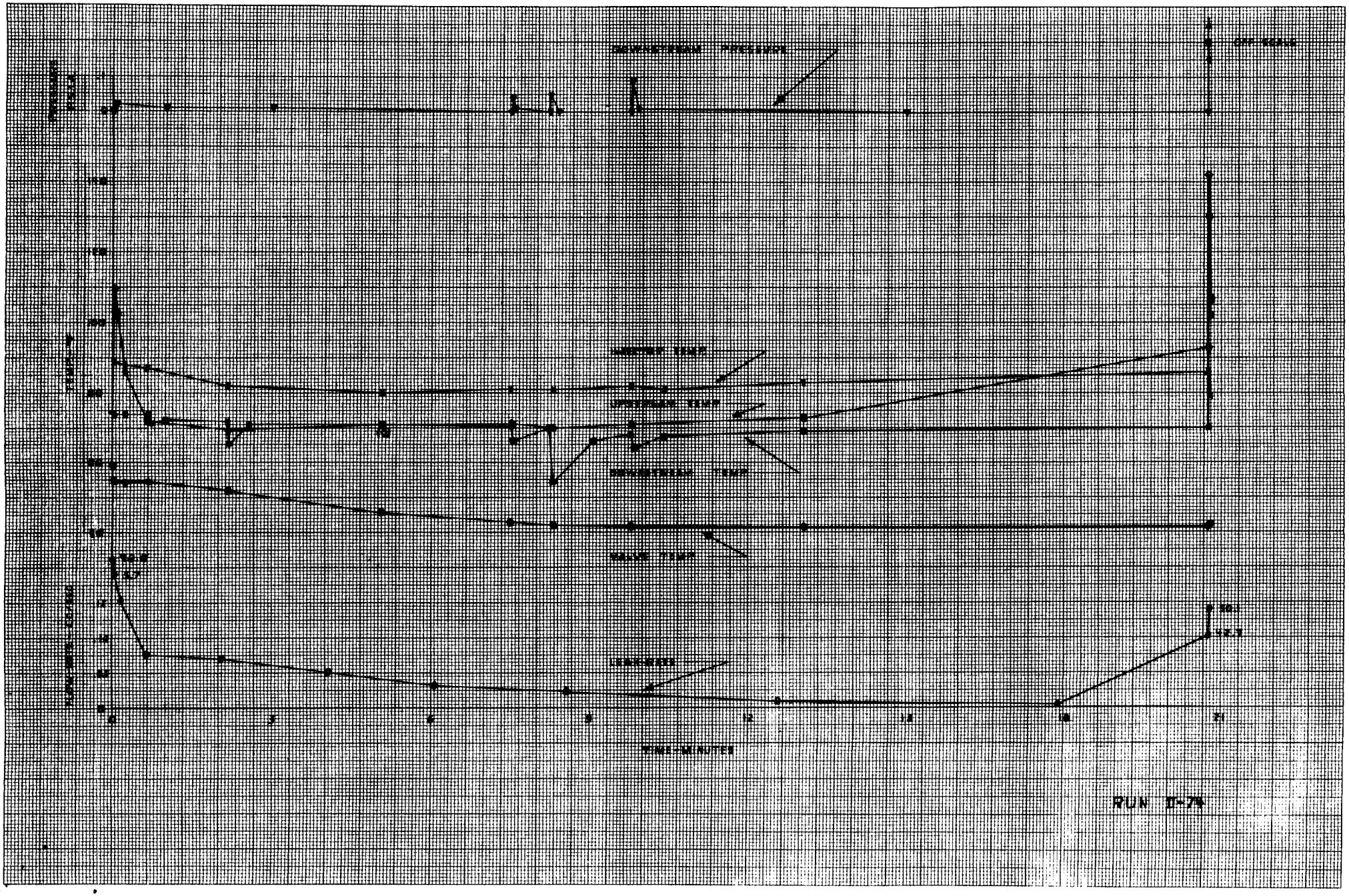
DOWNSTREAM PRESSURE
OFF SCALE
HEATER TEMP
UPSTREAM TEMP
BREAKTHRU TEMP
WALL TEMP
LEAKAGE
16.1
12.3
0
3
6
9
12
15
21
TIME-MINUTES
RUN II-74

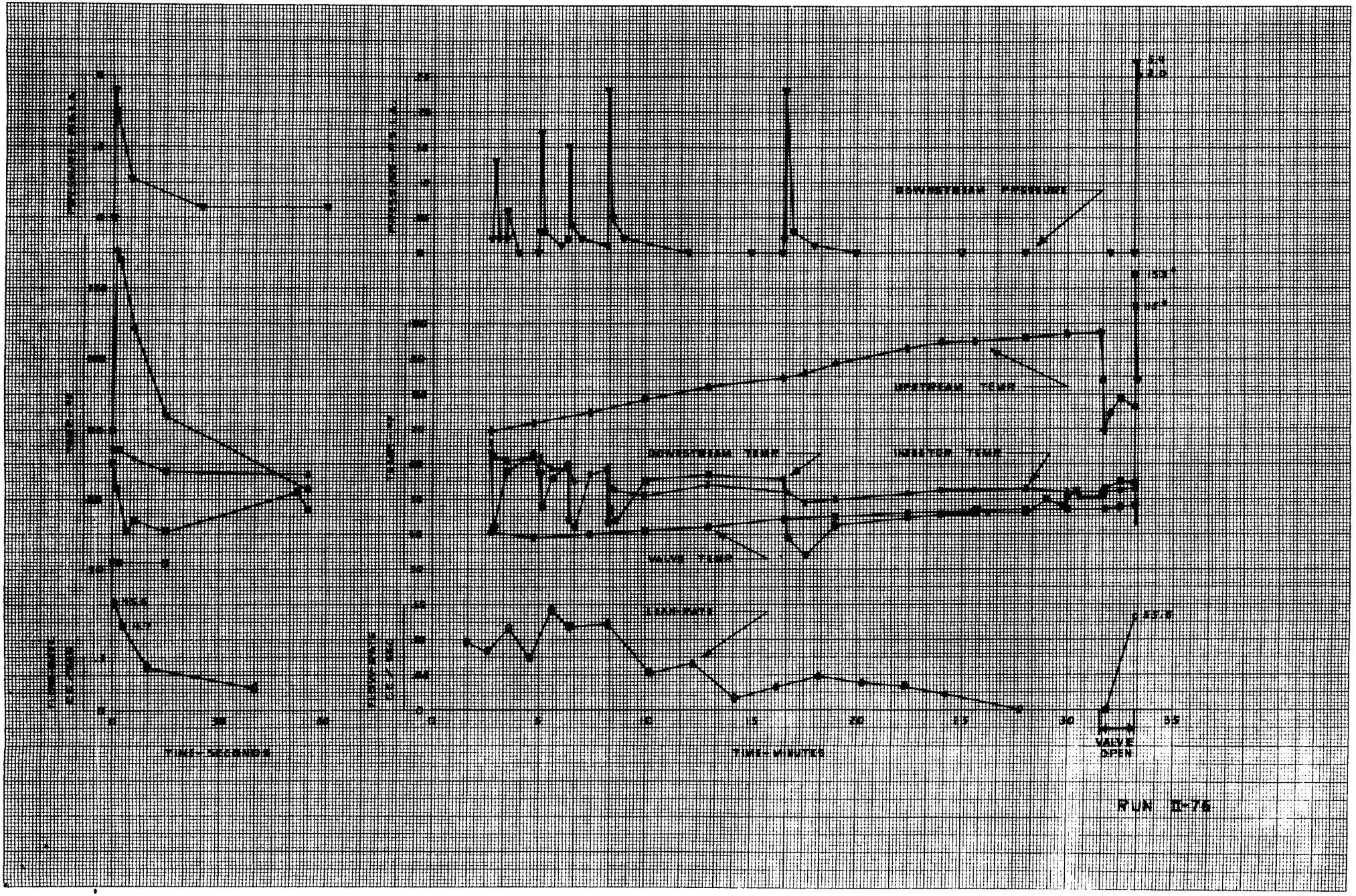
DOWNSTREAM PRESSURE
UPSTREAM TEMP
DOWNSTREAM TEMP
INLET TOP TEMP
VALVE TEMP
TIME-SECONDS
TIME-MINUTES
VALVE OPEN
RUN II-76

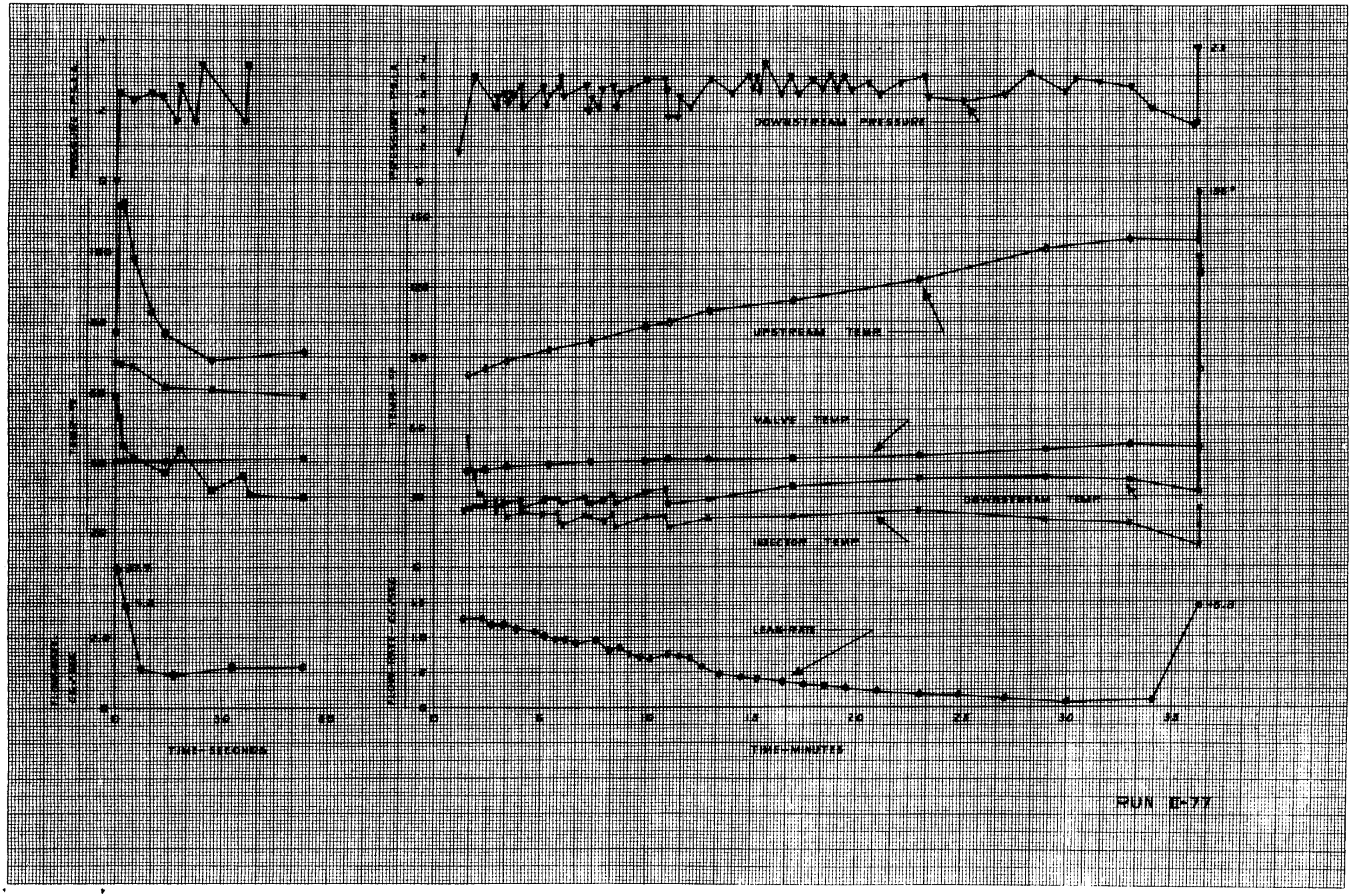
DOWNSTREAM PRESSURE
UPSTREAM TEMP
VALVE TEMP
DOWNSTREAM TEMP
INJECTOR TEMP
LEAK RATE
TIME-SECONDS
TIME-MINUTES
RUN E-77

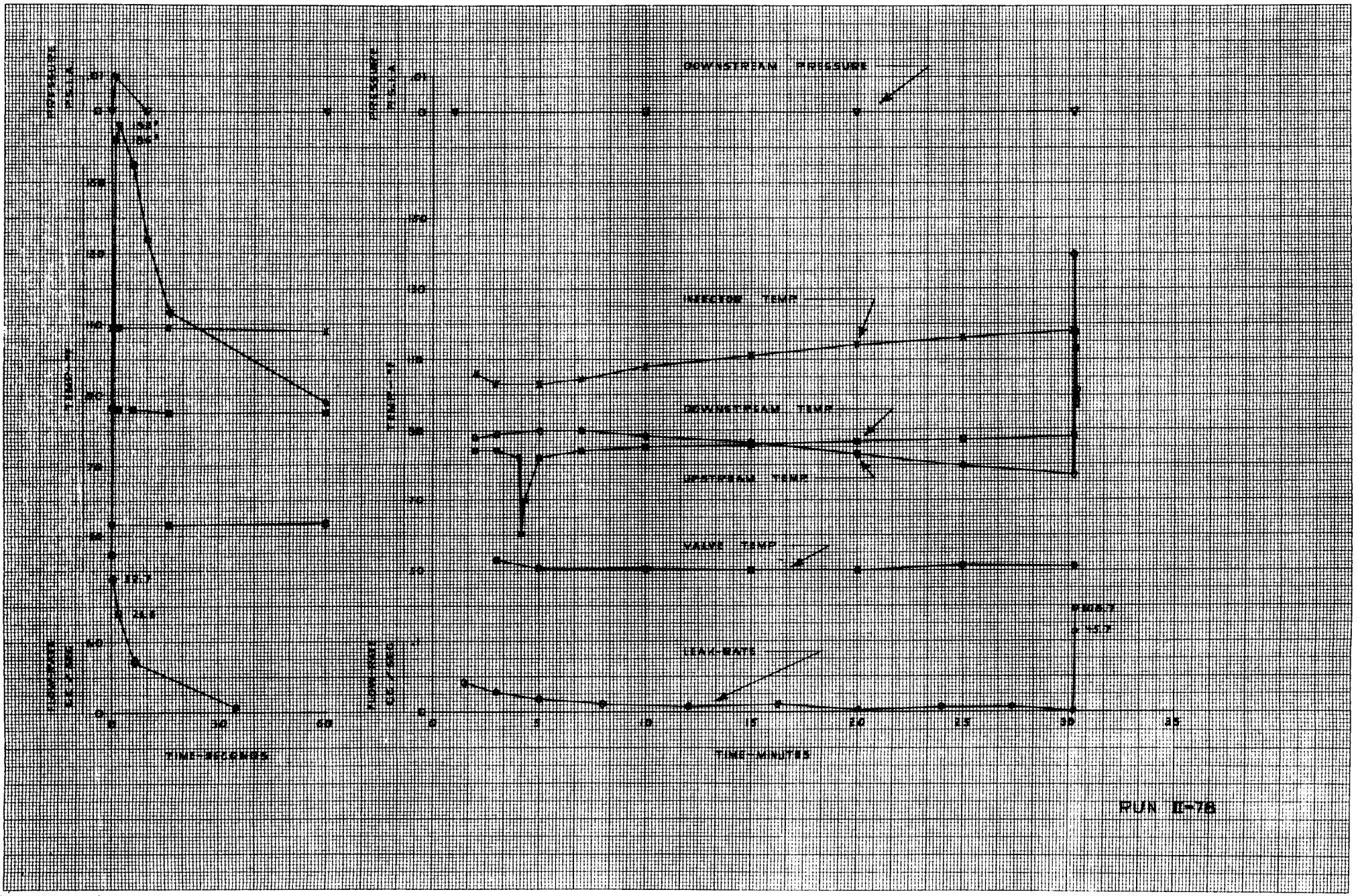
DOWNSTREAM PRESSURE
INJECTOR TEMP
DOWNSTREAM TEMP
UPSTREAM TEMP
VALVE TEMP
LEAK RATE
TIME-SECONDS
TIME-MINUTES
RUN II-78

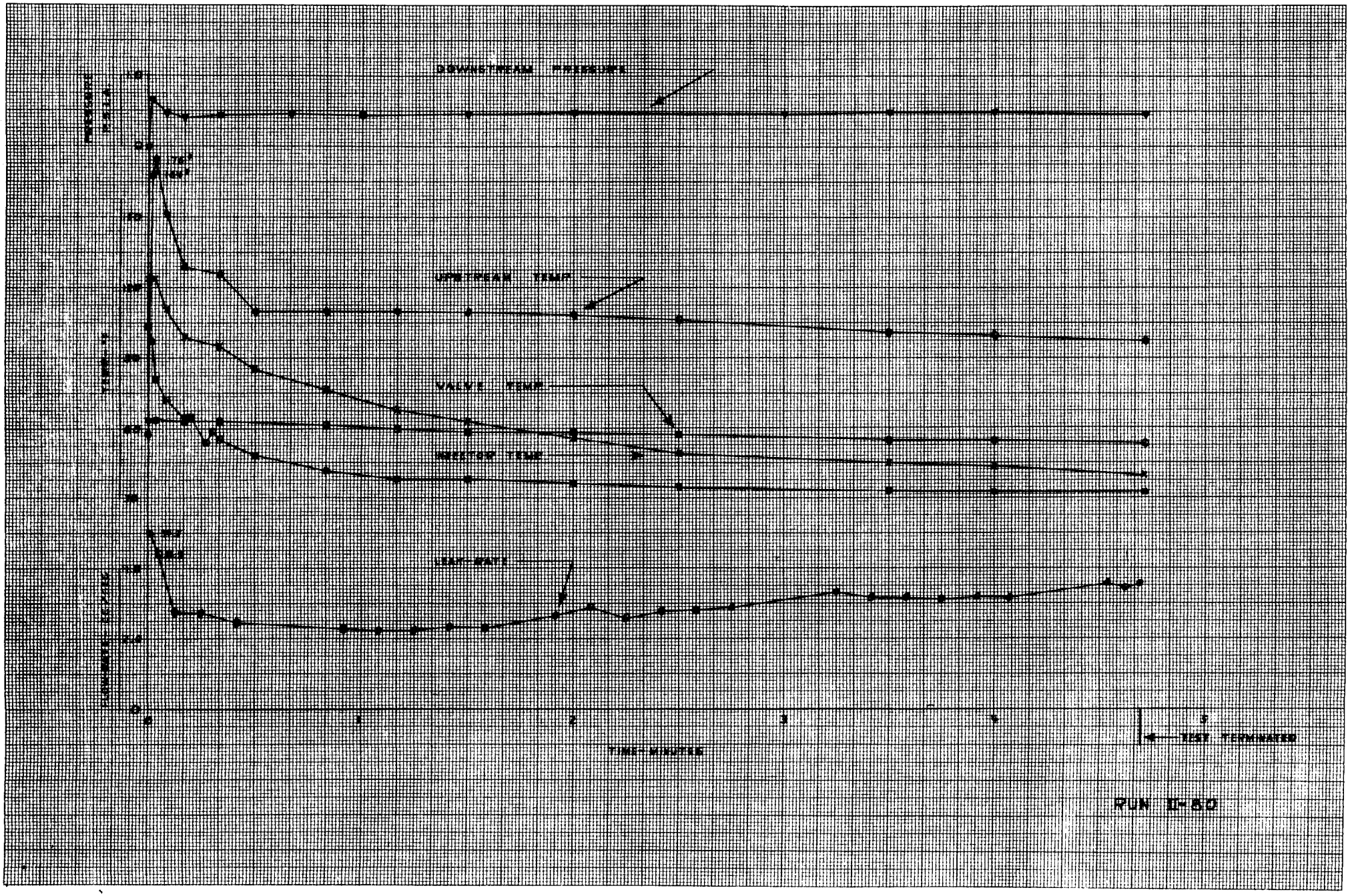
DOWNSTREAM PRESSURE
UPSTREAM TEMP
VALVE TEMP
INJECTOR TEMP
HEAT RATE
TIME-MINUTES
TEST TERMINATED
RUN II-80

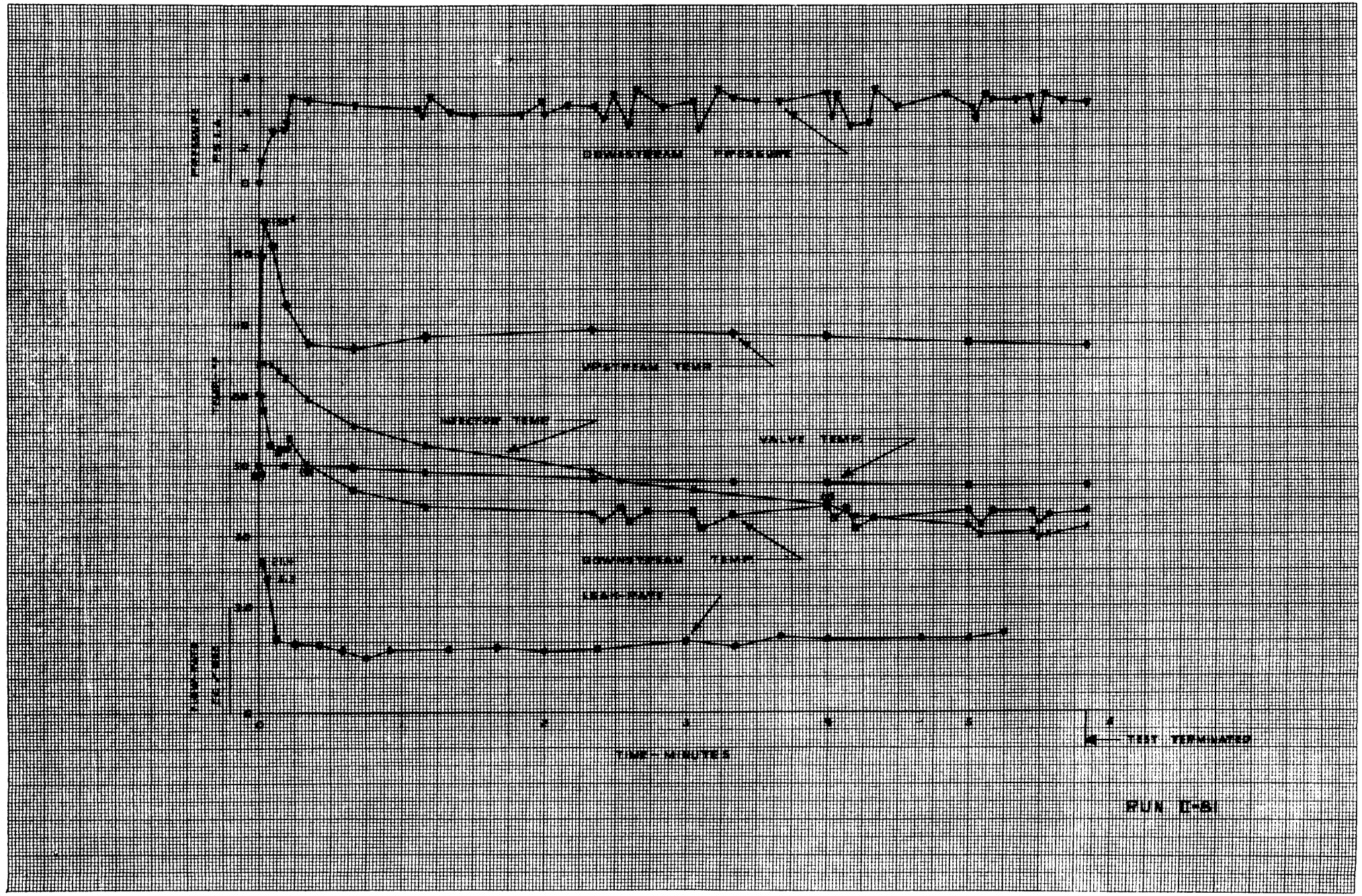
DOWNSTREAM PRESSURE
UPSTREAM TEMP
REACTOR TEMP
VALVE TEMP
DOWNSTREAM TEMP
LEAK-RATE
TIME - MINUTES
TEST TERMINATED
RUN II-61